A Study of the Growth of Pichia Membranaefaciens Utilising the Energy Obtained by the Oxidation of Different Metallic Hydroxides by Aeration

By S. RANGANAYAKI and Krishna BAHADUR

(Received May 27, 1954)

Introduction

Winogradsky observed long ago that micro-organisms can utilise the energy obtained by the oxidation of mineral substances for their life activity. This statement got confirmation from the findings of Temple and Colmer[1] who could grow *Thiobacillus ferroxidans* by means of energy obtained from the oxidation of ferrous ions.

I have succeeded in growing *Pichia membranaefaciens*[2] in cultures containing only one of such energy sources. In this paper, I am giving the results obtained by growing *this yeast* in cultures containing some metallic hydroxides which by slow aeration liberate energy required for growth. The hydroxides under study were manganese hydroxide, cobalt hydroxide, ferrous hydroxide, stannous hydroxide and cerous hydroxide.

Experimental

Several cultures, each containing 0.30 g. of sodium nitrate, 0.08 g. of potassium hydrogen phosphate, 0.006 g. of calcium carbonate and 0.009 g. of magnesium sulfate, were prepared. These minerals were put into 750 cc. flat bottom pyrex flasks and digested with dilute hydrochloric acid. The total volume of each culture was made to 500 cc. and the *p*H adjusted to 4.5. One gram of the freshly precipitated and dried hydroxide under investigation was added to each culture. The flasks were then cotton-plugged and sterilised by boiling at 15 lbs. pressure for 30 minutes in an autoclave. After cooling, these cultures were seeded with 0.2 cc. of an activated sample of *Pichia membranaefaciens*. This sample contained about 600 cells per cc.

Sterilised air was passed through each culture and the cell-count of the cultures was taken by the method described below. The temperature variation during the period of study was between 29.8°C and 33.0°C.

To take the cell-count of the cultures, first a culture solution was made by the following method. 0.20 g. of calcium carbonate, 0.25 g. of magnesium carbonate, 0.20 g. of sodium chloride, 0.20 g. of potassium sulfate, 0.20 g. of disodium hydrogen phosphate, 10 g. of sucrose and 2.5 g. of ammonium sulfate were weighed out into a flask. These were digested with dilute hydrochloric acid and the total volume of the culture was made up to one litre, adjusting the *p*H to 4.5. Twenty grams of agar-agar were added to it and the solution was sterilised by boiling at 10 lbs. pressure for 30 minutes. On cooling, it solidified. This solution was warmed by keeping it in a water bath. Five cc. of this melted solution were put into a sterilised Petri dish with the help of a sterilised pipette. The solution to be tested was shaken well and 1 cc. of this was added to the agar-agar culture in the Petri dish before it solidified. The dish was closed with the upper lid and kept in an incubator for 24 hours. A small star-like yeast colony developed around each cell. By counting these stars, the number of yeast cells was known. Ten of such Petri dishes were prepared for each culture whose cells were to be counted and the average of these ten countings is shown in the tables.

One culture was kept as control, in which all the other substances were present in the same amount except the source of energy. This control culture was also seeded with the same amount of yeast and aerated similarly. Its cell-count after 2 days and onwards was always zero.

Results

The results obtained by counting the cells in each culture are tabulated below:

No. of days after seeding	Average cell-count					
	Control	Manganese hydroxide	Cobalt hydroxide	Ferrous hydroxide	Stannous hydroxide	Cerous hydroxide
1	0.2	1.8	11.0	1.5	0.5	0.0
3	0.0	3.5	15.0	2.0	1.0	0.0
6	0.0	2.5	19.0	1.0	0.8	0.0
8	0.0	1.5	20.0	0.5	0.1	0.0
14	0.0	0.0	8.0	0.0	0.0	0.0
22	0.0	0.0	2.0	0.0	0.0	0.0
24	0.0	0.0	0.0	0.0	0.0	0.0

1) K. L. Temple and A. R. Colmer, *J. Bact.*, **62** 605-11 (1951).

2) According to the classification scheme of Lodder and Kreger-van Rij.

Discussion

The culture containing cobalt hydroxide as the source of energy material shows good growth of yeast; moreover this growth continues for a fairly long time. The death of yeast in the control culture is due to the fact that it did not contain any source of carbon. Cerous hydroxide is poisonous for the growth of yeast and no yeast cell is seen at any stage. The other hydroxides favour yeast growth in the following order: manganese hydroxide, ferrous hydroxide and stannous hydroxide.

In these cultures, the energy needed for the growth and life activity of the yeast is supplied by the slow oxidation of these hydroxides by aeration. The carbon needed for making the body of the yeast is obtained by the fixation of atmospheric carbon dioxide. Probably the energy needed in this fixation is supplied by the oxidation of the hydroxide.

In these cultures, it is seen that the yeast stops growing after some time and later on, dies out completely as the aeration continues. This is perhaps due to this fact, that the carbon compound synthesised by the fixation of atmospheric carbon dioxide is in a form which can only partially satisfy the carbon need of the organism. It may be that yeast needs carbon food of some other type which cannot be synthesised by this method. Therefore the growth of yeast stops and further aeration in the absence of the essential carbon food proves fatal to the yeast.

Summary

When in *Pichia membranaefaciens* cultures, all other nutrients are present except the carbon source and the hydroxide of some metal is added and the culture aerated, a growth of yeast is observed. Maximum growth is observed in the case of cobalt hydroxide. Cerous hydroxide is poisonous and does not favour any growth.

Chemistry Department, Allahabad University, Allahabad, India

Distribution of Fluorine in Various States in Terrestrial Waters

By Shigeki KOBAYASHI

(Received April 28, 1953)

Introduction

Despite an accumulation of the fluorine studies in terrestrial waters, the distribution of the element in its various states remains untouched, a problem particularly important from the viewpoint of its pathology and hygienics. Filling in the lack of knowledge is the primary motive for the present study.

In effect, the author applied Sanchis' method[1] of fluorine determination in four different ways to thirty-nine samples of various kinds of terrestrial waters in Japan and established the distribution of the element in the three following different states:

(A). The fluorine, which can be determined when Sanchis' method is applied to the supernatant water obtained by keeping the sample still until the suspended matter settles down. This comprises the fluoride ions preexistent as well as those which can be liberated from certain kinds of complexes such as the ions of silicofluoride or aluminofluoride under the conditions of the application of the method.

(B). Other kinds of dissolved fluorine, which can be converted into silicofluoric acid when the supernatant water is condensed into a smaller volume and treated with concentrated sulfuric or perchloric acid.

(C). The fluorine of the suspended matter, which can be converted into silicofluoric acid when the original sample is evaporated nearly to dryness and treated with concentrated sulfuric or perchloric acid.

Experimental

The sample is cautiously shaken so that the suspended matter is uniformly distributed, and then divided into two fractions.

Fraction 1 is left still until the suspended matter completely settles. The supernatant water is siphoned out into a separate vessel. To a measured portion (50-100 ml.) Sanchis' method is applied directly (a). Another portion is made slightly alkaline with sodium carbonate solution and evaporated nearly to dryness. Then it is distilled with the addition of sufficient amounts of solid silver sulfate and powdered quartz or glass, and some 5 ml. of concentrated sulfuric or perchloric acid. The fluorine in the distillate is determined

1) J. M. Sanchis, *Ind. Eng. Chem.*, Anal. Ed., 6, 134 (1934).

by Sanchis' method[2,3] (b).

Fraction 2 is shaken again and Sanchis' method is applied to a measured portion of the uniformly distributed suspension (c). Another portion of the same suspension is processed similarly as in (b), and the fluorine content of the distillate is finally determined (d).

By the following equations, the individual amounts of the element in the three different states can be calculated from the data, (a), (b), (c), and (d).

Fluorine in state (A) (a)
" " " (B) (b)—(a)
" " " (C) (d)—(b)

Results

The samples vary one from another in the distribution of the element in its three different states, but can be classified into the four following states, as given in Table I.

TABLE I

DISTRIBUTION OF VARIOUS FORMS OF FLUORINE IN TERRESTRIAL WATERS

Waters of Type 1, (a=b=c=d)

Sample	Source	a mg/L	b mg/L	c mg/L	d mg/L
No. 1	Well, Gamagori, Aichi Pref.	0.15	0.15	0.15	0.15
2	Well, Gamagori, Aichi pref.	0.15	0.15	0.15	0.10
3	Well, Oi, Gifu Pref.	0.25	0.35	0.30	0.30
4*	Well, Kasamatsu, Gifu Pref.	0.45	0.50	0.45	0.45
5*	Well, Sendanbayashi, Gifu Pref.	3.8	3.9	3.8	3.8
6	Well, Sendanbayashi, Gifu Pref.	0.10	0.10	0.10	0.10
7	Well, Sendanbayashi, Gifu Pref.	0.10	0.10	0.10	0.10
8	Well, Kamioka, Gifu Pref.	0.10	0.10	0.10	0.10
9	Spring "Kikusuisen", Yōrō, Gifu Pref.	0.25	0.30	0.25	0.30
10	Thermalsprings "Sakakibara-onsen", Sakakibara, Mie Pref.	3.5	3.5	3.5	3.4
11	The botten water of Lake "Kizaki-Ko", Kitaazumi, Nagano Pref.	0.40	0.35	0.40	0.40
12*	River "Wada-gawa", Shimizubara-mura, Nagano Pref.	0.75	0.75	0.75	0.75
13(a)	River "Yumata-gawa" just up its confluence with River "Mizumata-gawa", Nagano Pref.	2.0	2.0	2.0	2.1
14	River "Toyo-kawa" Miya, Aichi, Pref.	0.45	0.40	0.45	0.40
15	River "Sugo-gawa", Okazaki, Aichi Pref.	0.10	0.10	0.10	0.10

Waters of Type 2, (a=c<b=d)

Sample	Source	a mg/L	b mg/L	c mg/L	d mg/L
No. 16	Well, Gamagori, Aichi Pref.	0.25	0.50	0.25	0.50
17*	Well, Higashikata, Ehime Pref.	0.35	0.60	0.35	0.55
18*	Well, Ōsato, Aichi Pref.	1.7	2.1	1.6	2.1
19	Thermalsprings "Kinryu-onsen" Nagashima, Gifu Pref.	2.0	2.4	1.9	2.4
20	River, Shimecha, Hokkaido.	0.20	0.30	0.15	0.25
21*	River "Takase-gawa", Motoki, Tokiwa-Mura, Nagano Pref.	0.70	1.0	0.75	1.1

2) H. H. Willard and O. B. Winter, *Ind. Eng. Chem., Anal. Ed.*, **5**, 7 (1933).

3) H. Okuno, *J. Faculty Sci., Hokkaido Imp. Univ.*, **3**, (3), 101, (1942).

Waters of Type 3, (a=c<b<d)

Sample	Source	a mg/L	b mg/L	c mg/L	d mg/L
No.22(b)	Well, Sakae-machi, Nagoya City.	0.15	0.40	0.15	1.2
23*	Well, Yokomichi, Ehime Pref.	0.30	0.45	0.30	0.60
24	River "Aki-gawa", Ōi, Gifu Pref.	0.30	0.40	0.25	0.75
25	River "Ibi-gawa", Wakino, Gifu Pref.	0.10	0.30	0.15	0.50

Waters of Type 4, (a=b=c<d)

Sample	Source	a mg/L	b mg/L	c mg/L	d mg/L
No. 26	Well, Ōi, Gifu Pref.	0.35	0.40	0.40	0.90
27	Thermalsprings "Yunoyama-Onsen", Yunoyama, Mie Pref.	12.0	12.5	12.0	20.0
28	The surface water of Lake "Kizaki-ko", Kitasazumi, Nagano Pref.	0.40	0.35	0.40	0.60
29	Swamp "Nakano-sawa", Tokiwa-mura, Nagano Pref.	0.60	0.65	0.60	0.90
30	River "Kago-gawa" just up its confluence with River "Takase-gawa", Nagano Pref.	0.25	0.25	0.25	0.70
31	River "Kashima-gawa", Ōide, Nagano Pref.	0.25	0.25	0.25	0.75
32	River "Titi-gawa" at the foot of Mt. Shiroyama, Nagano Pref.	0.40	0.45	0.45	0.60
33*	River "Takase-gawa", Kutsukake, Tokiwa-mura, Nagano Pref.	0.75	0.80	0.75	1.25
34(c)	River "Takase-gawa" near Kuzu-onsen, Nagano Pref.	2.2	2.2	2.2	3.6
35*	River "Takase-gawa" about 2.5 km. down streem from Kuzu-onsen, Nagano Pref.	0.80	0.80	0.85	1.6
36	River "Mizumata-gawa" just up its confluence with River "Yumata-gawa", Nagano Pref.	2.1	2.0	2.1	2.5
37	River "Kiso-Gawa", Enakyo, Gifu Pref.	0.25	0.25	0.25	0.55
38	River "Togi-Gawa", Togi, Ishikawa Pref.	0.30	0.30	0.25	0.40
39	Water-fall "Yōrō-no-taki". Yōrō, Gifu Pref.	0.30	0.30	0.35	0.50

* Cases of mottled enamel of teeth were found among the people, usually using this water for drinking.
(a), (c) Sample contaminated with thermalsprings water.
(b) Turbid.

Type 1. This type of water dissolves one or more kinds of the ions belonging to (A), but contains no other fluorine compound either dissolved or suspended.

Type 2. This type of water contains the fluorine of (B) in addition to one or more kinds of the ions belonging to (A), but no suspended fluorine compound.

Type 3. This type of water contains one or more kinds of the ions belonging to (A) as well as the fluorine belonging to (B) and (C).

Type 4. This type of water contains one or more kinds of the ions belonging to (A) as well as fluorine (C), but none of (B).

From the result it may be seen that the

statistic exploration of fluorisis cases can be successful only when it is done simultaneously with a differential determination of fluorine in various states in the water, which if ever has seldom been the case in the foregoing studies.

The author expresses his sincere appreciation to Professors K. Sugawara and S. Oana of Nagoya University for their guidance and suggestions. He is also indebted to Dr. T. Koyama and Mr. Y. Morita for their advice and to the members of the Sugiyama Women's College for their help in the present research.

Chemical Laboratory,
Sugiyama Women's College,
Nagoya

Dielectric Behaviour of Hydrated Crystals. II. Potassium Mercury (II) Chloride Monohydrate and Ammonium Mercury (II) Chloride Monohydrate[1]

By Ryôiti KIRIYAMA and Hideko IBAMOTO

(Received October 10, 1953)

Introduction

The water molecule in a salt hydrate crystal, which does not directly coordinate with the metal ion and is situated in an open space in the crystal lattice, will differ to a certain degree from the directly coordinated water molecule in the dielectric behaviour relating to the dipole orientation of the water molecule. In the present paper, potassium mercury (II) chloride monohydrate, $K_2HgCl_4 \cdot H_2O$ and its isomorphous crystal, ammonium mercury (II) chloride monohydrate, $(NH_4)_2HgCl_4 \cdot H_2O$ are dealt with as the typical examples containing the interstitial water of crystallization as confirmed by the X-ray analyses.

Crystal, Specimen and Equipment

A large single crystal of $K_2HgCl_4 \cdot H_2O$ are grown by slow cooling from seed crystal in a slightly supersaturated aqueous solution contained in a glass vessel dipped in a water-thermostat. This solution has been prepared from potassium chloride and mercuric chloride according to the phase diagram. It requires about four or five weeks to obtain a suitable, large, transparent, single crystal.

The crystal of the ammonium salt is obtained in a similar way.

The specimen is made by cutting and grinding, and is inserted directly between silver- or platinum-coated electrodes for the measurement of the capacity and the equivalent resistance of the crystal condenser in a way similar to that described in the previous paper.[2]

Result of Dielectric Measurement

(a) **$K_2HgCl_4 \cdot H_2O$.** The permittivities of this rhombic crystal at a room temperature are as follows: $\epsilon_a = 6.7 \pm 0.3$, $\epsilon_b = 6.1 \pm 0.2$, $\epsilon_c = 17.5 \pm 1.0$ (15°C, at 3 Mc and 5 kc). There is a marked anisotropy between the permittivities parallel and perpendicular to the *c*-axis. The temperature dependences of the permittivities and the dielectric losses are shown in Fig. 1, and the temperature coefficients $\frac{1}{\epsilon}\left(\frac{d\epsilon}{dT}\right)$ are as follows:

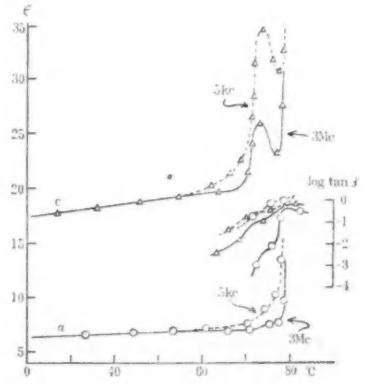

Fig. 1. The temperature dependences of the dielectric behaviour of $K_2HgCl_4 \cdot H_2O$

1) Parts of this investigation were separately read before the annual meetings of the Chemical Society of Japan in April 1949 and 1950, the annual meeting of the Crystallographic Society of Japan in May, 1950 and the Second International Congress of Crystallography at Stockholm in July, 1951.

2) R. Kiriyama and H. Ibamoto, This Bulletin, **27**, 32 (1954).

	−170——−120°	−120——−40°	−40——+70°
a	3×10^{-4}	7×10^{-4}	1×10^{-3}
c	4×10^{-4}	7×10^{-4}	3×10^{-3}

In these measurements, the average rate of heating is 0.2° per minute. The behaviour along the *b*-axis is almost similar to that along *a*. Above 70°C, there is a dispersion between 3 Mc and 5 kc along the *c*-axis, and the permittivity-temperature curve shows a peak at about 110°, while there is no such peak either along the *a*-axis or along the *b*-axis, and the dispersions along these axes are considerably small compared with that along *c*. At about 117°, sudden increases of the permittivities are observed in both *a*-and *c*-directions. When a considerable amount of phosphorus pentoxide powder has been spread at the bottom of the measuring cell, this steep increase at 117° diminishes and a maximum permittivity become measurable, then the ϵ-T curve shows a second peak at certain degrees higher than 117°. Therefore, it may be concluded that the increase at 117° is due to the surface conduction in the adsorbed layer of the dehydrated water molecules on the crystal surface. Similar phenomena were observed in the course of the dielectric measurements of $K_2CuCl_4\cdot 2H_2O$, $(NH_4)_2CuCl_4\cdot 2H_2O$ and $Sr(HCO_2)_2\cdot 2H_2O$ when the dehydration took place suddenly.[2]

Sometimes we observed a rather rapid increase of ϵ_c at a far lower temperature than that observed in the ordinary case and there arises a terrace on the low temperature side of the peak at 110° in the ϵ_c-T diagram. But this phenomenon is not reproducible and differs somewhat from others. Such a non-reproducible phenomenon may be attributed to some lattice imperfections of the crystal and a qualitative explanation will be given in the next paper of our studies.

For the purpose of making clear the cause of the anomaly at about 110°C, we carried out also the measurement of the time dependence of ϵ_c at constant temperatures, three different points being so chosen out of the temperature region where the anomaly is observed to be of significance from the view point of the results of X-ray experiments. The results are shown in Fig. 2. In the ϵ_c-time diagrams, the curve for 82.5° has two low peaks whereas that for 94° has only one high peak and that for 102.5° has also one high peak which lies nearer to the ordinate axis than that for 94°. After 300–500 hours, these curves seem to tend to an asymptotic value of about 13–15. According to the X-ray experiment mentioned below, the ordinary form transforms gradually into the high temperature form above 82°C. However, the transition velocity from the low temperature form into the high temperature one is so very little above the transition point, that the maximum ϵ_c which corresponds to the peak at about 110°C on the ϵ_c-T curve in Fig. 1 will appear very late as is seen for the appearance of the second peak in the ϵ_c-time curve for 82.5°. And the higher the temperature, the larger the transition velocity, and therefore the corresponding maximum ϵ_c at the higher temperature will appear in the earlier stage of the ϵ_c-time diagram.

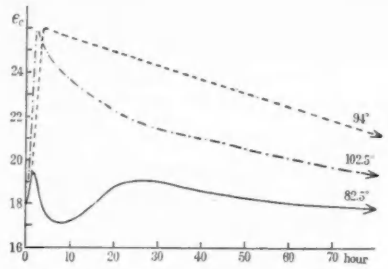

Fig. 2. The time dependences of ϵ_c at constant temperatures for $K_2HgCl_4\cdot H_2O$

(**b**) $(NH_4)_2HgCl_4\cdot H_2O$. The permittivities at 18°C are ϵ_a 7.2, ϵ_b 6.5, ϵ_c 22.3 at 3 Mc. There is also a marked anisotropy observed in the case of the potassium salt mentioned in (**a**). The temperature dependences of the dielectric behaviour are shown in Fig. 3. The sign of the temperature coefficient of the permittivity along each crystallographic axis of the ammonium salt is positive in the neighbourhood of the room temperature, but at lower temperatures the temperature coefficient of ϵ_a becomes negative. It may be

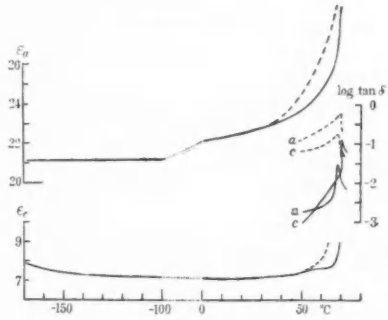

Fig. 3. The dielectric behaviour of $(NH_4)_2HgCl_4\cdot H_2O$. Samples are sandwiched in two mica foils in these cases. Full line-3 Mc, broken line—5 kc.

worth noticing that the negative sign of the temperature coefficient of the permittivity at low temperatures was also found in another ammonium salt, $(NH_4)_2CuCl_4 \cdot 2H_2O$.[2]

In ϵ-T diagram of this ammonium mercury (II) salt, a peak which is seen in the case of the potassium salt just below the dehydration temperature is not observed. But careful tracing of the ϵ-T curve suggests that such a peak may also exist so closely below the dehydration temperature that the peak can not be separated from the steep increase of ϵ in the neighbourhood of the dehydration temperature.

Results of X-ray and Thermal Investigations of $K_2HgCl_4 \cdot H_2O$

The change of the crystal structure is investigated by Laue patterns taken with the incident beam parallel to the *b*-axis at various temperatures (Table I). These results show that the crystal lattice is collapsing gradually above about 82°C. The Debye photographs of the initial and the final stages of 300 hours-heating are taken using Cu $K\alpha$ radiation with Ni-filter at various temperatures (Table II).

From these Laue and Debye photographs, it is concluded that the potassium salt gradually transforms from the low temperature form to the high temperature one above 82°C. The indices of the Debye patterns of this high temperature form are determined wholly in reference to the indices of the ordinary low temperature form, notwithstanding that the relative intensities of the Debye patterns of the high temperature form are essentially different from those of the low temperature one (Table V).

Table I

Structure change of $K_2HgCl_4 \cdot H_2O$ observed from Laue patterns

T(°C)	time(hour)	lattice
25	3	low temperature form
55	3	low (no change)
81	3	low (no change)
107	3	low (Laue spots weaken)
125	3	no spots, fiber patterns of KCl
155	(3)	Debye-rings of KCl only

The second column shows the time of exposure at the temperature given in the first column except the last case. The photograph of the last case was taken also for 3 hours-exposure after 300 hours-heating at 155°.

Table II

Structure change of $K_2HgCl_4 \cdot H_2O$ observed from Debye photographs

T(°C)	initial 10 hours	final 10 hours
25	low	low
60	low	low
75	low	low
80	low	—
82	—	low-high (mixed)
85	low	—
91	—	high (broad)
100	high (broad)	high
120	high (broad)	high (sharp)
128	—	high (sharp)
145	—	high (weak), KCl (strong)

Moreover, the dilatometric experiment using toluene as the dilatometer-liquid shows no discontinuity throughout this transition, whereas the case using mercury shows distinct bending of the dilatometric curve at about 82°. These results suggest that the fine powders of the high temperature form produced by the lattice breaking of the low temperature form are easily wetted by mercury but not by toluene, and there must exist a lattice transformation at about 82° without detectable volume change.

Besides these, the thermal analysis curve obtained by S. Seki and H. Chihara in this laboratory shows that there is no appreciable heat absorption at about the transition point but there are two peaks at 115° and 123°. In this experiment, the average rate of heating is 1.6° per minute and this rate is considerably faster than that in the case of the dielectric measurement. Therefore, the two peaks at 115° and 123° in the thermal analysis curve may be attributed to the latent heat of the delayed lattice transformation and those of the vaporization of the water liberated from the collapsing lattice and of the sublimation of mercuric chloride produced by the decomposition of this double salt respectively.

The microscopic observation of the surface after the partial dehydration at 120° shows numerous small pits distributed randomly on the *c*-plane and a few semi-cylindrical swellings along the *c*-axis on the *a*-plane. Moreover, in the course of the observation of the change of the optical properties with a polarizing microscope for the transparent thin plates, some stripes along the *c*-axis appear on the surface of the *a*-plane as the temperature rises and then the crystal collapses gradually, but many nuclei of dehydration are seen at the same time on the *c*-plane, and as the number of the nuclei increase,

the crystal plate loses its transparency. By the way, these partly dehydrated specimens are considerably hard and tough and they appear in white unglazed ceramic feature.

Discussion

(a) Anisotropy of the Room Temperature Permittivities. For the purpose of discussing the dielectric polarization of this rhombic crystal in the first place, the permittivity along each crystallographic axis is compared with the square of the refractive index for the corresponding axis (Table III).

TABLE III
REFRACTIVE INDICES FOR NaD[3] AND PERMITTIVITIES OF $K_2HgCl_4 \cdot H_2O$

n_a (α) 1.648	n_a^2 2.72	ε_a	6.7
n_b (γ) 1.699	n_b^2 2.89	ε_b	6.1
n_c (β) 1.678	n_c^2 2.82	ε_c	17.5

In this case, the maximum polarization in the optical frequency region is directed along its *b*-axis while that in the radio-frequency region is along its *c*-axis.

The crystal structure of the low temperature form of the potassium salt belongs to space group $Pbam$—V_h^1 and has a unit cell of $a=8.27$, $b=11.63$, $c=8.89$ kX containing four formula units.[4] There is a mirror plane perpendicular to the *c*-axis, therefore the dipoles of a pair of water molecules should be cancelling each other in the direction of the *c*-axis, and this cancellation is confirmed at a room temperature as a fixed four-proton system by the proton nuclear magnetic resonance absorption experiment using single crystals.[5] Consequently, the large polarization along the *c*-axis is mainly due to the atomic polarization of mercury which is surrounded by a less symmetrical chlorine octahedron and may be easily polarizable along the *c*-axis. In fact, the position of the mercury atom is 0.2 Å apart from the center of gravity of the chlorine octahedron (Fig. 4). Such an atomic

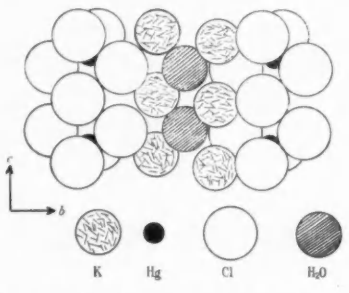

Fig. 4(a). Packing schema of the atomic arrangements in $K_2HgCl_4 \cdot H_2O$

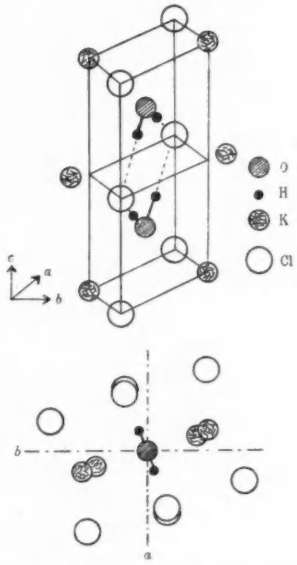

Fig. 4(b). The perspective and projection of the atomic arrangements around the pair of the water molecules in $K_2HgCl_4 \cdot H_2O$

polarization is somewhat analogous to that of the titanium atom in the ferroelectric barium titanate crystal.

In the case of the ammonium mercury (II) chloride monohydrate, the anisotropy of the permittivities, namely the far larger value of ε_c compared to those of ε_a and ε_b, may be attributed to the same cause as in the potassium salt.

(b) The High Temperature Modification of the Potassium Salt. Based on the facts that no detectable volume change is observed at the transition point, and also that the position as well as the indices of the X-ray reflections of the high temperature form coincide completely with those of the ordinary form, it may be concluded that the unit-cell dimensions of the high temperature form must be the same at the transition temperature as those of the low temperature form.

The analysis of the crystal structure of this high temperature form seems to be too difficult to determine precisely from the known data of the Debye photographs only. Fortunately, there are at least two clues for

3) P. Groth, "*Chemische Krystallographie*," Teil **1**, 360 (1906).
4) C. M. MacGillavry, J. H. de Wilde and J. M. Bijvoet, *Z. Krist.*, **100**, 212 (1938).
5) J. Itoh, R. Kusaka, Y. Yamagata, R. Kiriyama and H. Ibamoto, *J. Phys. Soc. Japan*, **8**, 233 (1953).

this crystal structure; one is the above invariableness of the lattice constants at the transition point, and the other the indefinite proportion of the water content in the high temperature form, i.e. the occupation of the possible interstitial positions of the lattice by the water molecules. From these considerations we have tried to determine the atomic arrangement of the high temperature form assuming that the corresponding space group is $Pbnm$—V_h^{16} and all chlorine atoms are in almost hexagonal close packing. The most probable crystal structure for the present among many possible models is gvien after successive trial and error approximations. The atomic coordinates and the relative intensities $I_{obs.}$, the squares of the structure factors $F^2_{cal.}$ of the Debye-patterns are shown in Tables IV and V respectively.

TABLE IV

ATOMIC PARAMETERS OF THE HIGH TEMPERATURE FORM OF $K_2HgCl_4 \cdot H_2O$[6]

$Pbnm$—V_h^{16}, a=8.3, b=11.6, c=8.9 Å, Z=4.

		x	y	z
Hg	(4c)	0.40	0.22	0.25
K(I)	(4a)	0.00	0.00	0.00
K(II)	(4b)	0.50	0.00	0.00
Cl(I)	(4c)	0.75	0.06	0.25
Cl(II)	(4c)	0.25	0.44	0.25
Cl(III)	(8d)	0.25	0.19	0.00

The structure principle of the high temperature form is that the mercury atom is surrounded by four chlorine atoms forming a deformed tetrahedron and the potassium atom by slightly deformed chlorine-octahedron. Strictly speaking, such a structure

TABLE V

INTENSITY RELATIONS OF DEBYE-PATTERNS OF $K_2HgCl_4 \cdot H_2O$

			low form		high form	
d (kX)		(hkl)	$I_{obs.}$	$F^2_{cal.}$	$I_{obs.}$	$F^2_{cal.}$
6.75		(110)	vs	0.4	m	0.
5.85		(020)	m	0.2	m	0.1
5.38		(111)	—	0.	s	0.7
4.85		(021)	—	0	m	0.1
4.45		(002)	w	0.1	w	0.1
4.35	$HgCl_2$	(001)	—	—	w-s	—
4.15		(200)	m	0.4	—	0.
3.91		(210)	—	0.	m	0.4
3.72		(112)	vs	1.0	—	0.
3.53		(022)	s	0.7	s	0.4
3.52		(130)				
3.38		(220)	vw	0.1	w	0.2
3.26		(131)	w	0.3	w	0.4
3.13	KCl	(200)	—	—	m-vs	—
3.05		(202)	s	1.0	—	0.
3.00	$HgCl_2$	(200)	—	—	vw-w	—
2.94		(212)	m	0.4	vs	1.0
2.93		(040)				
2.76		(041)	—	0.	m	0.4
2.76		(132)	—	0.1		
2.74		(140)	vw	0.2	—	0.1
2.69		(222)	vs	0.9	vw	0.4
2.69		(310)				
2.64		(301)	—	0.	—	0.4
2.58		(311)	—	0.	vw	0.1
2.52		(123)	—	0.	—	0.4
2.50		(320)	vw	0.2	—	0.
2.43		(042)	w	0.5	—	0.
2.40		(321)	—	0.	w	0.6
2.38		(240)	w	0.4	—	0.
2.25		(330)	vs	1.2	vs	1.0
2.23		(150)				
2.23		(004)				
2.23		(223)				
2.21	KCl	(220)	—	—	vw-w	—
2.18		(322)	—	0.	w	0.5
2.17		(151)	—	0.		
2.11		(114)	m	1.2	vvw	0.
2.10		(242)				
2.02		(303)	s	0.7	w	0.7
2.02		(250)				
2.02		(401)				
2.02		(340)				
1.95		(420)	m	0.9	w	0.4
1.94		(060)				

6) *cf.* Internationale Tabellen zur Bestimmung von Kristalstrukturen, (1938).

without the water molecule is not a high temperature modification of the monohydrate and the remaining water molecules in the lattice are probably in some interstitial positions. From the existence of the reflection of (110) which is a forbidden reflection for the high temperature space group, it will be concluded that in the high temperature form after the phase transition there remain also in several places the tunnel structures parallel to the c-axis, and the water molecules enclosed in these tunnels may have some chances of forming chain-like associations parallel to the c-axis within an adequate temperature range.

(c) The Structure of the Ammonium Mercury (II) Chloride Monohydrate, $(NH_4)_2HgCl_4 \cdot H_2O$. The isomorphism of the ammonium salt and the potassium salt has been confirmed by us structurally by means of X-ray methods. The ammonium salt has a unit cell of the dimensions a=8.50, b=11.97, c=9.19 Å (Cu $K\alpha$=1.542 Å) containing also four formula units. The ammonium salt is so sensitive to moisture that it is difficult to keep the crystal sample without lattice collapsing at just below the dehydration tem-

perature for several hours necessary to obtain the Debye photograph. Therefore, it could not be decided whether or not the hign temperature form of $(NH_4)_2HgCl_4 \cdot H_2O$ exists in a temperature range just below the dehydration point.

(d) The Temperature Dependences of the Permittivities. Now it is to be discussed what is the cause of the anomalous dispersion which appeared in $K_2HgCl_4 \cdot H_2O$ along the *c*-axis above the transition temperature. The result of the X-ray analysis of the low temperature form shows that there is a characteristic tunnel structure which contains water molecules only. This tunnel is strangulated by the surrounding atoms, consisting of a train of cocoon-shaped spaces with narrow and wide passages alternately. Water of crystallization in such spaces may be looked upon as a zeolitic water, but at room temperatures the fast that the orientations of the water molecules are fixed in the crystal lattice is confirmed. Moreover, there are no marked dispersions in the permittivity-temperature diagrams below the transition point 82° for the practically perfect crystal. Thus it may be concluded that the water molecules in the crystal lattice of the low temperature form are not movable in the whole range of temperatures below the transition point, this water of crystallization being not typically zeolitic.

The phase transition proceeds gradually and the atomic displacements of the chlorines are the smallest and those of the mercuries the largest among the three sorts of atoms, chlorine, potassium and mercury. Besides these, most of water molecules diffuse into the newly constructed lattice and take some suitable interstitial positions, but some of water molecules remain in the remnants of the tunnel structure as described in (**b**). The water molecules confined in these closed capillaries parallel to the *c*-axis will have some chances of chain-like associations of the water dipoles as the lattice loosens moderately when the temperature is maintained in an adequate range. Thus the high ϵ_c appears in consequence of the formation of chain-like clusters of the water dipoles parallel to the *c*-axis and not of the independent simple rotation of the water dipoles. The higher the temperature, the more violent the thermal motion and the more such clusters of water molecules will dissociate. Besides these, the dehydration through the collapsing lattice will become remarkable. The dissociation of the dipole clusters and the diminution of the numbers of the water molecules both cause the dielectric polarization to fall down above 110° as the experiment shows.

Based on this consideration, the changes of ϵ_c at three constant temperatures in the anomalous temperature region may be explained as follows. The first peak on the curve at 82.5°C may be due to the chain-like association of the water molecules enclosed in some original tunnel-structures which have probably some sort of lattice defects of their atomic arrangements. As the lattice transformation proceeds slowly at the constant temperature, these original tunnel-structures will be obstructed gradually and then the chance of the association will be diminished. Therefore, the polarization due to such dipole clusters will fall down, giving a peak of maximum polarization as seen in the figure (Fig. 2). However, in the course of the rearrangement of the atoms, the original tunnel-structures may remain in several places containing water molecules. As this newly constructed lattice is loosened gradually again, these water molecules which have had no chance of dipole association up to this stage owing to the original narrow passages of the tunnel-structure will be able to pass through it and may have some chances of association. Therefore, the dielectric polarization along this direction of the tunnel-structure will rise again. However, these enclosed water molecules may escape rather easily through the loosening lattice and then the polarization will diminish gradually in progress of time. Thus there appears the second peak as seen in the figure. The change at 94° or 102.5° may be explained in a similar way. At such higher temperatures, the transition proceeds rather quickly and the two peaks as seen in the process at 82.5° will fuse in one, and the saddle-shaped fall between two peaks will not be observable in either cases at 94° or 102.5°.

In $(NH_4)_2HgCl_4 \cdot H_2O$, the existence of the high temperature form is not certain as mentioned in (**c**). But the analogous feature of the permittivities below the dehydration temperature may be explained in the same way as in the case of the potassium salt.

The dielectric behaviour and the problem of the zeolitic water of crystallization of potassium tin (II) chloride monohydrate, $K_2SnCl_4 \cdot H_2O$, of which structure is similar to the mercury salts dealt with in the present paper, will be reported in the following paper, Part III.

Department of Chemistry, Faculty of Science, Osaka University, Nakanoshima, Osaka

Dielectric Behaviour of Hydrated Crystals. III. Potassium Tin (II) Chloride Monohydrate and Barium Nitrite Monohydrate[1]

By Ryôiti KIRIYAMA and Hideko IBAMOTO

(Received October 10, 1953)

Introduction

The water of crystallization in potassium mercury (II) chloride monohydrate, $K_2HgCl_4 \cdot H_2O$, which is apparently zeolitic from the view point of the atomic arrangement in its crystal, is fixed tightly in the lattice and shows no orientation polarization of its dipole at a room temperature as reported in the previous paper.[2] The crystal structure of potassium tin (II) chloride monohydrate, $K_2SnCl_4 \cdot H_2O$ closely resembles to that of $K_2HgCl_4 \cdot H_2O$ and in both crystals, a pair of the water molecules which are crystallographically equivalent are enclosed in a cocoon-shaped space facing each other. Brasseur and Rassenfosse who analysed the crystal structure of $K_2SnCl_4 \cdot H_2O$ stated that the water of crystallization is zeolitic based on its continuous dehydration with temperature.[3] It is worth while to decide whether or not the water of crystallization of this crystal is truly zeolitic from the view point of the dielectric behaviour of single crystals as done on other salt hydrates previously reported by the present authors.[2,4]

Although the crystal structure of barium nitrite monohydrate, $Ba(NO_2)_2 \cdot H_2O$ has never been fully analysed, the position of the barium ion has been determined. From the consideration based on the corresponding space group of this crystal structure and the position of the barium ion, it was presumed that the water molecule of this monohydrate is enclosed in a tunnel structure coming from the hexagonal spiral configuration of the lattice and that the water is probably zeolitic.[5] Therefore, it is also interesting to investigate the behaviour of the dielectric properties of this crystal from the standpoint of the dipole orientation and to compare the result with those of the other related crystals.

Crystal, Specimen and Equipment

Transparent, large, single crystals of $K_2SnCl_4 \cdot H_2O$ could not be obtained until now owing to the fact that the effective velocity of crystal growth is exceedingly small. Thus usual crystals exhibit milky white appearance, are more brittle than the transparent ones obtained by us and contain more or less inclusions of the saturated solution between the bundle-shaped fragments parallel to the *c*-axis.

We have succeeded in obtaining these transparent crystals suitable for dielectric measurements (the area perpendicular to the crystallographic axes should be larger than $10 \times 10\,mm^2$) by careful regulation of the temperature of the water-thermostat and the composition of the aqueous solution of this double salt. The composition was maintained usually in excess of the stoichiometric amount of potassium chloride. Besides these, the solution contained a small amount of hydrochloric acid and several grains of metallic tin for the purpose preventing the stannous ion from oxidation. The time required was more than two months.

Frequently, translucent and opalescent crystals were obtained, probably because of a small fluctuation of the temperature of the thermostat or a slight deviation of the composition of the solution. Such crystals have also been investigated for the purpose of comparing the dielectric behaviour of the transparent crystal with that of this translucent one.

Barium nitrite was prepared from double decomposition of barium chloride and sodium nitrite or barium chloride and silver nitrite. The large, transparent, yellow-coloured, single crystal of barium nitrite monohydrate grew up easily from the seed crystal in its aqueous solution. The obtained crystal has the shape of a hexagonal prism with a pyramidal top, but belongs to the class of hexagonal trapezohedron, 62-D_3; as the X-ray data show. Colourless crystal could not be obtained and the experiment has been performed using these yellow-coloured crystals.

Good crystals have been selected by a polarizing microscope beforehand, and the specimens for the dielectric measurements are made by cutting and grinding these crystals and pasted by tin-foils with vacuum-grease.

The equipment is the same as those in the previous papers.[2,4]

1) Parts of this investigation were separately read before the annual meeting of the Crystallographic Society of Japan in May, 1950, at that of the Chemical Society of Japan in April, 1951, and at the Second Congress of the International Union of Crystallography at Stockholm in July, 1951.

2) Part II: R. Kiriyama and H. Ibamoto, This Bulletin, **27**, 317 (1954).

3) H. Brasseur and A. de Rassenfosse, *Z. Krist.*, **101**, 389 (1939).

4) Part I: R. Kiriyama and H. Ibamoto, This Bulletin, **27**, 32 (1954).

5) A. Ferrari and L. Cavalca, *Periodico Mineral*, (Rome), **17**, 125 (1948); *Structure Reports* for 1947–1948, Vol. **11**, 355.

Result

(a) **$K_2SnCl_4 \cdot H_2O$**. The permittivities of this rhombic crystal are as follows: $\epsilon_a = 7.3$, $\epsilon_b = 10.1$, $\epsilon_c = 10.0$ (at 15°C; at 5 kc and 3 Mc). There are no dielectric dispersion at a room temperature on the transparent crystals, but a considerable dispersion along the *c*-direction and small dispersion along the *a*-direction are observed with the translucent crystals. Moreover, of the milky-white, opaque crystals the permittivities can not be measured in every direction of the principal axes owing to remarkable conduction.

Thus we have performed further measurements using the transparent crystals throughout the present experiment and the results for somewhat imperfect crystals will be quoted only in comparison with those for the perfect, that is, the transparent ones.

The temperature dependences of the permittivities and the dielectric losses are plotted in Fig. 1. While the values of permittivities

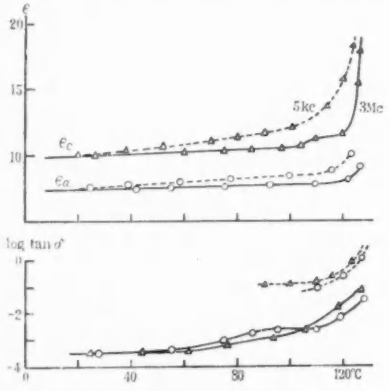

Fig. 1. The temperature dependences of the dielectric behaviour of $K_2SnCl_4 \cdot H_2O$.

are found reproducible in every repeated experiment, the temperature at which considerable dielectric losses appear becomes somewhat lower for every successive experiment. There are distinct dielectric dispersions at higher temperatures, a little along the *a*-axis and considerable along the *c*-axis, between 3 Mc and 5 kc as seen in Fig. 1.

The temperature coefficients of the permittivities $\frac{1}{\epsilon}\left(\frac{d\epsilon}{dT}\right)$ in the temperature range between 20° and 100°C are:

along *a* 6×10^{-4} (3 Mc), 14×10^{-4} (5 kc);
along *c* 6×10^{-4} (3 Mc), 23×10^{-4} (5 kc).

(b) **$Ba(NO_2)_2 \cdot H_2O$**. The room temperature permittivities at 3 Mc and 5 kc are: $\epsilon_a = 8.1$, $\epsilon_c = 7.4$. These values are equal in the limit of experimental error to those at 3 Mc previously reported.[5]

Their temperature coefficients are as follows: along *a* 3×10^{-4}, along *c* 6×10^{-4} in the temperature range between −170° and 80°C.

Up to about 90°C where the dehydration occurs, the permittivities increase monotonously and above 90° the slope of the ϵ-T curve becomes a little steeper than below and at about 100° the values increase rapidly owing to the surface conduction originated by the dehydrated water molecules. The temperature dependence at 3Mc, as an example, is shown in Fig. 2.

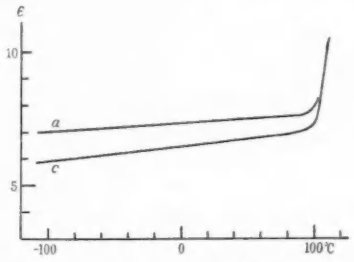

Fig. 2. The temperature dependences of the permittivities of $Ba(NO_2)_2 \cdot H_2O$.

Discussion

(a) **$K_2SnCl_4 \cdot H_2O$**. The anisotropy of the permittivities at room temperature is rather small and the direction of the maximum polarization is in the direction of the *b*-axis and not the *c*-axis. The refractive indices of this crystal were measured by us by means of the minimum deviation method using the prisms obtained by cutting and polishing the transparent, single crystals. The indices and other optical properties are listed in Table I.

TABLE I

OPTICAL CONSTANTS OF $K_2SnCl_4 \cdot H_2O$

Optically negative, axial plane—*b* (010), acute bisectrix—*a*-axis, (*a*-axis—*X*, *b*-axis—*Y*, *c*-axis—*Z*)[7]

	589mμ	546mμ	436mμ	ε
n_a (α)	1.672	1.685	1.732	7.3
n_b (β)	1.693	1.707	1.752	10.1
n_c (γ)	1.749	1.757	1.798	10.0

It is probable that the direction of the maximum optical polarization coincides with that of the crystallographic *c*-axis because of the dense arrangement of chlorine atoms forming $(SnCl_4)_\infty$ chain along the *c*-axis. However, in spite of its chain-like arrangement of $(HgCl_4)_\infty$ along the *c*-axis, the crystal of $K_2HgCl_4 \cdot H_2O$ does not direct the

maximum optical polarization to that axis.[2] Moreover, it is noticeable that the maximum dielectric polarization of this tin salt occurs in the direction of the *b*-axis and not in the *c*-axis whereas in the case of the mercury salt its ϵ_c has much larger value than the others, ϵ_a and ϵ_b.

According to the analyses of the crystal structures, the mercury salt belongs to space group $Pbam$-V_h^9 but the tin salt to $Pbnm$-V_h^{16} in spite of the very similar atomic arrangements.[8,3] However, the results of the proton nuclear magnetic resonance absorption experiments of these crystals suggest that the space group of the tin salt is not *Pbnm* but *Pbam* which is identical with that of the mercury salt.[9] Therefore, it is confirmed that these two salts are not only isomorphous morphologically but also isostructural with each other.

The main difference of the atomic arrangements of these crystal structures is that the tin atom is surrounded by six chlorine atoms in a deformed octahedron; four are near and two in horizontal are distant, taking the *c*-axis as the vertical direction, while the chlorine octahedron surrounding the mercury atom in the mercury salt is much more deformed than that of the tin salt, namely the almost horizontal two chlorines are near, the other two are remote and the remaining two are more distant (Fig. 3).

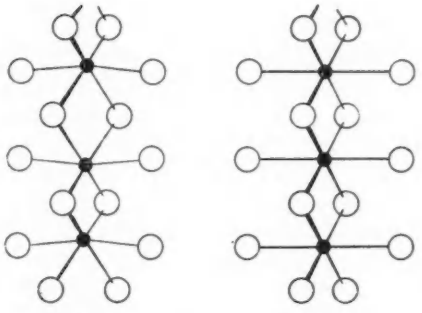

$(HgCl_4)_\infty$ $(SnCl_4)_\infty$

Fig. 3. The difference of the atomic arrangements between $(HgCl_4)_\infty$ and $(SnCl_4)_\infty$ chain contained in $K_2HgCl_4 \cdot H_2O$ and $K_2SnCl_4 \cdot H_2O$ respectively.

From these different metal-chlorine distances, it may be concluded that, on the one hand, the two long horizontal Sn-Cl bonds in the $SnCl_6$-octahedron are almost purely ionic and the remaining four are much more covalent than these, and, on the other hand, two short horizontal Hg-Cl bonds in the deformed $HgCl_6$-octahedron are much more covalent than the remaining four Hg-Cl bonds which may be ionic. The electron cloud of a chlorine atom in such a partially ionic, covalent bond as in the oblique Sn-Cl or in the horizontal Hg-Cl may be much more polarizable than that in the purely ionic metal-chlorine binding. Owing to this polarizing effect, the electronic polarization of the tin salt in the vertical direction will become much larger than that expected simply from the dense arrangement of chlorine atoms along the *c*-axis in the form of $(SnCl_4)_\infty$-chain. On the contrary, the electron cloud of the chlorine atoms in the mercury salt may be more polarizable in the horizontal Hg-Cl direction and less in the oblique ones for light waves. As the result of this polarizing effect, the electronic polarization in the horizontal plane (the maximum refractive index γ is equal to 1.699, which lies along the *b*-axis) may become slightly superior to that in the direction perpendicular to this plane (along *c*, $\beta = 1.678$) overcoming the polarization effect of the dense arrangement of the chlorine atoms in $(HgCl_4)_\infty$-chain parallel to the *c*-axis. These are the principal causes of the essential difference of the optical anisotropies between two isostructural crystals.

By the way, it has been recognized generally that the more ionic the bond nature, the larger the atomic polarization or the infrared polarization. From this point of view, it may be assumed that the value of the atomic polarization of the tin atom in the tin salt may be maximum in the direction of the *b*-axis along which the largest component of the ionic Sn-Cl binding is directed. Owing to this large atomic polarization, the direction of the maximum deformation polarization will tend to the *b*-axis overcoming the considerably large electronic polarization along *c*. On the contrary, in the case of the mercury salt, the large atomic polarization of the mercury atom along the *c*-axis in the deformed chlorine-octahedron will contribute greatly to the deformation polarization as discussed in the previous paper[2] and the electronic polarization perpendicular to this axis will make less contribution to the whole deformation

6) R. Kiriyama, *Kagaku*, **17**, 239 (1947) (in Japanese).
7) P. Groth, *Elemente d. physik. chem. Krystallographie*, 171 (1921).
8) C. M. MacGillavry, J. H. de Wilde and J. M. Bijvoet, *Z. Krist.*, **100**, 212 (1938).
9) J. Itoh, R. Kusaka, Y. Yamagata, R. Kiriyama and H. Ibamoto, *J. Phys. Soc. Japan*, **8**, 293 (1953).

polarization, then the direction of the maximum deformation polarization will agree with the c-axis.

The temperature dependences of the permittivities of this tin salt are plotted in Fig. 1, where ϵ_b is omitted as its curve runs almost precisely on that of ϵ_c especially below 100°C. There are distinct dispersions of the permittivities above the room temperature, but there is no anomalous behaviour such as seen in the mercury salt, and the permittivities and the dielectric losses increase monotonously until the dehydration occurs, and at the dehydration temperature the permittivities increase suddenly as the ordinary hydrated salts.[4]

The result of the thermal analysis shows that there are no peaks up to the dehydration temperature 127°C, and this temperature is fairly coincident with that of the sudden increase of the permittivities 125°C. Moreover, the X-ray oscillation photographs taken at various temperature show that there are no structural changes between a room temperature and 125°C.

Thus we may conclude that the water molecules at the cocoon-shaped interstitial positions can move slightly as the temperature rises above about 105°C. This temperature corresponds to the point of inflection on the ϵ_c-T curves at 3 Mc (Fig. 1). And it is also concluded that from the temperature dependence and the frequency dependence of the permittivities and the dielectric losses the potential barrier against the dipole orientation of the water molecules will be lowered gradually as the temperature rises up to 125°C. And at this temperature the crystal lattice begins to collapse and then the dehydration through the breaking lattice takes place intensely.

In the case of the translucent crystal, the permittivities and the dielectric losses are much larger than those of the perfect, transparent crystal, especially in the c-direction. It may be also concluded that there are some lattice defects and the water molecules have some chances to form chain-like molecular clusters in the c-direction as assumed in the case of the high temperature form of $K_2HgCl_4 \cdot H_2O$.[2] The larger values of the permittivities along the c-axis and the irreproducibillity of them in the translucent crystal of the tin salt may be explained by this model. The remarkable conductivity found in the measurement for the opaque crystal of the tin salt may be attributed to the electrolytic conduction of the saturated solution contained in crystals as the form of liquid inclusion.

(b) $Ba(NO_2)_2 \cdot H_2O$. There are no appreciable dielectric dispersions up to the dehydration temperature in barium nitrite monohydrate. Moreover, the proton magnetic resonance absorption experiment using single crystals carried out by us shows that the water molecules are fixed in the crystal lattice at room temperature and no indications of the protonic movements in the lattice can be detected.[10] Thus, we may conclude from the results of the dielectric measurement that the water of crystallization in such monohydrates as $K_2HgCl_4 \cdot H_2O$, $(NH_4)_2HgCl_4 \cdot H_2O$ and $K_2SnCl_4 \cdot H_2O$ or $Ba(NO_2)_2 \cdot H_2O$ is not movable in the open space of the crystal lattice in spite of the zeolitic feature presumed from the position of the water-oxygen but that it orientates itself into a fixed direction stabilizing the crystalline field by its dipole moment. However, it is noticeable that the imperfect crystals of these substances have often tunnel-like capillaries and the water molecules enclosed in these capillaries will show various kinds of anomalous dielectric behaviour even at room temperature. From these considerations, it will be rather important to reexamine the behaviour of the so-called "zeolitic water" in the hydrated crystals, which might have been misjudged owing to some imperfections of their crystals used for the thermal or dielectric experiments.

In conclusion the authors wish to express their thanks to Prof. I. Nitta for his encouragent and suggestions during this work. Their thanks are also due to Dr. S. Seki and Mr. H. Chihara for their kindness in carrying out the thermal analysis experiment. The expense of this work was partly defrayed by the Scientific Research Grant from the Ministry of Education.

Department of Chemistry, Faculty of Science, Osaka University, Nakanoshima, Osaka

10) J. Itoh, R. Kusaka and R. Kiriyama, *J. Phys. Soc. Japan* (in press).

Studies on the Condensation Polymers of Aromatic Acetoxy Carboxylic Acids

By Hajime HASEGAWA

(Received December 2, 1953)

Introduction

Much work has been done by many investigators on the syntheses of polyesters, especially on the polymers of aliphatic hydroxy carboxylic acid and the copolymers of mono- and di-basic carboxylic acids and glycols. But, as for the syntheses of the polymers of aromatic hydroxy carboxylic acid, no systematic study has been made, although Einhorn[1] made the dimer of salicylic acid by heating with phosphorus oxychloride and Anschütz[2] made the tetramer of it by the same method. This method was used in the present research. In the case of salicylic acid, the formation of the high polymer was not observed. However, in the case of *o*-acetoxy benzoic acid (aspirin), the resin-like substance was obtained. It was considered to be the polymer of salicylic acid, for the violent evolution of acetic acid was observed throughout the reaction with the marked increase of the molecular weight. Starting from this result, the author obtained the high polymers of various kinds of aromatic acetoxy carboxylic acid by heating. The process of the formation of polymers was followed by determining the molecular weight of the resins formed, at several stages of the reaction. From the data obtained, the effect of the position of acetoxy group and carboxyl group on the reactivity of the monomers, was considered. In the case of acetamino carboxylic acids, the formation of the polymer of the high molecular weight by heating was not observed.

Experimental

The monomers used for this research were prepared by the following procedures.

I) *o*-Acetoxy benzoic acid. Aspirin for medical use was purified. M. P. 135°C.

II) *m*-Acetoxy benzoic acid[3]. *m*-Hydroxy benzoic acid[4] was acetylated, using acetic anhydride. M. P. 131°C.

III) *p*-Acetoxy benzoic acid[5] was prepared by the action of acetic anhydride on *p*-hydroxy benzoic acid[6] which was synthesized from salicylic acid. M. P. 182°C.

IV) 3-Acetoxy naphthoic acid-(2)[7] was synthesized from 3-hydroxy naphthoic acid-(2). M. P. 174°C.

V) 2, 4-Diacetoxy benzoic acid[8]. β-Resorcylic acid[9] made from resorcinol by Kolbe-Schmitt method was acetylated. M. P. 134°C.

VI) 3, 5-Diacetoxy benzoic acid[10] was made by acetylating 3, 5-dihydroxy benzoic acid[11] by acetic anhydride. M. P. 155°C.

VII) *o*-Acetamino benzoic acid[5] was made by acetylating *o*-amino benzoic acid. M. P. 180°C.

VIII) *p*-Acetamino benzoic acid[12] was prepared by the action of acetyl chloride on *p*-amino benzoic acid. M. P. 253°C.

IX) 2-Acetoxy-4-acetamino benzoic acid. PAS for medical use, was acetylated by acetic anhydride. The product was recrystallized from hot water which contained a small quantity of alcohol, and was identified with the diacetyl compound of PAS by measuring the acetyl value of the product. Yield-70% of the theoretical amount. M. P. 184°C, with decomposition.

The condensation of the monomers shown above was carried out as follows; 10 g. of monomers were heated in a hard test tube of 1.5 cm. diameter during a definite time at the suitable temperature for each compound, which was listed in Table I. The acetic acid evolved in this reaction was carried off on the outside of a test tube by a slow current of dry carbon dioxide.

o-Acetoxy benzoic acid was chosen as the standard substance for comparison. Hence the process of the reaction of this compound was observed in detail at three different temperatures, 170°C, 240°C and 240°C. This monomer reacted smoothly at these temperatures. Contrary to this compound, *m*-acetoxy benzoic acid, *p*-acetoxy benzoic acid and 3, 5-diacetoxy benzoic acid did not react at 200°C. Therefore, the reaction temperature of 240°C was chosen for these compounds. *p*-Acetamino benzoic acid was heated at 300°C, because it reacted smoothly at the higher temperature than its melting point. The polymerization of the other compounds was carried out at two different temperatures (200°C and 240°C), as shown in Table I.

The molecular weight of the resins synthesized in this way was measured by the cryoscopic method using nitrobenzene as the solvent for the

1) A. Einhorn, *Ber.*, **34**, 2352 (1901).
2) R. Ansuchütz, *Ber.*, **25**, 3506 (1892).
3) A. Heintz, *Ann.*, **153**, 340 (1870).
4) H. Offermann, *Ann.*, **280**, 6 (1894).
5) A. Kauffmann, *Ber.*, **42**, 3482 (1903).
6) H. Kolbe, *J. prakt. Chem.*, (2) **11**, 24 (1875).
7) H. Gradenwitz, *Ber.*, **27**, 2624 (1894).
8) M. Bergmann, *Ber.*, **52**, 379 (1919).
9) A. Clibbens, *J. Chem. Soc.*, **107**, 1494 (1915).
10) F. Mauthner, *J. prakt. Chem.*, **136**, 205 (1933).
11) L. Barth, *Ann.*, **159**, 222 (1871).
12) G. Heller, *Ber.*, **43**, 2574 (1910).

TABLE I

Monomer	Reaction temp. (°C)	Color	Solubility in nitrobenzene	Transparency
o-Acetoxy benzoic acid	170	CL→CL	+	
	200	CL→LB	+	TR
	240	P→B	+	
m-Acetoxy benzoic acid	240	B→B	+	TR
p-Acetoxy benzoic acid	240	W	−	OP
3-Acetoxy naphthoic acid-(2)	200	LB→B	+	TR
	240	B→BB	+	
2, 4-Diacetoxy benzoic acid	200	CL→OY	+	TR
	240	OY→R	+	
3, 5-Diacetoxy benzoic acid	240	LB(F)→B(F)	+	TR
o-Acetamino benzoic acid	200	OY	−	TR
	240	R→BB	−	
p-Acetamino benzoic acid	300	LY	−	OP
2-Acetoxy-4-acetamino benzoic acid	200	RB→BB	−	STR

Color; CL=Colorless, LB=Light brown, P=Pink, B=Brown, W=White, BB=Brownish black, OY=Orange yellow, R=Red, LY=Light yellow, RB=Reddish brown, (F)=Fluorescence.
Solubility; +: Soluble, −: Insoluble.
Transparency; TR=Transparent, OP=Opaque, STR=Semitransparent.

polymers of acetoxy compounds, and phenol as the solvent for the polymers of acetamino compounds.

Results and Discussion

i) **The Properties of Polymers.**—With the increase of the molecular weight, the colors of synthetic resins obtained from *o*-acetoxy benzoic acid, *m*-acetoxy benzoic acid, 3-acetoxy naphthoic acid-(2), 2, 4-diacetoxy benzoic acid and 3, 5-diacetoxy benzoic acid change from colorless to brown (Table I), and their hardness increases, and the solubility decreases. Most of them are soluble in nitrobenzene, phenol and pyridine, but are insoluble in alcohol, ether, chloroform and carbon tetrachloride. The resins of the lower molecular weight slightly dissolve in benzene and acetone, but, with the increase of the molecular weight, they become insoluble in these solvents.

The polymers obtained from *p*-acetoxy benzoic acid and *p*-acetamino benzoic acid were opaque solids and did not dissolve in any solvents. The resins obtained from *o*-acetamino benzoic acid and 2-acetoxy-4-acetamino benzoic acid dissolved in phenol and cresol, but did not dissolve in other solvents.

The polymer (A in Table II) of 2, 4-diacetoxy benzoic acid obtained by heating at 240°C during 4 hrs., and the polymer (B in Table II) of 3, 5-diacetoxy benzoic acid obtained by heating 240°C during 6 hrs. are slightly soluble in nitrobenzene, phenol and pyridine, and the remaining part swells greatly. The degrees of swelling are given in Table II.

TABLE II

DEGREE OF SWELLING (% in volume).

Solvent	Phenol	Nitrobenzene	Pyridine
Polymer (A)	600	430	Soluble
Polymer (B)	280	300	300

ii) **The Change of Molecular Weight.**—The

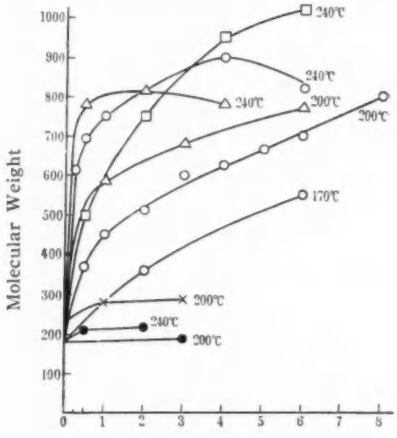

○ *o*-Acetoxy benzoic acid
□ *m*-Acetoxy benzoic acid
△ 3-Acetoxy naphthoic acid-(2)
● *o*-Acetamino benzoic acid
× 2-Acetoxy-4-acetamino benzoic acid

Fig. 1

data obtained by measuring the molecular weight in the course of polymerization are shown in Fig. 1 and Fig. 2.

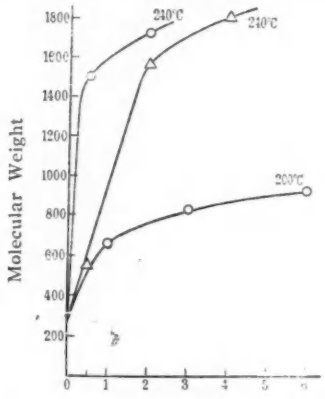

○ 2,4-Diacetoxy benzoic acid
△ 3,5-Diacetoxy benzoic acid
Fig. 2

In these figures, the important points will be the maximum value (p in Table III) of the degree of polymerization (molecular weight of the polymer/molecular weight of its monomer), which can be obtained in the course of reaction, and the reaction velocity (V in Table III) at t (time in hour)=0, which is expressed in the ratio of the change of the degree of polymerization to the change of hour. For example, these values of *o*-acetoxy benzoic acid are calculated as follows:

$$P = 890/180 = 5.0$$

$$V(200°C) = \frac{(370/180)-1}{1/2} = 2.1$$

As seen from this Table, there is some relation between the chemical structures of monomers and the values of V. Namely, almost the same value of V are observed for *o*-acetoxy benzoic acid and 2,4-diacetoxy benzoic acid. Furthermore, the value of V for *m*-acetoxy benzoic acid is almost the same as the value of V for 3,5-diacetoxy benzoic acid, which is smaller than the value of V for *o*-acetoxy benzoic acid and 2,4-diacetoxy benzoic acid at 240°C. This fact tells us that the monomers, which have the acetoxy group at the ortho-position to the carboxyl group, react faster than the monomers having the acetoxy group at the meta-position to the carboxyl group. But the value of P of *m*-acetoxy compounds is larger than the value of P of the corresponding *o*-acetoxy compounds. Therefore, it seems that *m*-acetoxy benzoic acid and 3,5-diacetoxy benzoic acid are suitable for the preparation of the high polymer of aromatic acetoxy carboxylic acid. As for the value of V of *p*-acetoxy benzoic acid, it cannot be obtained in this research. Therefore, the stability of *p*-acetoxy benzoic acid cannot be discussed in comparison to *o*-acetoxy compounds. However, considering the fact that *p*-acetoxy benzoic acid does not react at 200°C, it seems that *o*-acetoxy compounds react faster than *p*-acetoxy benzoic acid[13]. As for the values of V and P of 3-acetoxy naphthoic acid-(2), they are less than those of *o*-acetoxy benzoic acid. Contrary to the case of acetoxy carboxylic acid, the values of V and P of acetamino compounds are very small. The fact that the color of the product changes rapidly to dark brown may be due to the decomposition of the polymer formed. Therefore, the high polymer will not be obtained from aromatic acetamino carboxylic acid.

TABLE III

Monomer	Reaction temp. (°C)	V	P	Molecular weight
o-Acetoxy benzoic acid	170	0.5	5.0	895
	200	2.1		
	240	9.7		
m-Acetoxy benzoic acid	240	3.6	5.6	1016
3-Acetoxy naphthoic acid-(2)	200	1.6	3.5	811
	240	4.7		
2,4-Diacetoxy benzoic acid	200	1.7	7.2	1720
	240	10.6		
3,5-Diacetoxy benzoic acid	240	3.0	7.7	1820
o-Acetamino benzoic acid	200	0.03	1.2	220
	240	0.4		
2-Acetoxy-4-acetamino benzoic acid	200	0.2	1.2	287

The polymers (A and B in Table II) obtained from 2,4-diacetoxy benzoic acid and 3,5-diacetoxy benzoic acid swell greatly as shown above. These monomers have three functional groups. Therefore, it will be reasonable to assume that their polymers swell, owing to the net work structure formed by the cross linkage, and also their high

13) Y. Tsuzuki, This Bulletin, **5**, 282 (1950).

molecular weight. 2,4-Diacetoxy benzoic acid and 3,5-diacetoxy benzoic acid will be useful to the formation of the net work structure in the polymer.

Summary

We carried out a fundamental research for synthesizing high polymers of aromatic acetoxy carboxylic acid, and observed the influence of the position of the acetoxy group, and found that *m*-acetoxy benzoic acid, 3,5-diacetoxy benzoic acid and 2,4-diacetoxy benzoic acid, are superior as the monomer for the preparation of high polymers of aromatic acetoxy carboxylic acid.

I wish to express my hearty thanks to Prof. K. Yamamoto and Mr. K. Shibata for their kind guidance and valuable suggestions in this study.

Department of Applied Chemistry, Faculty of Science and Engineering, Waseda University, Tokyo

The Thermal Polymerization of Acetylene. On the Formation of Cyclooctatetraene

By Zenichiro KURI

(Received January 26, 1954)

Introduction

It has been known for a long time that acetylene is readily but intricately polymerized on heating,[1-4] giving a complex of unsaturated hydrocarbons as well as benzene.[2,10] Nevertheless, in the flow method at the suitable velocity, the propagation stops up to the tetramer and all the products obtained are volatile.[5] On the mechanism of the polymerization Pease, Taylor, and others[5,6,9,10,11] have pointed out from the over-all reaction rate that acetylene reacts in the bimolecular way and so the dimerization of acetylene determines the over-all rate.

On the structure of dimer produced in the primary acts of the photopolymerization of acetylene, Kemula[7] supposed that it would be vinylacetylene. Mignonac[8] got the product consistent with C_4H_4 in the thermal polymerization, but said no word about what it was. Recently Bergman,[12] supposing vinylacetylene to be the dimer, explained the Reppe reaction forming cycloöctatetraene (C.O.T.) under the high pressure.

Some experiments were performed assuming the dimer to be vinylacetylene, and the results were as follows;[13] if one uses a mixture of vinylacetylene and acetylene in the reaction, benzene constituting the main product in the polymerization decreases and also, when making C.O.T. by the catalytic method with high pressure, one can not get any C.O.T. if one uses vinylacetylene as the starting material.

Here, supposing cyclobutadiene (C.B.D.) to be the dimer in the thermal polymerization as well as in the photopolymerization[14] we investigated the thermal polymerization anticipating the formation of C.O.T. by dimerization of C.B.D. and we have obtained C.O.T. as expected.

Experiments

I. Thermal Reactivities and Analysis of C.O.T.

a) Thermal Changes of C.O.T. C.O.T., being a cyclic conjugated double-bonded compound, has unlike benzene little resonance energy and much reactivity.[15,16] It is so labile thermally and photochemically that it causes decomposition, polymerization, and isomerization at high temperatures.[17,18]

1) W. Bone, *J. Chem. Soc.*, **93**, 1197 (1908).
2) N. Zelinsky, *Ber.*, **57**, 264 (1924).
3) H. W. Walker *J. Phys. Chem.*, **31**, 970 (1927).
4) E. Hague, *J. Chem. Soc.*, 378 (1929).
5) R. N. Pease, *J. Am. Chem. Soc.*, **51**, 3470 (1929).
6) P. Schlaepfer and M. Brunner, *Helv. Chim. Acta*, **13**, 1125 (1930).
7) W. Kemula and S. Mrazek, *Z. phys. Chem.*, B**23**, 358 (1933).
8) G. Mignonac and E. Ditz, *C. r.*, **199**, 367 (1934).
9) H. Austin Taylor and A. V. Hook, *J. Phys. Chem.*, **39**, 811 (1935).
10) T. Fujisaki, *J. Inst. Fuel Japan*, **20**, 782 (1941).
11) H. D. Burnham and R. N. Pease, *J. Am. Chem. Soc.*, **64**, 1404 (1942).
12) E. Bergman, "Chemistry of Acetylene Compounds", **91**, (1948).
13) T. Fujisaki, *J. Inst. High Press. Gas Japan*, **15**, 244 (1951).
14) Z. Kuri and S. Shida. This Bulletin, **25**, 116 (1952).
15) I. Tanaka and S. Shida, ibid., **23**, 54 (1950).
16) Y. Mori, I. Tanaka, and S. Shida, ibid., **23**, 168 (1950).
17) I. Tanaka, S. Miyakawa, and S. Shida, ibid., **24**, 119 (1951).
18) I. Tanaka, unpublished.

Thus we adopted the flow method in the thermal polymerization of acetylene and quickly introduced the reaction products to a trap to get C.O.T.

b) Analysis of C.O.T. C.O.T. was analysed by the polarography[19] as in the case of our previous work.[14] Its half wave potential was -1.49 volts vs. S.C.E. At the sensitivity of 2.4×10^{-3} μA/mm. of the galvanometer 1 mm. displacement of the diffusion current corresponded to 2.79×10^{15} molecules of C.O.T. at the experimental conditions.

II. Experimental Details

a) Apparatus and Methods. Acetylene gas was purified by the normal method. The whole arrangement of the experiment is shown in Fig. 1. Purified acetylene is led through A into a liquid air freezing trap B, where the non-condensable gas is removed from the solidified acetylene through a vacuum pump and is fractionated into a reservoir C. From the reservoir, pure acetylene goes through a quartz reaction tube D heated by an electric furnace E, passing a dry ice trap F into the liquid air trap B. Reaction products caught in the trap F are evaporated back into the reaction tube D, after the experiment and are analysed spectrographically in the gas phase.

For the analysis of C.O.T., products in the trap F were directly distilled into a tiny ampoule G using the dry ice bath, and then the ampoule was cut off at the neck. Its contents were dissolved into ethanol-tetramethylammoniumbromide solution, which was submitted to the polarographic analysis.

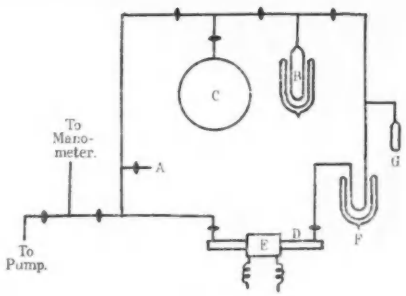

Fig. 1

b) Products of the Reaction. The absorption spectra of the reaction products are shown in Fig. 2. We see the products are benzene in the main and styrene in part. Besides them strong absorption lines characterized by 2808, 2720, 2687Å were always seen in the products of the photopolymerization, but in this case no trace of these lines belonging to the unknown substance appeared. This was a marked difference between the two cases. We suppose that the unknown substance is the intermediate of the polymerization and that it may be polymerized by heating in the thermal polymerization, for those lines disappear rapidly when irradiated with a mercury lamp. The absence of any thermal cracking can be inferred from the fact that there were not found any trace of the spectral lines of toluene and not any carbon or other sediments on the wall after the experiments.

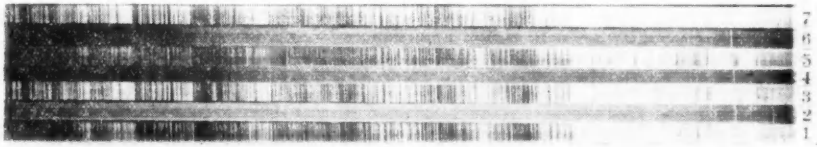

(1), (3), (5) and (7) Iron spectrum (2) Blank (4) Spectrum of the products at 10 mmHg. (6) The same at 5 mmHg.

Fig. 2. Spectra of the products.

c) The Rate of Formation of C.O.T. under the Varied Pressure of Acetylene. If we put the volume passed at the pressure of p mmHg at the experimental temperature, V cc., the pass-time in the furnace, t sec., the height of diffusion current of the polarogram of C.O.T., h mm. (1 mm. corresponds to m mols of C.O.T.), the concentration of acetylene, A mol/cc., we can describe the rate of formation of C.O.T. in terms of the concentration of acetylene as follows.

$$dC/dt=hm/Vt=k_eA^n. \qquad (1)$$

Putting $h/Vt=H$, $\log H$ is seen linear to $n\log A$ and the constant n is determined as far as the reaction satisfies eq. (1). Using the pressure p instead of A, $\log H$ was, in Fig. 3, plotted against $\log p$ at each temperature.

Fig. 3 shows $n=2$ from the slope. It is because of the decomposition of C.O.T. that the line at 575°C lies beneath the one at 570°C. This fact is also seen by the deviation of $\log k_e$ at 575°C. from the straight line vs. $1/T$ as will be written below.

d) The Rate of C.O.T. under the Varied Temperature. At the constant pressure of 250 mmHg, the logarithm of the rate constant k_e of C.O.T. formation was plotted against the reciprocal of the reaction temperature T°K. Fig. 4 shows the result. $\log k_e$ is linear against $1/T$ over the range of 525 and 570°C. The point at 575°C. deviates from the line, which means the decomposition of C.O.T. above at this temperature.

We get the activation energy $E_e=46900$ cal. from the slope of the straight line in Fig. 4. So, the rate of C.O.T. formation is obtained as follows.

19) R. M. Elofson, *Anal. Chem.*, **21**, 917 (1949).

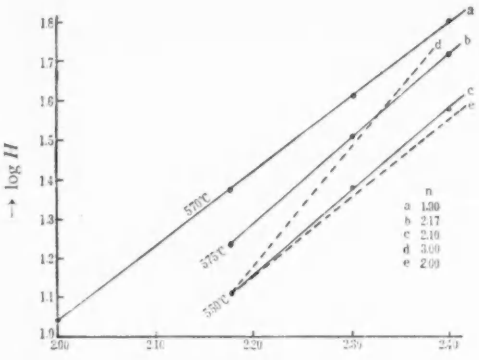

Fig. 3. Rate of formation of C.O.T. vs. acetylene pressure.

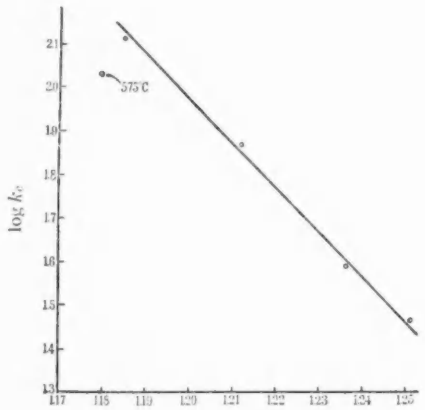

Fig. 4. Rate of formation of C.O.T. vs. reaction temperature.

$$dC/dt = 1.50 \times 10^{11} \exp(-46900/RT) \cdot A^2 \text{ mol. cc.}^{-1} \text{ sec.}^{-1} \quad (2)$$

Discussion of the Experimental Results

As we could determine the rate of formation from acetylene of C.O.T. as stated above, we assumed the following steps of the reaction mechanism.

$$2\ C_2H_2 \xrightarrow{k_1} \begin{matrix} CH{-}CH \\ \| \quad \| \\ CH{-}CH \end{matrix} \quad (3)$$

$$\begin{matrix} CH{-}CH \\ \| \quad \| \\ CH{-}CH \end{matrix} + C_2H_2 \xrightarrow{k_2} \text{or X} \quad (4)$$

$$2 \begin{matrix} CH{-}CH \\ \| \quad \| \\ CH{-}CH \end{matrix} \xrightarrow{k_3} \quad (5)$$

For simplicity we will abbreviate the concentrations as follows; acetylene A, cyclobutadiene D, benzene B, cycloöctatetraene C, the unknown intermediate X. Under the condition of rapid flowing, we can ignore the steps forming higher polymers than C_8H_8. Then in the stationary state

$$dD/dt = 1/2k_1A^2 - k_2DA - k_3D^2 = 0 \quad (6)$$

$$dB/dt = k_2DA \quad (7)$$

$$dC/dt = 1/2k_3D^2 \quad (8)$$

From eq. (6) we obtain as the stationary dimer concentration

$$D = \frac{-k_2 + \sqrt{k_2^2 + 2k_1k_3}}{2k_3} \cdot A \quad (9)$$

Here the negative root was omitted. We get from eqs. (7), (8) and (9)

$$dB/dt = \alpha\{(1+k_1/\alpha)^{1/2} - 1\}A^2 \quad (10)$$

$$dC/dt = 1/2[\alpha\{1-(1+k_1/\alpha)^{1/2}\} + k_1/2]A^2, \quad (11)$$

where $\alpha = k_2^2/2k_3$. The value of k_1/α in eqs. (10) and (11) is of the smaller order than 10^{-3} as far as the values of $(2E_2 - E_3)$ are below 25 kcal. In fact the value of k_1/α is much smaller because the one of $(2E_2 - E_3)$ is smaller as will be stated below. Thus simplifying eqs. (10) and (11) by the binominal theorem

$$dB/dt = 1/2k_1A^2 \quad (12)$$

$$dC/dt = \frac{k_1^2k_3}{8k_2^2} A^2 \quad (13)$$

We compare eqs. (13) and (2) to find them to be of the same form. The details of the rate constants of eq. (13) may be written as follows,

$$\frac{k_1^2k_3}{8k_2^2} = \frac{(p_1Z_1)^2p_3Z_3}{8(p_2Z_2)^2} \exp -2(E_1 - E_2 + E_3/2)/RT \quad (14)$$

p_1Z_1 in eq. (14) is given as 4×10^{10} (525~570°C) by Kamenetskii.[20] Z_2 and Z_3 are of the order of 10^{11}. Inserting these values we obtained $p_2^2/p_3 = 10^{-5}$ from the theoretical formula (14) and the experimental one (2). Substituting the various values of p_2 we find the corresponding ones of p_3 as follows.

p_2	10^{-1}	10^{-2}	10^{-3}	10^{-4}	10^{-5}	10^{-6}
p_3	10^{3}	10^{1}	10^{-1}	10^{-3}	10^{-5}	10^{-7}

In general the simpler the reacting molecules, the greater is the steric factor[21] and so $p_2 > p_3$ may be considered. From the values of p_2 and p_3 cited above, p_2 must be $<10^{-5}$, which follows $10^{-5} > p_2 > p_3$. If the dimer would be assumed to have the structure like butadiene biradical, its steric factor p_3 may be approximately of the same order with that

20) D. A. Frank-Kamenetskii, *Acta Phys. Chim. R.S.S.U.*, **18**, 148 (1943).
21) H. Eyring, "The Theory of Rate Process", McGraw-Hill Book Co. (1941) p. 19.

of dimerization of butadiene which is of 10^{-4}.[22] This value of p_3 disagrees with $10^{-5} > p_2 > p_3$.

If C.B.D. is assumed to be the dimer, its steric factor of dimerization p_3 may be greater than that of chain structure 10^{-4}, because the steric factor of the reaction forming a non-linear complex tends to have the greater one than that of the reaction forming a linear complex.[21] Hence, when p_3 of dimerization of C.B.D. is assumed to be 10^{-3}, $p_2=10^{-4}$ is obtained; that is $p_2 < p_3$, which disagrees with the conditions $p_2 > p_3$ mentioned in the case of the chain structure. But that may be explained as follows; the activated state of dimerization of C.B.D. in eq. (5) has a looser structure than that of eq. (4); consequently, ΔS^* of eq. (5) is greater than that of eq. (4).

Comparing the exponential terms of eqs. (2) and (14) we obtain

$$2(E_1-E_2+E_3/2)=46900 \text{ cal.}$$

As $E_1=29900$ cal according to Kamenetskii[20]

$$E_2-E_3/2=6450 \text{ cal.}$$

Here, E_2 will be of the order of 7~8 Kcal because it is the activation energy for the chain propagation.[11] Consequently E_3 becomes 1~3 Kcal which is so small that this corresponds to the assumption that the reactive dimers react to give C.O.T. as shown in eq. (5).

By calculating the ratio of yields of benzene and C.O.T. from eqs. (12) and (13), we obtain

$$B/C=\frac{4k_2^2}{k_1k_3}$$

$$=\frac{4(p_2Z_2)^2}{(p_1Z_1)(p_3Z_3)}\exp(E_1-2E_2+E_3)/RT \quad (15)$$

That is, the ratio of benzene and C.O.T. is independent of the pressure of acetylene. In fact inserting the values

$$p_2^2/p_3=10^{-5},\ E_2-E_3/2=6450 \text{ cal}$$

etc., into eq. (15) we may compare the evaluated ones and the experimental ones as shown in Table I. The former will not be so accurate, since the experimental values were obtained by assuming the whole weight of the products to be that of benzene which is the main product. Nevertheless they coincide considerably well with each other and especially $(B/C)_{o's}$ shows independence of pressure.

TABLE I

THE RATIO OF BENZENE AND C.O.T., OBSERVED AND CALCULATED

Temp. °C	Press. mmHg	B/C obs.	B/C calc.
535	250	1.59×10^3	3.72×10^3
550	250	1.28×10^3	3.02×10^3
	200	1.10×10^3	
570	250	4.59×10^2	2.37×10^3
	200	4.10×10^2	
	100	4.22×10^2	

Hence for increasing the yield of C.O.T. it is very efficient to diminish the exponential term of eq. (15) and so the yield as well as the rate of formation of C.O.T. will be increased very greatly if we can decrease, by the use of catalyser, for example, the value E_1, the largest among E_1, E_2, and E_3. On the other hand since the rate of formation of C.O.T. is proportional to the square of acetylene pressure, we may conclude from eqs. (13) and (15) that the use of high pressure and suitable catalyser diminishing E_1 will produce the large yield of C.O.T. This agrees qualitatively with the fact that Reppe[23] obtained C.O.T. in good yield using high pressure and nickel catalyser.

The existence of C.B.D. has not yet been proved, but Kamenetskii[24] considered from the chemical analysis of the polymerization products that the structure of dimer will be C.B.D. or methylenecyclopropene; and again C.B.D. was supposed to be the dimer by Reppe[23], too, who expected but did not succeed in finding C.O.T. in the thermal polymerization products and who said that C.O.T. is too labile thermally to be found in the products.

Concerning the stability of C.B.D., strain energy due to the bent C—C bonds is not so decisive according to Coulson[25], as Penney[26] denied its existence. C.B.D. is probably more stable in a rectangular form having the stretched single bonds than in a square form, after the calculation by Craig[27] and Coulson[28].

It is true that we can not determine these things only by the kinetic consideration we made, and we dare not insist upon our opinion. However from the view-point that the activation evergy E_2 and E_3 are very small, we may state the dimer will not be vinylacetylene but a more reactive and radical-like substance. This might be explained by the butadiene biradical, but we prefer C.B.D.

22) W. E. Vaughan, *J. Am. Chem. Soc.*, **54**, 3863 (1932).
23) W. J. Reppe, "Acetylene Chemistry" (P. B. Report 18852-s) (1949).
24) D. A. Frank-Kamenetskii, *C. R. Acad. Sci. U.S.S.R.*, **37**, 137 (1942).
25) C. A. Coulson and E. M. Moffitt, *Phil. Mag.*, **40**, 1 (1949).
26) W. G. Penney, *Proc. Roy. Soc.*, A**144**, 166; A**146**, 223 (1934).
27) D. P. Craig, *J. Chem. Soc.*, 3175 (1951).
28) C. A. Coulson, Private communication to S. Shida.

CHEMISTRY HALL LIBRARY

at present from the view-point concerning the values of the steric factors p_2 and p_3.

Summary

C.O.T. was found polarographically to exist in the thermal polymerization products of acetylene at the flow method. There did not occur any thermal cracking process below the temperature 570°C. on the experimental conditions. The polymerization of acetylene is fundamentally a bimolecular reaction and the dimer is supposed to be cyclobutadiene from the point of view of the steric factors of the reaction. Benzene is formed by the combination of cyclobutadiene and acetylene. C.O.T. is formed by the dimerization of cyclobutadiene; the rate of C.O.T. formation is of the second order in respect of acetylene. The activation energy and frequency factor of the rate is 46900 cal/mol and 1.50×10^{11} cc. $mol^{-1}. sec^{-1}$., respectively.

The ratio of yield of C.O.T. and benzene is independent of the pressure of acetylene and dependent of the temperature. In order to increase the ratio the activation energy E_1 must be lowered. The high yield of C.O.T. in the Reppe reaction was considered qualitatively.

The author expresses his deepest gratitude to Dr. S. Shida for his encouragement and advice. We are indebted to the budget of the Ministry of Education for our experiments.

Laboratory of Physical Chemistry, Tokyo Institute of Technology, Ohokayama, Meguroku, Tokyo

---

Reactivity of Coke. II. Effects of Heat Treatment of Cokes on Their Specific Surface Areas and Absolute Specific Reaction Rates with Carbon Dioxide at 950°C

By Yoshio KAWANA

(Received February 5, 1954)

Introduction

The reactivity of coke may be considered to depend mainly on its surface properties, crystallographic structure and the catalytic effects of ash in it. These properties are all changed considerably by heat treatment. Accordingly, knowledge on changes of physical and chemical properties of coke by heat treatment is very important for the consideration of the reactivity of coke. Since the conference on the ultra-fine structure of coals and cokes (London, 1943), the physical structure and surface chemical properties of coals and cokes have been actively studied.

The change of adsorption properties of coke or char by heat treatment has been obtained by Maggs[1] and Honda et al.[2] Recently, Boyer and Foucault[3] have obtained the variations of specific surface areas of cokes carbonized from four different coals below 1000°C. Walker et al,[4] and Jolley and Poll[5] discussed the surface area development of carbons during gasification reactions.

In our previous paper,[6] surface areas of cokes were obtained by adsorption of ammonia at 0°C using the simple B.E.T. method, and by these surface area values together with kinetic data, the carbon dioxide-coke reaction was discussed from the standpoint of the absolute reaction rates theory. In this paper, the author obtained the effects of heat treatment of cokes from 1000° to 2000°C on specific surface areas of cokes and absolute specific reaction rates of cokes with carbon dioxide at 950°C.

Experimental

Preparation of Coke Samples.—As original coals, Nakayama lignite, Mitsui Bibai coal, Yatake coal and Hongei anthracite were selected, and after crushing from 20 to 60 mesh (Tyler), their ash contents were reduced by the float-and-sink test in benzene-carbon tetrachloride solution.

1) F. A. P. Maggs, "Proc. Conf. Ultra-fine Structure of Coals and Cokes" B.C.U.R.A., London, 1944, p. 147.
2) H. Honda, Y. Kawana, K. Ouchi and K. Nagata, *J. Chem. Soc. Japan* (Pure chemistry section, in Japanese), **74**, 887 (1953).
3) A. Boyer and G. Foucault, *Compt. rend.*, **257**, 895 (1963).
4) P. L. Walker, R. J. Foresti and C. C. Wright, *Ind. Eng. Chem.*, **45**, 1703 (1953).
5) L. J. Jolley and A. Poll, *J. Inst. Fuel*, **26**, 33 (1953).
6) Y. Kawana, This Bulletin, **26**, 507 (1953).

TABLE I

PROXIMATE AND ULTIMATE ANALYSES OF ORIGINAL COALS

Original coals	Proximate analyses (%) standard basis				Ultimate analyses (%) dry basis					Calorific value (cal./g.)	Fuel ratio	Caking property
	Moisture	Ash	V.M.	F.C.	C	N	H	S	O+errors			
Nakayama lignite	9.95	5.70	44.75	39.60	62.40	1.19	4.96	0.39	24.73	5330	0.884	Non-caking
Mitsui Bibai coal	1.57	8.95	35.27	54.19	77.61	1.79	5.46	0.11	5.95	7650	1.57	Weakly caking*
Yatake coal	0.70	5.82	19.63	73.76	84.15	1.88	4.71	0.59	2.80	8180	3.76	Strongly caking
Hongei anthracite	1.78	1.90	6.79	89.53	91.02	0.98	3.39	0.39	2.29	8250	13.2	Non-caking

* Although Mitsui Bibai coal is usually classified as non-caking, the present sample with the preliminary treatment of reducing ash contents of the coal indicates weakly caking property.

The results of analyses of original coals after this treatment are shown in Table I. These coals were primarily coked at 950°C by an electric furnace, and then both Mitsui Bibai and Yatake cokes were again crushed from 20 to 60 mesh because they solidified in larger blocks, while the other cokes remained as they were. The primary cokes were separately heated in a vacuum carbon resistance furnace at various temperatures from 1000° to 2000°C. The time of heating to desired temperatures and the maximum pressure during heat treatment were respectively about 10—30 minutes and 5—26 mm Hg.

The analytical results and the density of these coke samples are as shown in Table. II.

TABLE II

ANALYTICAL RESULTS[(a)] AND DENSITIES[(b)] OF COKES HEATED AT TEMPERATURES FROM 1,000° to 2,000°C

Cokes		Temperature of heat treatment, °C 1000	1200	1400	1600	1800	2000
Nakayama coke	Moisture, %	8.84	8.29	4.14	1.02	—	0.27
	Ash, %	11.18	11.60	12.40	11.00	—	6.36
	Density, g/cc	1.572	1.809	1.571	1.482	—	1.436
Mitsui Bibai coke	Moisture, %	2.42	0.60	0.42	0.20	0.16	0.20
	Ash, %	16.52	17.72	16.97	14.94	13.41	9.56
	Density, g/cc	1.780	1.852	1.894	1.976	2.039	1.917
Yatake coke	Moisture, %	0.72	0.44	0.20	0.20	0.18*	0.24
	Ash, %	8.84	9.46	8.38	6.88	6.70*	4.62
	Density, g/cc	1.809	1.904	2.041	1.959	1.994*	1.927
Hongei coke	Moisture, %	5.52	1.36	0.28	0.14	0.16	—
	Ash, %	4.73	6.16	5.90	6.06	5.78	—
	Density, g/cc	1.808	1.671	1.676	1.674	1.659	1.650

(*a*) Standard basis (*b*) The densities of cokes were obtained from the usual liquid displacement method using water at 25°C. The air in the coke sample was eliminated as thoroughly as possible by the rotary pump. (*) This coke was treated at 1780°C.

Apparatus and Procedure.—The apparatus and procedure for determination of the surface area of coke and for reaction rates study of the coke-carbon dioxide system are the same as already stated in the previous paper.[5] The surface area of cokes was determined by the adsorption of ammonia at 0°C following the simple B. E. T. method.[7][8]

After measurement, the sample was heated and the adsorbed ammonia was thoroughly desorbed and then the reaction rates of coke with carbon dioxide at 950°C under constant volume were obtained by measuring the increase of the total pressure of this system against time.

Absolute specific reaction rates, K_a, expressed as the number of molecules reacted per sq. cm per second at 950°C when p_{CO_2}/p_{CO} was equal to unity, were obtained by the kinetic data together with the surface area determination as explained in detail in the first paper.

7) S. Brunauer, P. H. Emmett and E. Teller, *J. Am. Chem. Soc.*, **60**, 309 (1938).
8) S. Brunauer, L. S. Deming, W. E. Deming and E. Teller, ibid., **62**, 1723 (1940).

Results and Discussion

Variations of Specific Surface Areas of Cokes with Heat Treatment.—The B. E. T. plots of adsorption isotherms of ammonia at 0°C for various cokes heated at temperatures from 1000° to 2000° are shown in Fig. 1—Fig. 4. In lower temperatures of heat treatment, good straight lines are obtained, but

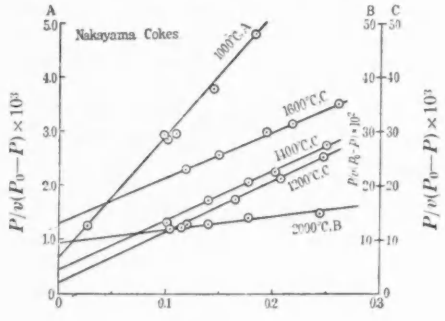

Fig. 1

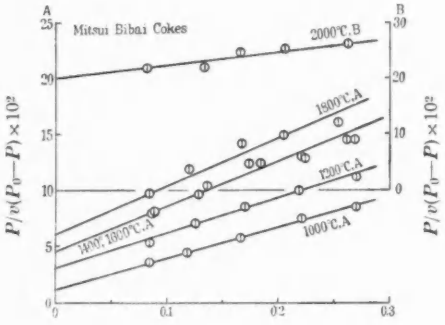

Fig. 2

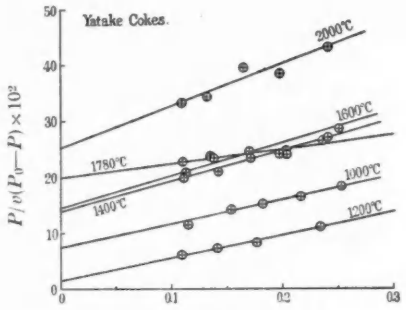

Fig. 3

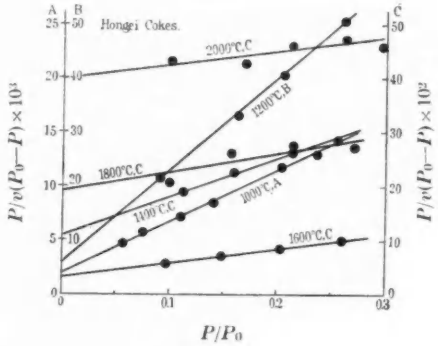

Fig. 4

above 1600°—1800°C, deviations from straight lines become larger and this may be ascribed to smaller adsorption volume. The errors in the surface area values coming from these deviations, however, may not be so large. Various values obtained from Fig. 1—Fig 4 by the usual procedures in the B.E.T. method are summarized in Table III.

TABLE III. EFFECTS OF HEAT TREATMENT OF COKES ON THEIR SURFACE PROPERTIES AND ABSOLUTE SPECIFIC REACTION RATES OF COKES WITH CARBON DIOXIDE AT 950°C

Cokes	Temp. of heat treatment, °C	Vacuum pretreatment °C, hr (mmHg)	Sample weights g	V_m cc	S m²	A m²/g	C	E_1-E_L cal/Mol	K	K_a molecules cm^{-2} sec^{-1}
Nakayama coke	1000	1000, 19 (10^{-4})	0.3924	43.1	149.4	381	36.3	1950	1.67	8.02×10^9
	1200	1100, 8 (10^{-5})	0.1566	10.5	36.4	232	43.2	2050	3.72	7.64×10^{10}
	1400	1100, 5 (10^{-4})	0.3179	10.5	36.4	115	21.2	1660	1.01	2.45×10^{10}
	1600	1100, 5 (10^{-4})	0.9002	10.9	37.8	42.0	7.09	1060	0.302	5.74×10^9
	2000	1100, 5 (10^{-4})	1.8291	2.80	9.71	5.31	3.89	740	1.75 1.61	1.28×10^{11} 1.17×10^{11}
Mitsui Bibai coke	1000	1000, 4.5 (10^{-3})	3.2387	3.63	12.6	3.89	19.7	1620	0.675	3.81×10^{10}
	1200	1100, 3.5 (10^{-3})	3.6872	2.86	9.92	2.69	12.3	1360	0.865	6.11×10^{10}
	1400	1100, 4 (10^{-3})	5.3936	2.20	7.63	1.41	10.1	1260	0.873	7.84×10^{10}
	1600	1100, 4.5 (10^{-4})	4.4478	2.20	7.63	1.72	10.1	1260	0.969	8.80×10^{10}
	1800	1100, 4.5 (10^{-4})	3.9977	2.03	7.04	1.76	8.02	1130	0.124	1.22×10^{10}
	2000	1100, 4.5 (10^{-4})	3.2879	2.29	7.94	2.41	2.18	420	1.05	9.20×10^{10}

	1000	1000,	$5(10^{-4})$	1.1308	1.92	6.66	5.89	7.57	1100	2.73	2.93×10^{11}
	1200	1100,	$2(10^{-3})$	2.3473	2.32	8.04	3.43	30.8	1860	1.39	1.23×10^{11}
Yatake	1400	1100,	$2(10^{-3})$	2.7940	1.49	5.17	1.85	4.81	850	1.67	2.27×10^{11}
coke	1600	1100,	$4(10^{-4})$	3.0608	1.38	4.78	1.56	4.98	870	0.722	1.06×10^{11}
	1780	1100,	$4(10^{-5})$	3.1939	2.20	7.63	2.39	2.27	450	0.925	8.45×10^{10}
	2000	1100,	$3(10^{-5})$	2.4947	0.96	3.33	1.33	4.25	790	0.310	6.57×10^{10}
	1000	1100,	$5(10^{-3})$	2.8936	21.4	74.2	25.6	21.2	1660	2.32	2.17×10^{10}
	1200	1100,	$5(10^{-3})$	1.7178	5.66	19.6	11.4	32.1	1890	2.76	1.00×10^{11}
Hongei	1400	1100,	$4(10^{-4})$	2.0311	1.24	4.30	2.11	7.37	1080	3.05	5.02×10^{11}
coke	1600	1100,	$4(10^{-4})$	6.1565	3.46	12.0	1.95	9.02	1190	2.92	1.60×10^{11}
	1800	1100,	$4(10^{-5})$	7.2682	1.90	6.59	0.91	2.75	550	1.35	1.36×10^{11}
	2000	1100,	$3(10^{-5})$	7.1644	1.53	5.30	0.74	1.65	270	0.0610	7.66×10^{9}

Before adsorption, coke samples were evacuated at higher temperatures to eliminate the surface oxide and residual volatile matters; "Vacuum pretreatment" in Table III shows the conditions of this preliminary treatment. The quantities of V_m, S, A and C in Table III are respectively monomolecular adsorption volume, total surface area, specific surface area and the B. E. T. constant. The quantity of (E_1-E_L) can be evaluated from C as usual.

The variations of (E_1-E_L) with heat treatment are also indicated in Fig. 5. For all

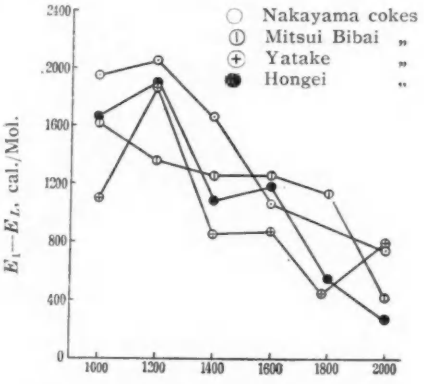

Temperature of heat treatment, °C

Fig. 5. Variations of E_1-E_L with heat treatment.

kinds of cokes, generally speaking, (E_1-E_L) decreases with the increase of heat treatment temperature and the difference due to the rank of original coals can not be clearly seen in Fig. 5. Except for Mitsui Bibai cokes, there seem to be maximum points of (E_1-E_L) at about 1000°−1200°C.

The variations with heat treatment of the specific surface area of cokes are illustrated in Fig. 6. The area of cokes carbonized from non-caking coals such as Nakayama lignite and Hongei anthracite in lower temperature of heat treatment is much larger than that

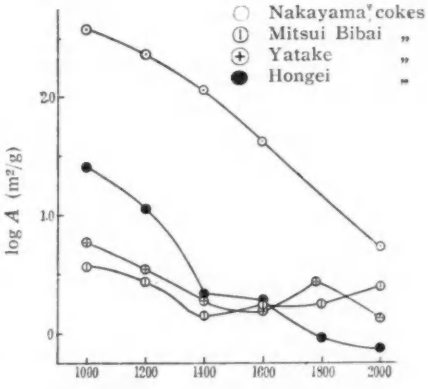

Temperature of heat treatment, °C

Fig. 6. Effects of heat treatment of cokes on their specific surface areas.

of cokes from other caking coals such as Mitsui Bibai and Yatake coals, but the values of the former cokes decrease rapidly with heat treatment temperature, while those of the latter cokes do not change so much by heat treatment and there may be minimum points at about 1400°−1600°C. The ratios of the area of coke heated at 2000°C to that at 1000°C are respectively about 1.4×10^{-2} for Nakayama, 6.2×10^{-1} for Mitsui Bibai, 2.3×10^{-1} for Yatake and 2.9×10^{-2} for Hongei cokes. It is very interesting to notice that there is a close relationship between the manner of decrease of the area of coke by heat treatment and the caking property of the original coal.

Recently, the views that amorphous carbon consists not only of the so-called "turbostratic structure"[9] but also of a third "three-dimensional covalent cross-linked structure", which plays a great role in the structure of chars and cokes, have been justified by X-ray studies[10] on carbonization products from

9) J. Biscoe and B. E. Warren, *J. Appl. Phys.*, **13**, 364 (1942).

10) J. Gibson, M. Hobhan and H. L. Riley, *J. Chem. Soc.*, **1946**, 458.

hexaiodobenzene and hexachlorobenzene and by the wet oxidation rates studies[11] of various kinds of amorphous carbons containing cokes. According to the magnetochemical studies[12] of coals and their related substances, the structure of chars and cokes depends much on both the carbonization temperature and the structure of starting substances; moreover the structure of coke carbonized at about 1100°C may be considered to consist mainly of the three-dimensional covalent cross-linked structure, the change of which to the turbostratic structure or to the graphite one may occur at temperatures higher than 1100°C.

The higher the temperature of heat treatment is, the more the three-dimensional covalent cross-linked structure of cokes is decomposed and the nearer it is to that of graphite; hence, in general, the surface area of cokes decreases with heat treatment temperatures. However, the structure of cokes depends on the kind or rank of original coals as well as the heat treatment temperature, so the specific surface area of cokes heated even at the same temperature may differ a great deal from each other.

It cannot be clearly explained why the specific surface area tends to increase above 1600°C for caking coals, but not for non-caking coals. As the temperature of 1600°C coincides with that of rapid graphitization of cokes,[13] there may be some special relation between the increase of the specific surface area and the graphitization of cokes from caking coals.

Variations with Heat Treatment of Absolute Specific Reaction Rates of Cokes with Carbon Dioxide at 950°C.—The values K and K_a in Table III are respectively rate constants and absolute specific reaction rates, expressed as the number of molecules reacting per sq. cm per second at 950°C when P_{co_2}/P_a equals unity in the reaction of coke with carbon dioxide, as defined in the first paper. The relations between K_a and the heat treatment temperature are also indicated in Fig. 7. Generally, a regular relation between K_a and the heat treatment temperature is neither seen for all kinds of cokes, nor is there a clear relation between K_a and the rank of original coals for all temperatures of heat treatment. Although the higher the temperature of heat treatment is, the more regular becomes the crystallographic structure of cokes, which approaches to that of graphite, there is not a general tendency of the decrease of K_a with the heat treatment temperature. The irregular changes of K_a by heat treatment may be due to the catalytic effects of the ash which coexists on the surface of coke, and the magnitudes of the changes are comparable with or are larger than those of the specific surface area decrease by heat treatment. According to this result, it may be said that the impurities in coke have stronger effects on the reactivity of coke than the surface area of coke has.

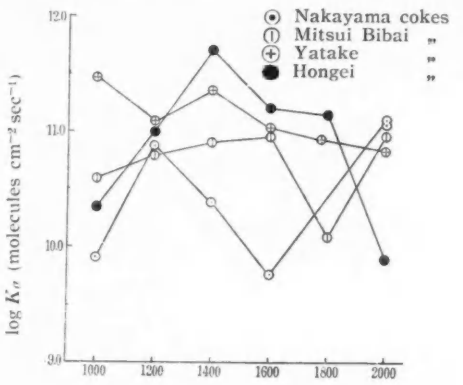

Fig. 7. Effects of heat treatment of cokes on absolute specific reaction rates of cokes with carbon dioxide at 950°C.

On the other hand, in our first paper, it has been concluded that the difference of K_a between pure amorphous carbon and pure graphite at the same temperature will be small, and that for carbons containing some impurities, the catalytic effects of the ash in carbons on the absolute specific reaction rates may be much greater than those of the difference of the crystallographic structure of carbons, that is, the degree of graphitization of carbon, from the absolute reaction rates study of various carbons with carbon dioxide. The same conclusion could again be derived from the above-mentioned results. That is, there are some effects which are much greater than those of the difference of the degree of graphitization of cokes, and these effects have been assumed to be the catalytic effects of the ash in coke.

Summary

The effects of heat treatment of cokes on their specific surface areas and absolute

11) H. E. Blayden and H. L. Riley, *J. Soc. Chem. Ind.*, **54**, 159T (1935); A. F. Balfour, H. E. Blayden, A. H. Carter and H. L. Riley, *J. Soc. Chem. Ind.*, **57**, 1 (1938); H. L. Riley, *J. Chim. Phys.*, **47**, 565 (1950).

12) H. Honda and K. Ouchi, *Reports of the Resources Research Institute* (in Japanese) No. 1 (1952).

13) H. Honda and K. Ouchi, *Sci. Rep.*, Tohoku Univ. Series 1, **37**, 55 (1953).

specific reaction rates of cokes with carbon dioxide at 950°C have been obtained by the same procedure as stated in the first paper.

Generally, the specific surface area of cokes decreases with heat treatment temperature, and the values for cokes from non-caking coals are much greater than those for cokes from caking coals in lower heat treatment temperatures, and there is a close relationship between the manner of decrease of the specific surface area of coke by heat treatment and the caking property of the original coal.

The changes by heat treatment of absolute specific reaction rates of cokes with carbon dioxide at 950°C are very irregular for all the temperatures. There are some effects, which are much greater than those of the difference of the crystallographic structure of cokes, on the absolute specific reaction rates of cokes with carbon dioxide. These effects have been assumed as the catalytic effects of the ash in coke, which may also be larger than those of the surface area of coke on the reactivity of coke.

The author wishes to express his earnest thanks to Mr. A. Baba, Dr. H. Honda and Mr. Y. Yoshida for their kind advice and interest in this study. The author's thanks are also due to Mr. R. Sato for his kind assistance in this experiment.

Shigen-Gijutsu-Shikenjo
Resources Research Institute
Saitama-Kawaguchi
Japan

Surface Chemistry of Synthetic Protein Analogues. IV. On the Monolayers of Electrolytic Synthetic Polypeptides, Poly-L-Glutamic Acid and the Copolypeptide of L-Lysine, L-Leucine and L-Glutamic Acid

By Toshizo ISEMURA and Kozo HAMAGUCHI

(Received March 22, 1954)

Introduction

In the preceding three papers of this series[1-3], we have reported on the properties of the monolayers of some synthetic polypeptides, all of which have non-electrolytic side chains. It was found that the polypeptides having sidechains which are less than four carbon atoms in length, such as poly-DL-norleucine, gave the surface pressure-area curves which closely resembled in shape those of natural proteins. In relation to only the length of side chains, poly-DL-norleucine may be a suitable one as a model of proteins. Strictly speaking, however, this polypeptide may be inadequate because of the lack of electrolytic nature.

The copolypeptide of L-lysine, L-leucine and L-glutamic acid which is described in the present paper should be a more promising protein model for the following three reasons: namely, (1)this copolypeptide has amino groups, carboxyl groups and non-polar hydrocarbon groups in side chains, (2) plausible length of side chain and (3) the configuration of L-type. All of these properties are found in natural proteins in general.

This polypeptide films gave the different surface pressure-area (F—A) and surface viscosity-area (η—A) curves on the substrates of various *p*H values and the results obtained are interpreted in terms of the ionization degree of its amino and carboxyl groups. In addition, further simplified, non-amphoteric, poly-L-glutamic acid monolayers on the substrates of different hydrogen ion concentrations were also examined.

The interest about these electrolytic polypeptides concentrate not only upon the protein model but also upon this polyelectrolytic behaviour of which investigations are recently developed by Kuhn and Katchalsky.[4,5] We have investigated the properties of these polypeptides monolayers from the viewpoint of polyelectrolyte in addition to the comparison of these polypeptides with natural proteins.

Experimental

Materials and Methods. The copolypeptide of

1) T. Isemura and K. Hamaguchi, This Bulletin, **25**, 40 (1952).
2) T. Isemura and K. Hamaguchi, ibid., **26**, 425 (1953).
3) T. Isemura and K. Hamaguchi, ibid., **27**, 125 (1954).
4) W. Kuhn, O. Kunzel and A. Katchalsky, *Helv. Chim. Acta*, **31**, 1994 (1948).
5) A. Katchalsky, *J. Polymer Sci.*, **7**, 393 (1951).

L-lysine, L-leucine, and L-glutamic acid and poly-L-glutamic acid were prepared by Dr. H. Tani and Mr. H. Yuki[6] and were used without any further purification. This copolypeptide was spread from its methanol solution and poly-L-glutamic acid from a solution in N/100 sodium hydroxide containing 1 percent isopropyl alcohol. The film of the polyelectrolyte is profoundly affected by the existence of a small amount of salt in the substrate In order to minimize the effect of various salt ions the *p*H of the substrates was adjusted inevitably only with hydrochloric acid or sodium hydroxide without using the buffer. The value of *p*H was measured by using the Beckman glass electrode. The change of the *p*H values before and after experiment, however, did not exceed 0.2 unit at most.

Surface pressure and surface viscosity measurements were carried out by the method of a hanging plate and of damped oscillatory motion of a disc, as reported in the previous papers.[1,3] The area per amino acid residue of the copolypeptide was calculated by assuming that the same ratio of L-lysine, L-leucine and L-glutamic acid as the initial monomer concentration ratio of this polymerization, 1:2:1, was maintained in the copolymer.

Results. The F—A and η—A curves of the copolypeptide on the substrates of different *p*H values were shown in Figs. 1 and 2. It was found

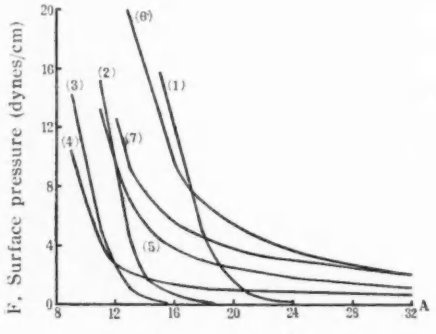

Fig. 1. Surface pressure-area curves for monolayers of the copolypeptide on the substrates of different *p*H values. Curve (1), *p*H 7, (2), *p*H 9.4, (3), *p*H 5.8, (4), *p*H 4.4, (5), *p*H 3.0, (6), *p*H 12.3, and (7) *p*H 1.6. (8°C).

from these figures that the F—A and η—A curves were varied with the substrate *p*H and that the F—A curves on the substrate of which *p*H values lie between 5.8 and 9.4 were of condensed type, but the more acidic or the more alkaline in the outsides of this *p*H range the substrate becomes, the more the F—A curves expand. Furthermore, while in this *p*H range the surface viscosity was very large even at lower pressure region—this is the analogous fact with the case of non-polar polypeptides[3]—it was not sensitive until the surface pressure became considerably high on the either side of this *p*H range. The surface viscosities decrease with the rise of temperature of the substrate at any *p*H value excepting at *p*H 7, where the effect of the temperature was reverse, i.e., the higher the temperature the larger was the viscosity. (Fig 3).

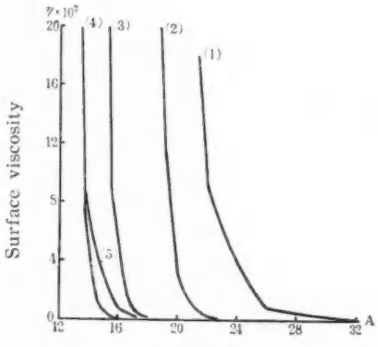

Fig. 2. Surface viscosity-area curves for monolayers of the copolypeptide on the substrate of different *p*H values. Curve (1) *p*H 7, (2) *p*H 8.3, (3) *p*H 9.2, (4) *p*H 5.8 and (5) *p*H 1.6. (7°C)

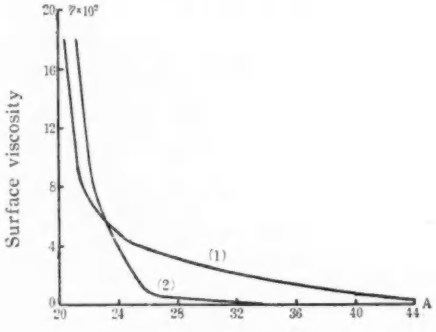

Fig. 3. Effect of temperature on surface viscosity-area curve for monolayer of the copolypeptide at *p*H 7. Curve (1) 14°C, (2) 7°C.

The F—A and η—A curves of poly-L-glutamic acid were shown in Figs. 4 and 5. Fig. 6 shows the relations of *p*H-area (at constant pressure), and *p*H-surface pressure (at constant area), namely curve (I) shows the plot of the area at 1 dyne/cm. against *p*H (ca. 10°C), curve (II) the same as curve (I) but at the temperature 21°C., curve (III) the surface pressure at 15 Å²/residue against *p*H, and curve (IV) the area at $\eta=10^{-2}$ surface poises

6) H. Tani, H. Yuki, K. Okawa, S. Sakakibara and C. Oizumi, *Seni Kagaku Kenkyusho Nenpo* (*Mem. Inst. Fiber Research*) **7**, 98 (1953).

against *p*H. It was noted that the area or surface pressure decreased steeply at about *p*H 4.6.

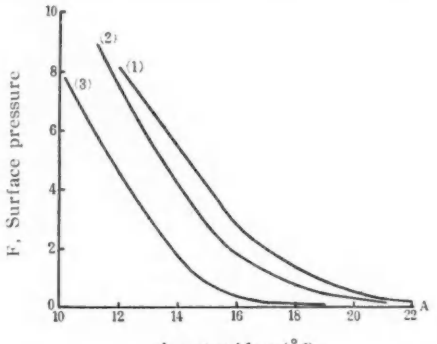

Fig. 4. Surface pressure-area curves for monolayers of poly-L-glutamic acid. Curve (1) *p*H 1.6～4.6, (2) *p*H 5.1 and (3) *p*H 5.6. (10°C).

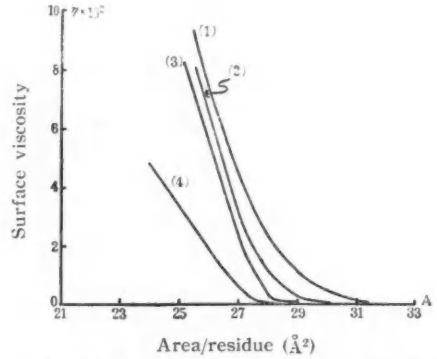

Fig. 5. Surface viscosity-area curves for monolayers of poly-L-glutamic acid. Curve (1) *p*H 1.6, (2) *p*H 3.0, (3) *p*H 4.4 and (4) *p*H 4.8. (22°C).

Discussion

Compressibility δ was calculated from the F—A curves at various *p*H by the equation

$$\delta = -\frac{1}{A}\frac{\partial A}{\partial F} \qquad (1)$$

and was plotted against the area. In Fig. 7 the area of the minimum compressibility ($\delta_{min.}$) appearing in the δ—A curves is plotted against the *p*H of the substrates.

The minima appear at *p*H 4.4 and 9.6 and the maximum at *p*H 7 in this curve. The area at $\eta = 2\times10^{-2}$ surface poise was plotted against *p*H in this figure and this relation is also of W-shape similarly. This relation resembles that found by Gorter, van Ormondt

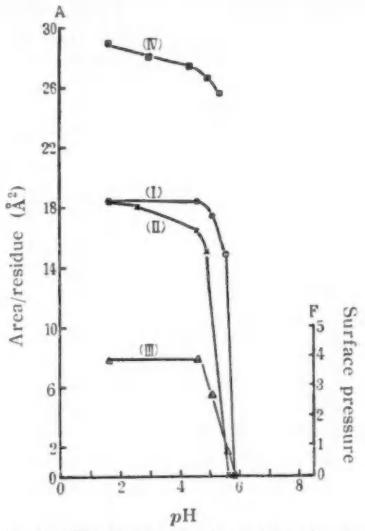

Fig. 6. Monolayers of poly-L-glutamic acid. Curve (I) Area at 1 dyne/cm.—*p*H curve at 10°C. (II) Area at 1 dyne/cm.—*p*H curve at 21°C. (III) Surface pressure at 15 Å²/residue—pH curve at 10°C. (IV) Area at $\eta = 10^{-2}$ surface poise—*p*H curve at 22°C.

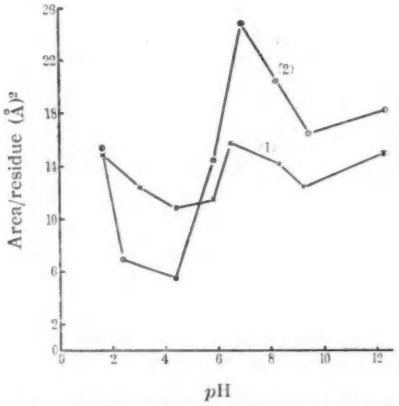

Fig. 7. Monolayers of the copolypeptide. (1) Area at compressibility minimum against *p*H curve, (2) Area at $\eta = 2\times10^{-2}$ surface poise against *p*H curve.

and Dorn,[7] who pointed out that the spreading was maximum at the isoelectric point of the protein. Later, the same relation was also recognized by Bateman and Chambers[8]

7) E. Gorter, J. van Ormondt and F. P. Dorn, *Proc. Kon. Akad.*, Amsterdam, **35**, 838 (1932), cited by McBain, "Colloid Science," (1950).

8) J. B. Bateman and L. A. Chambers, *J. Chem. Phys.*, **7** 244 (1939).

and others. Dervichian,[9] however, suggested that this phenomenon was ascribed to the maximum insolubility of proteins at the isoelectric point. In our case, however, the dependence of the area upon *p*H of the substrate may not be ascribed to the difference of solubility, because the solvent used for spreading is methanol and the area becomes again larger when the *p*H is sufficiently higher or lower.

When the copolypeptide was spread on a large area of the substrate, the polar as well as non-polar side chains and —CO—NH— groups in the main chain would be laid on the surface. With the compression of the film, the non-polar side chains tend to stand up perpendicularly to the surface in air, remaining the main chain on the surface of the substrate. Consequently, the long linear polypeptide would assume more or less extended structure in the spread monolayer.

Now, we shall consider on which *p*H lies the isoelectric point of this copolypeptide. At *p*H 7, some peculiar phenomena were observed, that is, (a), the maximum appeared in the A (at compressibility minimum)-*p*H curve (Fig. 7), (b) the surface viscosity is very high even in larger area and (c) the temperature dependence of the viscosity is opposite to that at the other *p*H values (Fig. 3). Since the number of $-NH_3^+$ ions might be the same as that of $-COO^-$ ions at the isoelectric point, it is probable that the number of salt-linkages between these ions is at its maximum and that the large network structure of the film may be completed. In such a state the resistance against shear becomes very large and the surface viscosity is expected to be high in a larger area. If the salt-linkages between these ions is possible, the degree of hydration and also the hydrophilic tendency of these groups decrease and so it is considered that the F—A curve at the isoelectric point develops from the larger area. With increasing or decreasing the *p*H of substrates from the isoelectric point, either positive or negative charge of the molecules exceeds the other and the number of salt-linkages between NH_3^+ and $-COO^-$ ions decreases. The decrease of the number of salt-linkages results in the lowering of surface viscosity, for the resistance against shear becomes necessarily smaller. All the results and considerations above mentioned lead us to the conclusion that the isoelectric point of this copolypeptide may lie at *p*H 7.

The surface viscosity of the protein monolayer is often discussed in terms of molecular shape in an analogous manner with the viscosity of its bulk solution.[10],[11] In our opinion, the surface viscosity may be entirely different from the bulk viscosity in nature. Therefore, it cannot be considered similarly.

It is well known that the polyampholyte, natural[12],[13] and synthetic,[14],[15] shows a minimum viscosity at its isoelectric point in the bulk solution. This is caused by the coiling of the polyelectrolyte chains by the intramolecular neutralization and no effective free charge in the molecule. On the other hand, the polyampholyte molecule in the monolayer is extended by the surface force. The number of positive and negative ionic groups is maximum in total even though the number of either ionic groups is equal to each other at isoelectric point. As a result, these ionic groups tend to interact intermolecularly forming salt-linkage. This is the reason of maximum surface viscosity and minimum bulk viscosity at isoelectric point.

Surface viscosity depends not only on the interaction between the molecules but also on the degree of molecular packing. There exist two extreme cases of orientation, one of which is that the side chains are directed perpendicular and the other, parallel to the water surface. Between these two extremes the forms or orientations which the polypeptide molecules may prefer on the water surface should be different from the substrate *p*H, depending on the degree of ionization of amino and carboxyl groups. Quantitative analysis of F—A and η—A curves is, therefore, very difficult.

As mentioned above, the F—A curves were of condensed type on the substrates of which *p*H values lie in the range between 5.8 and 9.4, but changed to expanded type if the substrate becomes more alkaline or more acidic than either end of this *p*H range. These facts also relate to the degree of ionization of carboxyl or amino groups; when the number of either positive or negative ions increases, the film expands by the electrical repulsion between the free charges.

The dependence of the degree of ionization (α) of the polyelectrolyte on *p*H may be expressed theoretically by the following equation,[5]

9) D. Dervichian, *Nature*, **144**, 629 (1939).

10) J. T. Davies, *Biochim. et Biophys. Acta*, **11**, 165 (1953).

11) K. Imahori, This Bulletin, **27**, 146 (1954).

12) E. K. Rideal, "Introduction to Surface Chemistry," p. 431, (1930).

13) H. B. Bull, *Trans. Faraday Soc.*, **36**, 80 (1940).

14) T. Alfrey Jr. and H. Morawetz, *J. Am. Chem. Soc.*, **74**, 436 (1952).

15) T. Alfrey Jr., R. M. Fuoss, H. Morawetz and H Pinner, ibid., 438.

$$p\mathrm{H}-pK_0=\log\frac{\alpha}{1-\alpha}+\frac{0.4343}{kT}\frac{\partial F(\nu)}{\partial\nu} \quad (2),$$

Where $F(\nu)$ is the free energy of electrostatic field of a molecule having ν ionized groups and K_0 the intrinsic dissociation constant. We cannot find out the relation of pH and α from equation (2), because of the difficult calculation of $F(\nu)$. However, according to Arnold and Overbeek,[16] pK_0 of polymeric acid obtained from extrapolation of titration data to a very low degree of ionization is practically equal to the dissociation constant of a monobasic acid of the corresponding monomeric acid composition. So, the degree of ionization α_L of amino groups and α_G of carboxyl group can be evaluated to a first approximation by assuming the dissociation constant of $-NH_2$ group of lysine (pK_{0L}) and of —COOH group of glutamic acid (pK_{0G}) to be 10.5 and 4.3, respectively, using the following simple equation,

$$p\mathrm{H}-pK_0=\log\frac{\alpha}{1-\alpha} \quad (3).$$

Havinga and M. den Hertog-Polak[17] suggested that the value of pH of the electrolytic surface film may be different from that of the bulk solution. On the other hand, Glazer and Dogan[18] showed that there exists little effect with the surface film of polyampholyte such as proteins. In the present calculation, the pH value of the bulk solution was used as that of the surface phase.

If we assume that the polymerization ratio of lysine and glutamic acid of this copolypeptide is 1 : 1 (this assumption is valid when the isoelectric point lies near pH 7 as mentioned above), equation:

$$|\Delta\alpha|=\alpha_L-\alpha_G \quad (4)$$

may be considered to give a measure of effective free charges. On the other hand, if the inter or intramolecular salt-linkages are possible, the probability of its linkage may be proportional to the product of α_L and α_G. Fig. 8 represents the relation of $|\Delta\alpha|$ and $\alpha_L-\alpha_G$ against pH.

As found from Fig. 8 the pH range in which F—A curves are of condensed type correponds to $\Delta\alpha$ of at most 5%. (In this pH range eqn. (3) may well be applied.) This copolypeptide has, however, the residues of

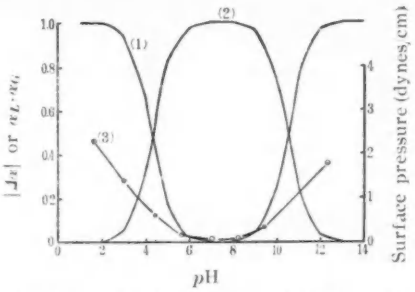

Fig. 8. (1) $|\Delta\alpha|$—pH curve, (2) $\alpha_L\cdot\alpha_G$—pH curve, (3) surface pressure at 30 Å²/residue—pH curve.

lysine, leucine and glutamic acid in the ratio of 1 : 2 : 1 as described above. So, this value of $|\Delta\alpha|$ corresponds to only about 1% ionization of the total number of side chains. It is unfortunate, however, that the pH range which gives the F—A curves of condensed type could not be examined in detail, because of the small amount of the sample. The films which gave the F—A curves of condensed type are characterized by the high viscosity even at low surface pressures (Fig. 9) and this fact corresponds to the cases of nonpolar polypeptides. From these results it is considered that in the pH range which gave the F—A curves of condensed type the molecules forming the film are in such a state that few free charges in molecules exist.

At pH 4.4, $\alpha_L-\alpha_G\fallingdotseq0.5$ (at this pH eqn. (3) cannot be applied but simply qualitatively), namely the number of $-NH_3^+$ ions is greater than that of $-COO^-$ ions by about 50% and the F—A curve is of expanded type. This value of $|\Delta\alpha|$ corresponds to about 10% ionization of the total number of side chains. The film which gives the F—A curves of expanded type is not sensitive for surface viscosity until the film pressure is rather high (Fig. 9). The plots of surface viscosity against surface pressure are shown in Fig. 9. The films which do not bear free charges, for instance, those of non-electrolytic or electrolytic polypeptides which are in the isoelectric state, show the steep curve (I) and increasing the free charges makes the curve flattened for the pressure axis (curve II). Joly[19] measured the surface viscosity against film pressure relations of natural proteins on the aqueous solution of 0.01 N hydrochloric acid. It is found from his results that the more alkaline the isoelectric point is, the more flattened are the η—F curves as shown in curve (II). Consequently,

16) R. Arnold and J. Th. G. Overbeek, *Rec. trav. chim.*, **64**, 190 (1950).
17) E. Havinga and M. den Hertog-Polak, *Rec. trav. chim.*, **71**, 64 (1952).
18) J. Glazer and M. Z. Dogan, *Trans. Faraday Soc.*, **49**, 449 (1953).
19) M. Joly, "Surface Chemistry." *Research* Supplement, Butterworth, p. 157 (1949).

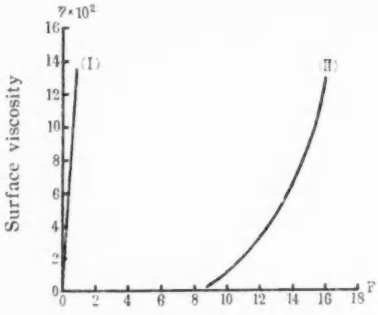

Fig. 9. Surface viscosity-surface pressure curves for monolayer of the copolypeptide. Curve (I) *p*H 7, (II) *p*H 1.6.

the change of the F—A curves to the expanded type must be ascribed to the electrical repulsion of the free charges in polypeptide molecules.

In Fig. 8 surface pressures at constant area are also plotted against the *p*H of the substrate. If the surface pressures exerted at constant area depend markedly on the electrical repulsion between free charges of the molecules, this F—*p*H curve must resemble the $|\Delta\alpha|$ *p*H—curve. This is in fact the case if F—*p*H curve is plotted at a larger area, for instance, 30 Å²/residue; with the lowering of $\Delta\alpha$, F becomes smaller and a minimum point appears at *p*H 7. This fact also supports the theory that the isoelectric point of this copolypeptide lies at *p*H 7. When the surface pressures at smaller area than 25 Å²/residue are plotted against *p*H, there exists discontinuity between *p*H 6 and *p*H 7 and the curve like $|\Delta\alpha|$—*p*H curve could not be obtained, since at such an area region surface pressure depends also on the form or orientation of the molecules.

As is shown in Fig. 7, surface area at constant pressure or at constant viscosity against *p*H curves is of W-shape, and now this curve will be examined in relation to the $|\Delta\alpha|$—*p*H and $\alpha_L\cdot\alpha_G$—*p*H curves. The $\alpha_L\cdot\alpha_G$—*p*H curve shows a maximum at the isoelectric point, *p*H 7, in other words, there exists maximum number of salt-linkages between $-NH_3^+$ and $-COO^-$ ions, the A—*p*H curve shows also a maximum at this *p*H. When the substrate becomes more acidic or alkaline from the isoelectric point, the area becomes smaller, and this region corresponds to the droop of the $\alpha_L\cdot\alpha_G$—*p*H curve. In this region the effect of $\alpha_L\cdot\alpha_G$ is more predominant than that of $|\Delta\alpha|$, i.e., the condensing effect of salt-linkages is more pronounced than the expanding effect of electrical repulsion by free charges. When the substrate becomes still more acidic or alkaline, the area becomes larger again and these regions correspond to the rise of the $|\Delta\alpha|$—*p*H curve, i.e., the effect of electrical repulsion ($|\Delta\alpha|$) is more predominant than that of salt-linkages ($\alpha_L\cdot\alpha_G$). It is of interest that two minima appearing in the curve of W-shape correspond to about pK_0 values of lysine and glutamic acid, respectively.

It is clear from the following reasons that the W-shaped A—*p*H curve is not due to the solubility of this copolypeptide into the underlying water as reported by Dervichian. In the case of poly-L-glutamic acid film, the increase of *p*H shifts the F—A curves to smaller area region and this is clearly due to the increasing solubility of the film substance. A sudden decrease in area and in pressure occurs at *p*H 4.6. The α value at this *p*H calculated from eqn. (3) is approximately equal to 0.6. In the case of the copolypeptide $|\Delta\alpha| \fallingdotseq 0.5$ at *p*H 4.4, based on eqn. (3). In this case, however, there exist the other residues of hydrophobic leucine and non-ionized glutamic acid and if the ratio of lysine, leucine and glutamic acid residues in the molecule is 1:2:1 as described above, this value of $|\Delta\alpha|$ corresponds to about 10% ionization of the total number of the side chains. In such a state, solubility effect cannot be considered in the light of our results of poly-L-glutamic acid.

Next, let us consider about the F—A and η—A curves of poly-L-glutamic acid. The displacement of the F—A curves to a smaller area with the rise of the *p*H of the substrate may be due to the increasing solubility of this polypeptide into the substrate by the ionization of carboxyl groups. It is an interesting fact that both the pressure at constant area and the area at constant pressure or surface viscosity decreased rapidly if the *p*H of the substrate exceeds 4.6. This value of *p*H corresponds to the pK' value of glutamic acid.

Berger and Katchalski[20] showed that the reduced viscosity of poly-aspartic acid solution increases rapidly at about *p*H 4.6. Although there have been no experiments on the viscometric behaviour of poly-glutamic acid to be compared with, our present monolayer results may correspond approximately to the bulk data. According to Katchalsky,[5] the rapid increase

20) A. Berger and E. Katchalski, *J. Am. Chem. Soc.*, **73**, 4084 (1951).

of reduced viscosity is due to the elongation of a polypeptide molecule by the electrical repulsion of ionized groups. If the elongation of a polymer molecule into a rod-like filament occurs, the film-forming molecules cannot remain on the surface and dissolve into the underlying water[21]. Our results represent the correspondence between the bulk and monolayer behaviour.

Summary

The surface pressure and surface viscosity of the spread monolayers of the copolypeptide of L-lysine, L-leucine and L-glutamic acid and of poly-L-glutamic acid were measured in relation to substrate *p*H.

The copolypeptide of L-lysine, L-leucine and L-glutamic acid.—The F—A curves in the range of *p*H 5.8 and 9.4 were of condensed type, but at both outsides of this *p*H range they were of expanded type. The area at constant pressure or surface viscosity against *p*H curves were of W-shape and a maximum appeared at *p*H 7. That the isoelectric point of the copolypeptide may lie at *p*H 7 was concluded from the observations of the monolayer properties. The W-shaped curve could be interpreted in terms of the ionization degree of amino and carboxyl groups. At the isoelectric point, *p*H 7, the surface viscosity became maximum. This is in contrast to the bulk viscometric behaviour of polyampholytes.

Poly-L-glutamic acid.—The area at constant pressure or surface viscosity and the pressure at constant area decreases rapidly if the *p*H of the substrate exceeds 4.6. This fact corresponds to the viscometric behaviour of electrolytic polypeptides in solution, i. e., when the elongation of a molecule by the electrical repulsion of ionized groups occurs, the rapid increase in viscosity and in solubility appears in solution and at monolayer, respectively.

The authors wish to express their sincere thanks to Dr. H. Tani and Mr. H. Yuki in the Faculty of Science at Osaka University who gave them the valuable samples of the synthetic polypeptides. A part of the expense for the experiments has been defrayed from a grant given by the Ministry of Education, to which the authors' thanks are also due.

The Institute of Scientific and Industrial Research, Osaka University, Sakai, Osaka

21) T. Isemura, H. Hotta and S. Otsuka,, This Bulletin, **27**, 93 (1954).

Colorimetric Microdetermination of Chromium and Manganese in Aqueous Solutions

By Akiya KOZAWA, Motoharu TANAKA* and Kumazo SASAKI

(Received March 31, 1954)

Introduction

Sometimes it becomes necessary to determine a small amount of chromium and manganese in natural waters and industrial solutions. Heavy metal impurities in the electrolyte (concentrated NaCl solution) have a marked influence on the chlorine-caustic electrolysis by the mercury cell process.[1] In the present study, the method of analysis of chromium and manganese in the electrolyte was established; ferric hydroxide was used as collector and reduction of ferric ion followed by aluminum hydroxide precipitation made it possible to separate chromium from manganese and iron.

Separation of Chromium from Manganese

Chromium and manganese being collected by ferric hydroxide, as will be described later, chromium must be separated from manganese and iron, both of which interfere more or less with the colorimetric determination of chromium.

If an acidic solution containing aluminum and ferrous ions is just neutralized with ammonium hydroxide to bromocresol purple, aluminum hydroxide is precipitated, while a bulk of ferrous iron remains in solution. In this procedure, chromium coprecipitates with aluminum hydroxide and thus manganese

* Department of Chemistry, Faculty of Science, Nagoya University.

1) Gösta Angel and Tage Lundén, *J. Electrochem. Soc.*, 99, 435 (1952).

together with a greater part of iron was separated from chromium.

The following experiment is carried out to check this point.

Various amounts of manganese and chromium are added to 25 ml. dilute sulfuric acid solution (1 : 50) containing 10 mg. of ferric iron and aluminum respectively and then one ml. of 5% hydroxylamine sulphate solution is added. And after boiling to hasten the reduction of any ferric iron to ferrous, the solution is cooled to room temperature and neutralized with ammonium hydroxide (1 : 5) using B. C. P. as indicator.

After filtration, aluminum hydroxide is dissolved with 10 ml. of hot sulfuric acid (1 : 20) and reprecipitated with ammonium hydroxide in the same manner.

Aluminum hydroxide containing chromium on the filter paper is dissolved with 10 ml. of sulfuric acid (1 : 20) and 1 ml. of 85% phosphoric acid,[2] and transferred to a 50 ml. volumetric flask. Chromium coprecipitated with aluminum hydroxide is oxidized to sexivalent state by silver peroxide.[2] After the decomposition of excess of the oxidizing agent by dipping the volumetric flask in boiling water for 2 or 3 minutes, the solution is cooled to room temperature by tap water. Distilled water is added to the mark and 2 ml. of 0.2% of diphenylcarbazide solution (acetone 1 : water 1) are added. The optical density of the solution is then measured by the spectrophotometer at the wave length of 540 mμ.

One ml. of 30% hydrogen peroxide solution and the excess of ammonium hydroxide are added to the jointed filtrates containing iron and manganese.[3] The solution is warmed to about 80°C.

Ferric hydroxide together with all of the manganese is filtered and dissolved with 10 ml. of hot sulfuric acid (1 : 40) containing a small amount of hydrogen peroxide. The solution is boiled to destroy hydrogen peroxide. Then it is transferred into a 25 ml. volumetric flask and manganese is oxidized to permanganate by silver peroxide.[3,4] After the excess of the oxidizing agent is decomposed by the same procedure as before, the volumetric flask is filled with distilled water to the mark and the optical density is measured at the wave length of 535 mμ.

If any chloride is present, the solution becomes turbid; an addition of mercuric sulfate[5] solution, however, is successfully employed to mask the silver chloride formation.

Results are shown in Table I.

TABLE I

SEPARATION OF Cr FROM Mn WHEN PRESENT TOGETHER

No. of experiment	Cr taken μg.	Cr found μg.	Mn taken μg.	Mn found μg.
1	0.0	0.0	44	41
2	4.0	4.0	88	88
3	8.0	8.2	0	0
4	8.0	8.3	22	23
5	8.0	8.2	22	22
6	16.0	16.4	66	68
7	100.	97.0	220	222
8	200.	196.	220	216

As shown in this table, 0—200 μg. of chromium and manganese can be separated and determined.

Coprecipitation of Cr and Mn with Ferric Hydroxide

One litre of water containing 10 mg. of ferric ion and various amounts of chromium and manganese are neutralized with excess of ammonium hydroxide at 30 to 40°C. The precipitate of ferric hydroxide with chromium and manganese is filtered and dissolved with 10 ml. of hot sulfuric acid (1 : 20) and determination of both elements is carried out by the same procedure as in section II. Table II shows the results.

TABLE II

COPRECIPITATION OF Cr AND Mn WITH FERRIC HYDROXIDE

No. of experiment	Cr taken μg.	Cr found μg.	error μg.	Mn taken μg.	Mn found μg.	error μg.
9	4.0	3.9	0.1	22	23	1
10	16.0	15.8	0.2	44	45	1
11	20.0	19.1	0.9	88	85	3
12	100.	97.0	3.0	110	112	2

We can thus determine manganese and chromium with the mean probable error of 2.5% and 2.4% respectively. Results for chromium appear to be slightly low. The use of an empirical curve is therefore recommended for the estimation of chromium.

When this method is applied to nearly saturated sodium chloride solution (purified electrolyte), particular attention should be taken to remove chloride ion by repeated precipitation of ferric and aluminum hydroxide. As shown in Table III, no trace of

2) M. Tanaka, This Bulletin, **23**, 165 (1950).
The interference of few mg. of iron can be avoided by phosphoric acid or fluoride.

3) M. Tanaka, *J. Chem. Soc. Japan, Pure Chem, Sect.*, **72**, 129 (1950).

4) Y. Murakami, This Bulletin, **22**, 159 (1949); K. Kimura and Y. Murakami, *Mikrochemie*, **36**, 727 (1950).

5) M. Tanaka, *J. Chem. Soc. Japan. Pure Chem. Sect.*, **72** 136 (1950).

manganese or chromium was found in this sample, and the added amounts of these elements were almost quantitatively recovered.

TABLE III

ANALYSIS OF 500 ml. SAMPLE SOLUTION

No. of experiment	Cr added μg.	Cr found μg.	Mn added μg.	Mn found μg.
13	0.0	0.0	0	0
14	8.0	7.8	44	46
15	20.0	19.3	88	87
16	100.	96.0	110	102

Behavioar of Sexivalent Chromium

A sample solution after electrolysis by the mercury cell process contains some free chlorine, so chromium may exist as sexivalent. The brine sample after electrolysis is analysed by the above mentioned procedure; after removal of trivalent chromium and manganese ions by ferric hydroxide, the filtrate is acidified with sulfuric acid and warmed after addition of some sodium sulfite (2–3 g.) for the reduction of chromate to chromic state. Ten mg. of aluminum, collector of chromium, are added to the solution which is subsequently neutralized with excess of ammonium hydroxide. After filtration of aluminum hydroxide, chromium in the hydroxide is determined as is in the case of trivalent chromium. Results are shown in Table IV.

TABLE IV

ANALYSIS OF BRINE CONTAINING FREE CHLORINE

No. of experiment.	Cr III added μg.	Cr III found μg.	Cr IV added μg.	Cr VI found μg.	Mn added μg.	Mn found μg.
17	0.0	0.8	0.0	1.3	0	12
18	8.0	9.0	11.6	11.6	44	56

From these results, it will be clear that small amounts of chromate scarcely ever associate with ferric hydroxide precipitate in our procedure.

Summary

Chromium and manganese less than 100μg. in 500–1000 ml. of solution are separated from a bulk of the solution by ferric hydroxide precipitation and the separation of chromium from manganese and iron can be carried out by the reduction of ferric iron to ferrous followed by the precipitation of aluminum hydroxide. And each element was determined colorimetrically using the silver peroxide as oxydant. No coprecipitation of chromate could be observed in this procedure.

The writers wish to express their hearty thanks to Professor Ken Sugawara for his stimulating interest as well as constant encouragement in the course of this study.

Department of Applied Chemistry,
Faculty of Engineering,
Nagoya University,
Chikusa-ku, Nagoya

Mikroanalyse mit Hilfe von ionenaustauschenden Harzen. II. Über den Nachweis geringer Menge des Chroms mit Wasserstoffperoxyde

Von Masatoshi FUJIMOTO

(Eingegangen am 10. April, 1954)

Einleitung. Wie in der vorhergehenden Mitteilung[1] genau erwähnt, durch mikroanalytische Anwendung der ionenaustauschenden Harze wurde eine neue und verbesserte Tüpfelmethode vorgeschlagen. Bei gegenwärtigem Versuche, hat der Verfasser eine graue bzw. violette Färbung, die bei Anwesenheit von Chromat oder Bichromat mit Wasserstoffperoxyd in die hellgelben anionenaustauschenden Harzkörnchen entsteht, auf den Nachweis geringer Menge des Chroms angewendet und befriedigende Ergebnisse erhalten.

1) I. Mitteilung, Dieses Bulletin, **27**, 48 (1954).

Die in dieser Untersuchung benutzten anionenaustauschenden Harze. Zum Vergleich wurden folgende zwei Arten anionenaustauschender Harze verwendet:

Amberlite IRA-400: Ein aus Styrol und Divinylbenzol dargestelltes starkbasisches Harz von quartärem Ammoniumtypus.

Amberlite IRA-411 (oder XE-98): Ein ebenso starkbasisches Harz wie IRA-400 mit kleinerem Divinylbenzolgehalt.

Beide wurden, vor dem Gebrauch, durch zweimaliges Durchlaufen der 2 N Salzsäure und destilliertes Wassers in die RCl-Form übergeführt. Die Korngrösse ist ungefähr 30 Maschen von Tylerschem Normalsieb.

Versuchsanordnung. Auf einer weissen

Tüpfelplatte versetzt man mit einem Tropfen (0.02 ccm mit Kapillarpipette) der Versuchslösung[2] und einigen Harzkörnchen. Nach drei oder fünf Minuten stehen gelassen, fügt man dazu einen Tropfen verdünnter Schwefelsäure (oder Essigsäure[3]) und verdünnter Lösung des Wasserstoffperoxyds hinzu. Je nach der Mange der Chromat- bzw. Bichromationen in der Probelösung, färben sich die Harzkörnchen grau oder veilchenblau bzw. violettbraun, und diese werden in gleicher Weise als die in der vorhergehenden Mitteilung beobachtet.

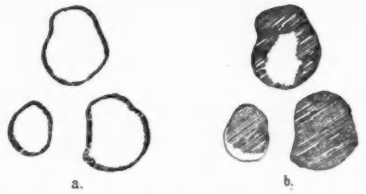

Abb. I. Schematische Darstellung der Färbung der Harzkörnchen
(Cr=2 γ/0.02 ccm als $K_2Cr_2O_7$)
a. = Amberlite IRA-400.
b. = Amberlite IRA-411.

Bestimmung der Bedingungen höchster Empfindlichkeit

1. Massflüssigkeit. Zu diesem Zweck, wurde eine Reihe der Lösungen des Kaliumbichromats (aus heissem Wasser umkristallisiert) dargestellt, deren 1 ccm 10.0 mg, 100-, 10.0-, und 1.00 γ von Chrom enthielten.

Alle folgende Vergleichungen der Bedingungen wurden mit einer Lösung ausgeführt, deren ein Tropfen (0.02 ccm) 2 γ von Chrom enthielt.

2. Einfluss der Harzart. Abb. Ia. und Ib. sind die schematische Darstellung der Färbung an Amberlite IRA-400 bzw. IRA-411. An der IRA-411 wird im Vergleich mit IRA-400 weitgehende Diffusion ins Harzkörnchen der gefärbten Schicht (mit schrägen Linien geschildert) beobachtet, jedoch, waren die Empfindlichkeiten für beide Harze deshalb durchaus dieselbe, weil Verdichtung gefärbter Ionen am Rande der IRA-400 Körnchen diese Differenz vollends kompensierte. Daher wurde bei allen folgenden Versuchen lediglich Amberlite IRA-411 als ein Vertreter angewendet

3. Einfluss der Konzentration der Schwefelsäure. Azidität des Reaktionsmittels wirkte beträchtlich der Reaktionsempfindlichkeit ein. In Tabelle I wird das Einfluss der Konzentration der Schwefelsäure auf der Färbung dargestellt:

TABELLE I

EINFLUSS DER SCHWEFELSÄUREKONZENTRATION AUF DER FÄRBUNG*

Für 2 γ Cr/0.02 ccm, mit (als $K_2Cr_2O_7$)		und 10 proz. H_2O_2
0.01 N H_2SO_4		nur hell grauisch braun,
0.1 N H_2SO_4		nur hell grauviolett,
1 N H_2SO_4		erst deutlich violett,
10 N H_2SO_4		ebenso deutlich violett.

* Salzsäure trat auch ganz gleichfalls auf.

Von diesem Experiment aus betrachtet, war die Anwendung der ungefähr 1 N Schwefelsäure wünschenswert.

4. Einfluss der Konzentration des Wasserstoffperoxyds. Da scheinlich die konzentrierte Lösung des Wasserstoffperoxyds die Färbung hemmte, wurde eine Reihe der Untersuchungen mit 1 N Schwefelsäure unter verschiedenen Konzentration am Wasserstoffperoxyd folgenderweise ausgeführt. Die Resultate der Experimente stehen in Tabelle II:

TABELLE II

EINFLUSS DER KONZENTRATION DES WASSERSTOFFPEROXYDS

Für 2γ Cr/0.02 ccm, mit 1 N H_2SO_4

		Nach 1,	5,	10,	15, und 25 Min.
und	30 proz. H_2O_2	+ + + +	++++	(+)(+)(+)(+)	(+)(+)(+)(+) − − − −
	10 proz. H_2O_2	+ + + +	++++	+ + + +	+ + + + (+)(+)(+)(+)
	1 proz. H_2O_2	(+)(+)(+)(+)	≒++≒	≒ ≒ ≒ ≒	≒ ≒ ≒ ≒ ≒ ≒ ≒ ≒
	0.1 proz. H_2O_2	− ± ± −	++++	+ + + +	± + + + + + + +

−: nicht erkennbar, ±: unsicher, (+): schwach, +: sicher, ≒: etwas stärker, ≒: intensiv gefärbt.

2) Nach der Oxydation des Chroms (III) zum Chromate oder Bichromate wird es hergestellt.

3) Die ausgeprägten Einflüsse der Essigsäure auf die scheinbare Deutlichkeit der Färbungen werden an anderer Stelle dieser Mitteilung eingehend erörtert (vgl. s. 350).

In Betracht der Deutlichkeit und der Beständigkeit von der Färbung, sei ein prozentige Lösung des Wasserstoffperoxyds empfehlenswert.

Auf solche Weise, mit Amberlite IRA-411, ein prozentigem Wasserstoffperoxydwasser und 1 N Schwefelsäure wurde folgender Versuch für Erfassungsgrenze durchgeführt.

Bestimmung der Erfassungsgrenze.[4] Die Resultate der Experimente stehen in Tabelle III:

TABELLE III

DIE RESULTATE DER EXPERIMENTE FÜR ERFASSUNGSGRENZE

Zeit nach der Mischung (Min)	Probe	Färbung an zwölf Vertiefungen											
1～2	A	−	−	−	−	−	−	−	−	−	−	−	−
	B	±	±	(+)	+	(+)	±	(+)	(+)	(+)	(+)	(+)	(+)
5～6	A	−	−	−	±	±	−	±	±	±	−	±	(+)
	B	(+)	(+)	+	+	(+)	(+)	+	+	(+)	(+)	+	+
10～15	A	±	−	±	±	±	±	±	±	±	−	±	±
	B	(+)	+	+	+	(+)	+	+	+	+	+	+	+

A: 0.2 γ Cr (als wässr. Lsg. des $K_2Cr_2O_7$) in 0.02 ccm Probelösung.
B: 0.3 γ Cr (als „ „ „ „) in 0.03 ccm Probelösung.
In Bezug auf den Zeichen, −, ±, +, usw., vgl. Tabelle II.

Die Erfassungsgrenze 0.3 γ unter Grenzkonzentration $1:1\times10^5$ für Chrom an dieser Reaktion wurde so festgestellt.

Bestimmung der Erfassungsgrenze für Chrom nach der Oxydation zum Chromate

1. Massflüssigkeit des Chromsalzes wurde aus der in 1 N Schwefelsäure gelösten Lösung des extrareinen Kalichromalauns, deren 1 ccm 0.87±0.003 mg von Chrom enthielt,[5] vorbereitet.

2. Auswahl des Oxydationsmittels. Folgende dreiartige Oxydationsmethoden wurden zu diesem Zweck angewendet, d.h., Oxydation (1) mit wärmer alkalischer Lösung von Wasserstoffperoxyd,[6] (2) mit heissem Bromwasser und (3) mit heisser gesättiger Lösung des Kaliumpermanganats.

Durch Methode (2) war die Oxydation ungeeignet. Methode (1) auch war dann nicht wünschenswert infolge der Niederschlagbildung falls andere Metallionen wie Eisen vorhanden waren, trotz seiner sehr glatten und befriedigenden Oxydationswirkung. Infolgedessen, wurde gegenwärtiger Versuch, mit Hilfe letzter Methode, d.h., durch Kochen der Probelösung mit einem Tropfen gesättiger Lösung des Kaliumpermanganats in einer Mikroeprouvette 1 bzw. 2 Min lang mit einem Mikrobrenner,[7] ausgeführt, dabei überschüssiges Reagens durch Zusatz von Wasserstoffperoxyd glücklicherweise entfärbt wurde.

In gleicher Weise wie die in Tabelle III durchgeführt, war die Erfassungsgrenze für Chromsalze nach der Oxydation zum Chromate 0.3 γ unter Grenzkonzentration $1:6.7\times10^4$.

TABELLE IV

EINFLÜSSE DER BEGLEITSTOFFE

Begleitstoffe	benutzter Verbindungstypus	Menge der Begleitstoffe	Nachweisbare Chrommenge	Grenzverhältnis	Anmerkungen
Fe^{2+} oder Fe^{3+}	$FeSO_4$ oder $FeCl_3$	430 γ	0.25 γ	$1:1.8\times10^3$	——
Ni^{2+}	$NiCl_2$	2.3 mg	0.64 "	$1:3.6\times10^3$	——
Co^{2+}	$CoCl_2$	2.7 mg	0.63 "	$1:4.4\times10^3$	——
Cu^{2+}	$CuSO_4$	1.4 mg	0.63 "	$1:2.2\times10^3$	——
Mn^{2+}	$MnSO_4$	Grosser Überschuss.	0.3 "	——	——
UO_2^{2+}	Uranylacetat	910 γ	0.62 "	$1:1.5\times10^3$	Neben Blindversuche.
CH_3COOH	Eisessig	Grosser Überschuss.	——	Ziemlich befördert die Färbung.	

4) Hinsichtlich der Bedeutung der Erfassungsgrenze, vgl. Fussnote 1).

5) Die Menge von Chrom wurde folgenderweise bestimmt: Nach der Oxydation mit heisser gesättiger Lösung des Kaliumpermanganats und der (1:1) Schwefelsäure, wurde die Probelösung mit Wasser abgekühlt, filtriert und mit destilliertem Wasser völlig ausgewaschen, wonach die ins Filtrat angesammelte Lösung des Chromats mit bestimmtem Überschusse der 0.1 N Massflüssigkeit des Mohrschen Salzes reduziert wurde, deren Überschuss mit einer Massflüssigkeit des 0.1 N Kaliumpermanganats titriert wurde.

6) Vgl. J. W. Mellor und H. V. Thompson, „A Treatise on Quantitative Inorganic Analysis", 2. Aufl. 1938, s. 533.

7) A. A. Benedetti-Pichler, „Introduction to the Microtechnique of Inorganic Analysis", 1. Aufl. 1942, s. 8.

Einflüsse der Begleitstoffe. Wegen hoher Spezifität der Reaktion konnte man alle Nachweise von Chrom, bei Anwesenheit des grösseren Überschusses von Eisen(II) (III)-, Nickel (II)-, Kobalt(II)-, Kupfer(II)-, Mangan (II)-, Uranyl (II) salze, bzw., Essigsäure, ohne Schwierigkeit durchführen. Die Resultate werden in Tabelle IV kurz gefasst.

Ausgeprägte Beförderung der Färbung mit Essigsäure.[8] Essigsäure befördert so ziemlich die Färbung, dass selbst die mit 1 N Schwefelsäure sich liefernde nur schwach graue Färbung durch ihren Zusatz zur deutlich veilchenblauen Färbung sich verändert. Dabei handelt es sich darum, dass vermutlich eine Art des intensiv gefärbten Chromkomplexsalzes mit Essigsäure sich bildet, jedoch, hier berührt man schlechthin empirischen Ergebnissen. Als Beispiel sei folgende Gegenüberstellung solches Verhältnis klar zu machen:

$$\left.\begin{array}{ll} \text{a)} & \text{RCl} + \text{Cr } 1\gamma^{*} \\ \text{b)} & \text{ROOC}\cdot\text{CH}_3 + \text{Cr } 1\gamma \\ \text{c)} & \text{ROOC}\cdot\text{CH}_3 + \text{Cr } 1\gamma \end{array}\right\} \xrightarrow[2\ \text{Min.}]{} + \left\{\begin{array}{l} 1\,\text{N } \text{H}_2\text{SO}_4 \\ 1\,\text{N } \text{H}_2\text{SO}_4 \\ 6\,\text{N } \text{CH}_3\text{COOH} \end{array}\right\} \xrightarrow[1\ \text{Min.}]{} + \text{ 1proz. } \text{H}_2\text{O}_2 :$$

* als eine Lösung des Kaliumbichromats in der Probelösung vorliegt.

Zum semiquantitativen Vergleich, stellte der Verfasser die scheinbare Intensität der Färbung durch eine Reihe der Zahlen, d. h., −, ±, (+), und +, durch 0, 1, 1.5, bzw. 2, dar. Folgende Abbildung stellt dieses Verhältnis für die an vier Vertiefungen der Tüpfelplatte ausgeführten Reaktionen schematisch dar.

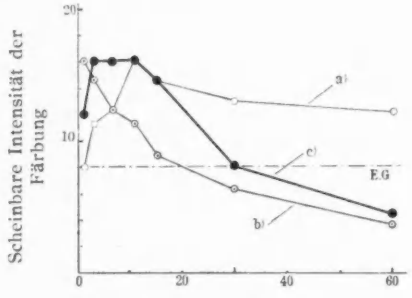

Abb. II. Schematische Darstellung der zeitliche Verwandlung von scheinbarer Intensität der Färbung.

Von dieser Abbildung aus betrachtet, wird es klar, dass, wegen seiner schnellen Entfärbung, Verfahren-b) für empfindlichen Nachweis unbequem ist, und dass c), im Vergleich mit a), dank seiner bis zu 10 Min nach der Mischung entstehenden deutlichsten und zwar beständigsten Färbung, als ein vorzüglichstes Verfahren betrachtet wird, trotzdem nach 10 Min die Färbung etwas schneller als a) verschwindet.

Durch Verwendung der Essigsäure an Stelle der Schwefelsäure wurde der Nachweis geringer Menge des Chromats bemerkenswerterweise deutlich, obgleich diese Erfassungsgrenze mit dem nach Tabelle III erhaltenen Werte identisch war, d. h., 0.3 γ von Chrom unter Grenzkonzentration $1 : 1\times10^{5}$.

Zusammenfassung

1. Eine empfindliche und sehr spezifische Nachweismethode für Chrom als Chromat mit Wasserstoffperoxyd wird durch einfachste Anwendung von der hellgelben starkbasischen anionenaustauschenden Harze festgestellt. (Vgl. Tabelle II und III).

2. Oxydation des Chroms zum Chromate wird mit heisser gesättigter Lösung des Kaliumpermanganats am günstigsten durchgeführt.

3. Verwendung der Essigsäure an Stelle der Schwefelsäure verbessert bemerkenswerterweise die scheinbare Deutlichkeit des Nachweises, wenn auch die Erfassungsgrenze gar nicht erhöht wird.

Zum Schluss möchte der Verfasser Herrn Prof. Dr. E. Minami für seine freundliche Anregungen über diese Untersuchung seinen herzlichen Dank aussprechen.

Laboratorium der analytischen Chemie,
Chemisches Institut der
wissenschaftlichen Fakultät,
Tokyo Universität, Tokyo

8) Über diese Wirkung wird der Verfasser später ausführlich diskutieren.

Mechanism of the Formation of Guanidine and its Derivatives by the Fusion of Dicyandiamide with Amine Salt

By Kiichiro SUGINO

(Received April 19, 1954)

This contribution is the abstract of my papers already published in Japanese in the Journal of the Chemical Society of Japan in 1939 and 1944.[1] Some new facts found by the further experiments are added.

I. Mechanism of the Reaction between Dicyandiamide and Ammonium Salt

Dicyandiamide is converted by its reaction with ammonium salt into guanidine salt.

$$C_2H_4N_4 + 2NH_3 \cdot HX = 2CH_5N_3 \cdot HX$$

This reaction was studied using several ammonium salts in fused state and also in aqueous solution.[2] The difference of the reaction velocity and the yield of guanidine salt due to the difference of ammonium salt was discussed systematically. For each salt, especially the nitrate, the conditions were determined under which the good yield of guanidine salt should be expected. The result was later applied to the commercial preparation of guanidine nitrate by Dr. K. Odo.[3]

The mechanism of this reaction has not yet been clearly explained except that biguanide salt is probably the intermediate product.[4] In order to clarify this mechanism, the following items were studied successively.

a) The condition of the formation of biguanide salt by the fusion of dicyandiamide with ammonium salt.
b) The fusion of biguanide monosalt* with ammonium salt.
c) The thermal decomposition of biguanide monosalt in fused state.

Quantitative determination of the reaction products, the measurement of the heating curve and also the heat of reaction were carried out for each reaction. The main results obtained are summarized as follows.

a) By the fusion of 1 mol. of dicyanidiamide with 2 mol. of ammonium salt, biguanide salt was first formed preceding the guanidine formation. But the former was converted to guanidine salt even at the temperature as low as 120°C according to the reaction (2, 2′) described later. The results are shown in Table I.

TABLE I

Dicyandiamide 4.2 g.
NH_4NO_3 8.0 g.
M. p. of the mixture, 116°C.

Temp. (°C)	Time (hr.)	Biguanide-HNO_3* (g.)	(%)	Guanidine-HNO_3** (g.)	(%)	Insoluble residue of water extraction (g)	Dicyandiamide (unconverted)
120	2	1.79	21.8	—	—	0.01	remains quantitatively
120	3	1.85	22.6	2.25	18.4	0.01	〃 〃
120	4	1.85	22.6	3.26	26.7	0.01	〃 〃

* Determined as nickel-biguanide and reduced to nitrate.
** Determined as picrate and reduced to nitrate.

TABLE II

Biguanide mononitrate 8.2 g.
NH_4NO_3 4.0 g.
M. p. of the mixture, 131°C.

Temp. (°C)	Time (min.)	Guanidine-HNO_3* (g.)	(%)	Insoluble residue of water extraction (g.)	Biguanide
above 180	10	11.7	96	0.02	trace
〃 180	17	10.7	88	0.02	〃

* Determined as picrate and reduced to nitrate.

1) K. Sugino, *J. Chem. Soc. Japan*, **60**, 351, 411 (1939); K. Sugino, M. Yamashita and S. Izumi, **65**, 265, 271 (1944); C.A., **35**, 5097 (1941); 3763c (1947).
2) K. Sugino, *J. Chem. Soc. Japan*, **60**, 267 (1939).
3) K. Odo, *J. Chem. Soc. Japan* (Industrial Chemistry Section), **52**, 210 (1949).
4) Blair, Braham *J. Am. Chem. Soc.*, **44**, 2342 (1922); Smith, Sabetta, Steibach, *Ind, Eng. Chem.* **23**, 1124 (1931).
* Biguanide dinitrate did not give any guanidine salt by its reaction with ammonium salt. The description of Smith, Sabetta and Steinbach (4) is erroneous.

b) By the fusion of 1 mol. of biguanide monosalt with 1 mol. of ammonium salt, corresponding guanidine salt was obtained in yield as same as that obtained by the reaction between 1 mol. of dicyandiamide and 2 mol. of ammonium salt. The results obtained using nitrate are shown in Table II.*

The phenomenon of the heat evolution due to the guanidine formation was observed in the heating curve of their reactions (Fig. 1).

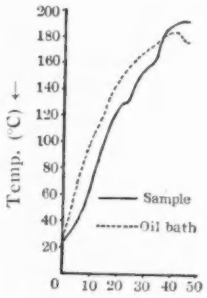

Fig. 1. Biguanide HNO_3 8.2 g. NH_4NO_3 4.0 g.

But it was not very great compared with the same phenomena found in the heating curve of the reaction between 1 mol. of dicyandiamide and 2 mol. of ammonium salt (Fig. 2). In order to clarify these observations,

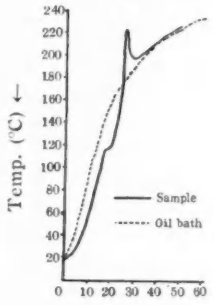

Fig. 2. Dicyandiamide 4.2 g. NH_4NO_3 8.0 g.

the heat of reaction of each reaction must be be determined. For this purpose, the heats of combustion and formation of dicyandiamide and biguanide mononitrate were measured by the usual method (calorimetrical), which were found to be as follows.

Substance	Heat of combustion per g.	Heat of combustion per mol. at constant pressure	Heat of formation per mol. from its elements at constant pressure** (ΔH_f)
Biguanide mononitrate	2274 cal	371.49 Kcal	−90.9 Kcal
Dicyandiamide	3926 cal	329.40 Kcal*	3.76 Kcal

* Later, the heat of combustion of dicyandiamide was measured by Salley and Gray (*J. Am. Chem. Soc.*, **70**, 2650 (1948)), his figure being 331.88 Kcal/mol.

** The heats of formation from the elements, ΔH_f, were calculated using 94.45 and 68.37 Kcal/mol. (18°C) for the heat of formation of gaseous carbon dioxide and of liquid water, respectively.[5] But recently, for these values, 94.05 and 68.32 Kcal/mol. (25°C, 1 atm.) seem to be used commonly.

For the heats of formation of ammonium nitrate and guanidine nitrate, the following data were taken from the literature.

Ammonium nitrate[5] ΔH_f/mol. −87.1 Kcal.,

Guanidine nitrate[5] ΔH_f/mol. −91.8 Kcal.

Then the heats of reaction of following reactions could be calculated which were given as follows.

$$NH_2\cdot C(NH)\cdot NH\cdot CN + NH_4NO_3 = (NH_2\cdot C(NH)\cdot NH\cdot C(NH)\cdot NH_2)HNO_3 + 7.6 \text{ Kcal}$$
$$(NH_2\cdot C(NH)\cdot NH\cdot C(NH)\cdot NH_2)HNO_3 + NH_4NO_3 = 2(NH_2\cdot C(NH)\cdot NH_2)HNO_3 + 5.6 \text{ Kcal}$$
$$NH_2\cdot C(NH)\cdot NH\cdot CN + 2NH_4NO_3 = 2(NH_2\cdot C(NH)\cdot NH_2)HNO_3 + 13.2 \text{ Kcal}.$$

These data seemed to correspond to the heat evolution in two heating curves.

c) The thermal decomposition of biguanide monosalt under fused state was found to give guanidine salt quantitatively as shown in Table III. Melamine was also found in a fair yield in the reaction product.

The most important observation was the existence of regenerated dicyandiamide in the reaction product when biguanide monosalt was cautiously decomposed under fused state at 190–195°C for 2–3 minutes so as to

5) Bichowsky und Rossini, "Thermochemistry of Chemical Substances," (Reinhold Publ. Corp.) 34 (1936).

* The same results were obtained using chloride or sulfate.

6) Calculated by the author from the data of Matignon, *Chem. Centr.*, (1892) II, 199.

TABLE III

Biguanide-mononitrate: 10.00 g. (m.p. 202–3°C).
Conditions: According to Fig. 3.

Guanidine nitrate*		Melamine**		
(g.)	(%)	From solution	From insoluble residue of water extraction (1.67 g.)	(%)
7.31	98.3	0.54	1.05	62
7.20	96.8	1.59 g. —		—

* Determined as picrate and reduced to nitrate.
** The amount of melamine is not quantitative.

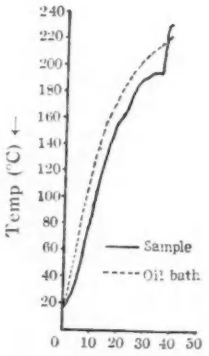

Fig. 3.

prevent spontaneous superheating due to the melamine formation*. For this purpose, about 2.0 g. or less amount of the sample must be used at a time. By extracting the pulverized reaction product by acetone and evaporating the extract to dryness, the crystal of dicyandiamide could be obtained. (From 15.00 g. of the reaction product, about 0.80 g. of dicyandiamide melting at 200°C was isolated. The melting point of the mixture of the sample with pure dicyandiamide was 203–205°C).

Then, the thermal decomposition of biguanide mononitrate may be represented as follows:

$$(NH_2\cdot C(NH)\cdot NH\cdot C(NH)\cdot NH_2)HNO_3 = (NH_2\cdot C(NH)\cdot NH_2)HNO_3 + NH_2\cdot CN$$
$$NH_2\cdot CN = 1/3\, C_3H_6N_6$$
$$(NH_2\cdot C(NH)\cdot NH\cdot C(NH)\cdot NH_2)HNO_3 = (NH_2\cdot C(NH)\cdot NH_2)HNO_3 + \tfrac{1}{2}NH_2C(NH)\cdot NH\cdot CN$$

As the result of these ovservations, the author proposed a mechanism which is summarised as follows.

1) Dicyandiamide is first converted into biguanide monosalt by the addition of 1 mol. of ammonium salt.

$$NH_2\cdot C(NH)\cdot NH\cdot CN + NH_3\cdot HX = (NH_2\cdot C(NH)\cdot NH\cdot C(NH)\cdot NH_2)HX \quad (1)$$

2) Biguanide monosalt is next converted into 1 mol. of guanidine salt and 1 mol. of cyanamide or ½ mol. of dicyandiamide by the thermal decomposition.

$$(NH_2\cdot C(NH)\cdot NH\cdot C(NH)\cdot NH_2)HX = (NH_2\cdot C(NH)\cdot NH_2)HX + NH_2\cdot CN \quad (2)$$
$$(NH_2\cdot C(NH)\cdot NH\cdot C(NH)\cdot NH_2)HX = (NH_2\cdot C(NH)\cdot NH_2)HX + \tfrac{1}{2}NH_2\cdot C(NH)\cdot NH\cdot CN \quad (2')$$

3) The cyanamide or dicyandiamide formed in nascent state, reacts immediately with ammonium salt to give 1 mol. of guanidine salt or 0.5 mol. of biguanide monosalt successively.

$$NH_2\cdot CN + NH_3\cdot HX = (NH_2\cdot C(NH)\cdot NH_2)HX \quad (3)$$
$$\tfrac{1}{2}NH_2\cdot C(NH)\cdot NH\cdot CN + \tfrac{1}{2}NH_3\cdot HX = \tfrac{1}{2}(NH_2\cdot C(NH)\cdot NH\cdot C(NH)\cdot NH_2)HX \quad (3')$$

The biguanide monosalt formed according to the reaction (3') is again decomposed to guanidine salt and dicyandiamide (2'). The reaction (2) and (3) may take place at higher temperatures (at least above 160°C), whereas the reaction (2') and (3') at lower temperatures.

II. Mechanism of the Reaction between Dicyandiamide and Aniline Hydrochloride

The mechanism of the reactian between dicyandiamide and aniline hydrochloride was studied in order to generalise the mechanism of guanidine formation by the reaction between dicyandiamide and ammonium salt.

In this case, it was well known that the phenylbiguanide-HCl (the primary reaction product) was formed quantitatively.[7] Then,

* The heats of reaction of (2), (2') are endothermic.

7) Lumière and Perrin, *Buli. soc. chim.*, [3] **33**, 205 (1905). Sugino et al, *Japanese Patent* 125272.

TABLE IV

Phenylbiguanide-HCl 15.00 g. (molar ratio 1)

Conditions* (A) 230°C. 2 min.
(B) 230°C. 2 min. after the heat evolution.
(C) 220–230°C. 2 min.

Reaction	Product	Monophenylguanidine***		Guanidine***		Diphenylguanidine		Inosoluble residue of Boiling water extraction (melamine derivatives)	Others
		Yield** (g.)	Molar ratio	Yield** (g.)	Moler ratio	Yield** (g.)	Molar ratio	Yield** (g.)	Yield** (g.)
(A) Thermal decomposition of phenylbiguanide-HCl		2.70	0.29	1.26	0.30	—	—	3.38	—
		2.81	0.30	0.96	0.23			3.40	2.87
(B) Reaction with ammonium chloride (3.78 g.)		4.68	0.49	1.88	0.45	—	—	1.66	1.57
(C) Reaction with aniline-HCl (9.12 g.)		4.72	0.50	0.67	0.16	5.55	0.37	3.22	2.40

* The mixture melted at (A) 237°C., (B) 230°C. and (C) 185°C. respectively and a small heat evolution occurred spontaneously at about 230°C. By maintaining the mixture at that temperature for 2–3 minutes after the heat evolution, no phenylbiguanide was already present in the fused mass.

** Due to the difficulty of the perfect separation of each product, the yield did not mean the total amount of each product and a part of them may be included in "others". But these data may seem to be useful to compare the amount of each reaction product between three reactions.

*** Determined as picrate and reduced to free base.

TABLE V

SCHEMES OF THE METHOD OF THE SEPARATION OF EACH REACTION PRODUCT

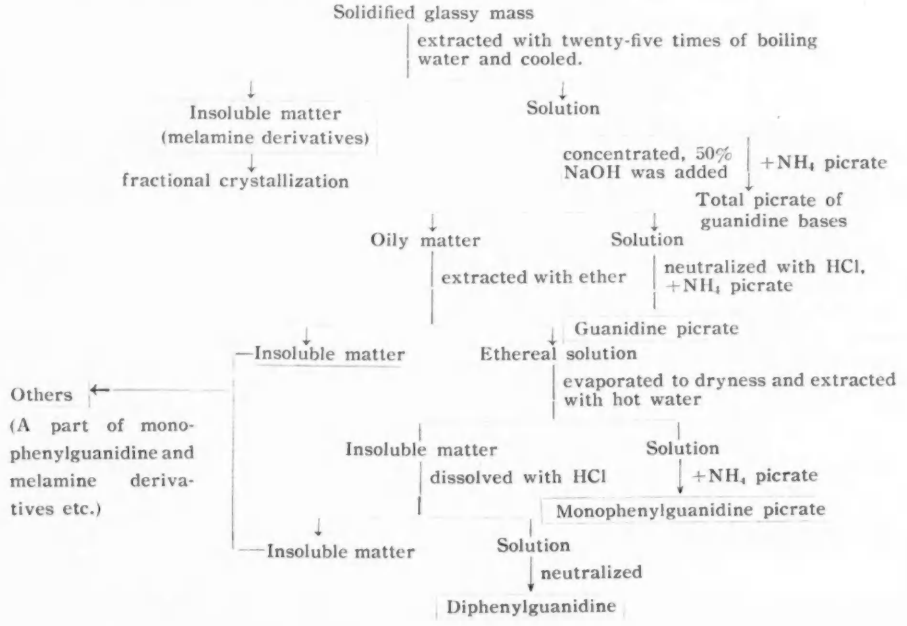

in fused state, the thermal decomposition of phenylbiguanide-HCl and the reaction between phenylbiguanide-HCl and aniline-HCl or ammonium chloride were studied successively.

An example of the quantitative separation of the products of three reactions is shown in Table IV and the method of the separation of each reaction product is also schematically shown in Table V.

It was first observed that the thermal decomposition of phenylbiguanide-HCl in fused state gave not only phenylguanidine-HCl, but also guanidine-HCl. This reaction may be represented as follows by referring the mechanism of the thermal decomposition of biguanide monosalt.

$$(C_6H_5NH\cdot C(NH)\cdot NH\cdot C(NH)\cdot NH_2)HX \longrightarrow \begin{cases} (C_6H_5NH\cdot C(NH)\cdot NH_2)HX + NH_2\cdot CN \\ (NH_2\cdot C(NH)\cdot NH_2)HX + C_6H_5NH\cdot CN \end{cases}$$

If an amine salt should be existed in the reaction mixture, the cyanamides formed would react immediately to give corresponding guanidine salts. So, by the use of ammonium salt, the salt of phenylguanidine and guanidine may be formed.

$$NH_2\cdot CN + NH_2\cdot HX \rightarrow (NH_2\cdot C(NH)\cdot NH_2)HX$$
$$C_6H_5NH\cdot CN + NH_2\cdot HX \rightarrow (C_6H_5NH\cdot C(NH)\cdot NH_2)HX$$

Also by the use of aniline HCl, the formation of the salt of phenylguanidine and diphenylguanidine may be expected.

$$NH_2\cdot CN + C_6H_5NH_2\cdot HX \rightarrow (C_6H_5NH\cdot C(NH)\cdot NH_2)HX$$
$$C_6H_5NH\cdot CN + C_6H_5NH_2\cdot HX \rightarrow (C_6H_5NH\cdot C(NH)\cdot NHC_6H_5)HX$$

The latter two reactions were verified by the experiment. By the fusion of cyanamide (1 mol.) or phenylcyanamide (1 mol.) with aniline HCl (1 mol.), the salt of phenylguanidine or diphenylguanidine was obtained in yield as high as 96% and 92% respectively.

As the result of these successive reactions, a rough estimate of the ratio of the amount of phenylguanidine, guanidine and diphenylguanidine formed by the following reactions may be as follows.

(A) Thermal decomposition of phenylbiguanide-HCl.

(B) The reaction of phenylbiguanide-HCl with ammonium chloride.

(C) The reaction of phenylbiguanide-HCl with aniline HCl.

	Monophenylguanidine	Guanidine	Diphenylguanidine
(A)	1	1	0
(B)	2	2	0
(C)	2	1	1

The results shown in Table IV were in good agreement with this conclusion. But in the reaction (C), the amount of diphenylguanidine seemed to be somewhat larger than that of the other two guanidines. By referring the result of methylbiguanide described later, it is generally noticed that the proportion of different kinds of guanidines formed in these reactions may depend upon the substituent of biguanide as later indicated by Oxley and Short.[8]

If the sufficient amount of amine salt should not exist in the thermal decomposition of phenylbiguanide-HCl, the cyanamides formed might react together and form a mixture of melamine derivatives. Throughout the above three reactions, some amount of melamine derivatives could always be found in the reaction product as shown in Table IV. Melamine derivatives from the reaction (A) and reaction (B) were found to consist mainly of the same compound which was identified as 2.4-dianilino-6-amino-s-triazine (diphenylmelamine). This compound could be synthetized by the mutual reaction of phenylcyanamide and cyanamide.

2.4-dianilino-6-amino-s-triazine.

From the reaction A.

M. p. 201–205°C., m. p. of picrate: 272°C.

Found: C, 64.72, 64.78, H, 5.93, 5.54, N, 30.22

From the reaction B.

M. p. 208–210°C., m. p. of picrate: 272°C.

Found: C, 64.71, 64.76, H, 5.23, 5.58, N, 31.27

From the mutual reaction of phenylcyanamide and cyanamide.

M. p. 197–202°C., m. p. of picrate: 272°C.

Found: C, 64.75, 64.75, H, 5.50, 5.38, N, 29.69

Calc. for $C_{15}H_{14}N_6$: C, 64.74, H, 5.05, N, 30.21

By summarizing these observations, the author determined the mechanism of the reaction between dicyandiamide and aniline-HCl which are now believed to be as follows.

$$NH_2\cdot C(NH)\cdot NH\cdot CN + C_6H_5NH_2\cdot HX = (C_6H_5NH\cdot C(NH)\cdot NH\cdot C(NH)\cdot NH_2)HX \quad (1)$$

$$(C_6H_5NH\cdot C(NH)\cdot NH\cdot C(NH)\cdot NH_2)HX \longrightarrow \begin{cases} (C_6H_5NH\cdot C(NH)\cdot NH_2)HX + NH_2\cdot CN & (2) \\ (NH_2\cdot C(NH)\cdot NH_2)HX + C_6H_5NH\cdot CN & (2') \end{cases}$$

$$NH_2\cdot CN + C_6H_5NH_2\cdot HX = (C_6H_5NH\cdot C(NH)\cdot NH_2)HX \quad (3)$$
$$(NH_2\cdot CN + NH_2\cdot HX = (NH_2\cdot C(NH)\cdot NH_2)HX)$$

$$C_6H_5NH\cdot CN + C_6H_5NH_2\cdot HX = (C_6H_5NH\cdot C(NH)\cdot NHC_6H_5)HX \quad (3')$$
$$(C_6H_5NH\cdot CN + NH_2\cdot HX = (C_6H_5NH\cdot C(NH)\cdot NH_2)HX)$$

8) Oxley and Short, *J. Chem. Soc.*, **1951**, 1252.

$$2C_6H_5NH\cdot CN + NH_2\cdot CN \rightarrow H_2N-\underset{\displaystyle N}{\overset{\displaystyle N}{\overset{\diagup\!\!\diagdown}{C}}}-C-NHC_6H_5 \quad (4)$$
$$\underset{\displaystyle N}{\overset{\displaystyle N}{\overset{\diagup\!\!\diagdown}{C}}}$$
$$NHC_6H_5$$

In the case of phenylbiguanide salt (a unsymmetrical biguanide), two reactions take place in the thermal decomposition. It is converted to (a) phenylguanidine salt and cyanamide and (b) guanidine salt and phenylcyanamide (2), (2′). The cyanamides formed in nascent state react immediately with amine salts and the corresponding salts of guanidines are formed (3), (3′). Some of the cyanamides react together and the phenyl derivatives of melamine (for example: 2.4-dianilino-6-amino-s-triazine (diphenylmelamine)) are obtained as byproducts (4).

III. Mechanism of the Reaction between Dicyandiamide and Methylamine Hydrochloride

The mechanism of the reaction between dicyandiamide and methylamine-HCl was also studied and was found to be almost the same as the case of aniline-HCl. For this purpose, a quantitative study of the following reactions was carried out just the same as in the case of the reaction between dicyandiamide and aniline-HCl.

1. The preparation of pure methylbiguanide-HCl.
2. The thermal decomposition of methylbiguanide-HCl.
3. The reaction between 1 mol. of methylbiguanide-HCl and 1 mol. of ammonium chloride.
4. The reaction between 1 mol. of methylbiguanide-HCl and 1 mol. of methylamine-HCl.
5. The reaction between 1 mol. of dicyandiamide and 2 mol. of methylamine-HCl.

The results obtained are summarized in Table VI.

TABLE VI

Methylbiguanide-HCl: 7.58 g. (molar ratio 1)
Conditions:* Temp. 190°C., Time 2 hrs.

Reaction \ Product	Methylguanidine picrate		Guanidine picrate		Dimethylguanidine picrate	Insoluble residue of water extraction (100 cc.)	Picrate of melamines**
	Yield (g.)	Molar ratio	Yield (g.)	Molar ratio	Yield (g.)	Yield (g.)	Yield (g.)
(A) Thermal decomposition of methylbiguanide-HCl	7.47	0.49	5.46	0.38	—	0.24	0.84
(B) Reaction with ammonium chloride, 2.68 g. (Molar ratio 1:1)	13.09	0.87	12.18	0.85	—	trace	
(C) Reaction with methylamine-HCl, 3.38 g. (Molar ratio 1:1)	15.89	1.05	5.51	0.38	undetermined	nearly zero	
(D) Reaction of dicyandiamide (4.20 g.) with methylamine-HCl, 6.75 g. (Molar ratio 1:2)	17.87	1.18	3.55	0.25	undetermined	trace	

* After two hours and at that temperature, no methylbiguanide was present in the fused mass.

** M.p. 282°C.

The preparation of methylbiguanide-HCl was carried out as follows.

Dicyandiamide (1 mol.) / Methylamine-HCl (1 mol.) —fused at 120-130°C, for 1 hr.→ —dissolved in hot water— < Insoluble matter / Filtrate — $CuCl_2$ (or CuCl) NH_3 soln. was added— < Filtrate / Pink colored precipitate —dissolved in HCl soln. / treated with H_2S→ CuS / Filtrate —evaporated→ Crude Methylbiguanide-2HCl —recrystallization from 80-90% alcohol→ Pure Methylbiguanide-2HCl —dissolved in water and neutralized with equiv. amount of NaOH→ NaCl / Methylbiguanide-HCl —extracted with abs. alcohol→ Pure Methylbiguanide-HCl.

The separation of methylguanidine and guanidine from the reaction mixture could be performed successfully by using the difference of the order of precipitation of those picrates. By adding a saturated solution of ammonium picrate in the reaction mixture, guanidine picrate was first precipitated and when the precipitation of guanidine picrate was almost completed, methylguanidine picrate began to precipitate. So, by carrying out the precipitation cautiously and also recrystallizing, those two picrates could be separated almost completely.

The results seemed to be very similar to that of the reaction of phenylbiguanide-HCl. First, methylbiguanide-HCl also yielded both the salt of methylguanidine and guanidine by the thermal decomposition in fused state just the same as in the case of phenylbiguanide-HCl. Cyanamide and methylcyanamide which were supposed to form at the same time reacted together to give melamine derivatives. By the presence of a suitable amount of an amine salt in the reaction mixture, these cyanamides, if they existed, must be converted to corresponding guanidines. In the case of NH_4Cl, therefore, guanidine and methylguanidine may be obtained and in the case of methylamine-HCl, methylguanidine and sym-dimethylguanidine may also be expected to form. So, similar to the case of phenylbiguanide, a rough estimate of the ratio of the amount of methylguanidine and guanidine formed by the following reactions may be expected as follows:—

(A) The thermal decomposition of methylbiguanide-HCl.

(B) The reaction between methylbiguanide HCl and ammonium chloride.

(C) The reaction between methylbiguanide HCl and methylamine-HCl.

	Methylguanidine	Guanidine
(A)	1	1
(B)	2	2
(C)	2	1

The results shown in Table VI were in good agreement with this assumption. The result of the reaction between 1 mol. of dicyandiamide and 2 mol. of methylamine HCl (D) was found to be almost the same as that of the reaction (C), but the amount of methylguanidine was somewhat larger than in the latter case.

About sym-dimethylguanidine, its confirmation was not carried out in the above experiment. But now, Mr. R. Kitawaki of my laboratory, has again been studying the same reaction in order to confirm this compound in the reaction product. He succeeded in isolating about 9.0 g. of N, N′-dimethylguanidine picrate from the reaction product obtained by the fusion of 21.0 g. of Dicyandiamide with 33.8 g. of methylamine-HCl at 190°C for 1 hr*.

M. p. 159–160°C.

After recrystallization: m. p. 172–4°C.

m. p. of N, N′-dimethylguanidine-HCl derived from the purified picrate: 151–2°C.

m. p. of the mixture of these samples with the same salts of N, N′-dimethylguanidine prepared by the reaction of methylamine with iodocyan or of monomethylcyanamide with methylamine. HCl.*

	Known sample	Mixture
picrate	177°C	175°C
hydrochloride	154°C	153–4°C

As the result of these observations, the mechanism of this reaction could also be formulated as follows.

$$NH_2\cdot C(NH)\cdot NH\cdot CN + CH_3NH_2\cdot HX = (CH_3NH\cdot C(NH)\cdot NH\cdot C(NH)\cdot NH_2)HX \quad (1)$$

$$(CH_3NH\cdot C(NH)\cdot NH\cdot C(NH)\cdot NH_2)HX \rightarrow (CH_3NH\cdot C(NH)\cdot NH_2)HX + NH_2\cdot CN \quad (2)$$

$$\rightarrow (NH_2\cdot C(NH)\cdot NH_2)HX + CH_3NH\cdot CN \quad (2')$$

$$NH_2CN + CH_3NH_2\cdot HX = (CH_3NH\cdot C(NH)\cdot NH_2)HX \quad (3)$$

$$(NH_2CN + NH_3\cdot HX = (NH_2\cdot C(NH)\cdot NH_2)HX)$$

$$CH_3NH\cdot CN + CH_3NH_2\cdot HX = (CH_3NH\cdot C(NH)\cdot NHCH_3)HX \quad (3')$$

$$(CH_3NH\cdot CN + NH_3\cdot HX = (CH_3NH\cdot C(NH)\cdot NH_2)HX)$$

Mutual reaction of cyanamides $\rightarrow$ Melamine derivatives (4)

In this case, the thermal decomposition of methylbiguanide hydrochloride takes place mainly to the side of methylguanidine formation (2), (This may be the influence of CH_3-group discribed above.) therefore the reaction product consisting of mainly methylguanidine-HCl and the amount of guanidine-HCl seemed to be relatively small. Also, a small amount of N, N′-dimethylguanidine was successifully found in it.

In 1922 Werner[9] also had carried out the reaction between dicyandiamide and methylamine-HCl. He supposed that methylguanidine was only the reaction product according to his supposed mechanism.

$$C_2H_4N_4 \rightleftharpoons 2NH_2CN$$

$$2NH_2CN + 2CH_3NH_2\cdot HX = 2(CH_3NH\cdot C(NH)\cdot NH_2)HX$$

$$C_2H_4N_4 + 2CH_3NH_2\cdot HX = 2(CH_3NH\cdot (NH)\cdot NH_2)HX$$

* Unpublished papers of R. Kitawaki,

9) Werner, *J. Chem. Soc.*, **121**, 1790 (1922).

He obtained a picrate which melted at 285°C. and supposed it to be methylguanidine picrate. But the melting point of methylguanidine picrate is about 200°C according to many other researches.[10] This erroneous observation induced the following two erroneous explanations of other investigators. Schenck[11] supposed the picrate obtained by Werner to be ethylenediguanidine picrate and also Kapeller[12] supposed the same picrate to be a mixture of dicyandiamide and picric acid. These observations, of course, were also erroneous. This question continued to be unsolved till 1943, when the author has again studied this reaction.

The author also obtained a picrate melted at 285°C in the reaction product of this reaction. According to the author's mechanism, it was obviously certain that this picrate was a mixture of a large amount of guanidine picrate and a small amount of methylguanidine picrate. It was first formed by adding the picrate solution in the solution of reaction product due to the difference of precipitation velocity of two picrates.

In conclusion, the author wishes to express his thanks to Mr. M. Yamashita for his valuable collaboration in the part III of this research.

Laboratory of Organic Electrochemistry,
Department of Chemical Engineering,
Tokyo Institute of Technology,
Ookayama, Tokyo

10) Phillips, Clarke, *J. Am. Chem. Soc.*, **45**, 1756 (1923).
11) Schenck, *Z. physiol. Chem.*, **155**, 306 (1926).
12) Kapeller, *Ber.*, **59**, 1652 (1926).

Electrolytic Reduction of Dicyandiamide

By Kiichiro SUGINO

(Received April 19, 1954)

This contribution is the abstract of my paper[1] already published in Japanese in the Journal of the Chemical Society of Japan in 1939. Some new and revised explanations are added.

For the structure of dicyandiamide, Bamberger[2] proposed cyanoguanidine formula ($NH_2 \cdot C(NH) \cdot NH \cdot CN$) and with this, he could explain very smoothly the formation of guanidine and methylamine from dicyandiamide by the reduction with Zn and HCl (1893). Bell[3] (1926) however, repeated this experiment and he found that by hydration preceding the reduction (even in cold solution), guanylurea was formed instead and consequently he was led to adopt the original cyclic formula for dicyandiamide. So, it seemed to me that there were many problems regarding the reduction of dicyandiamide. For these reasons, an investigation was made to answer the following two questions.

1. Does dicyandiamide reduce directly ?
2. What kinds of products are given by the reduction ?

As the result of many experiments, it was found that dicyandiamide could be reduced directly only by the electrolytic reduction under special conditions (1% aq. solution of dicyandiamide acidified with H_2SO_4 amounting to 1%).

I. The case in which the electrolysis was stopped so as to let the catholyte remain acidic.

The conditions and the results obtained are shown in Table I.

A new compound (a base) was found to be formed by the following reduction.

$$C_2H_4N_4 + 4H \rightarrow C_2H_8N_4$$

This new compound seemed to be very unstable and could exist only in an acidic medium at room temperature. So, when the electrolysis was stopped so as to let the catholyte still remain acidic and a saturated solution of picric acid was added to the catholyte, the new compound could be precipitated as dipicrate.

Color: Light yellow (plate or needle)

m.p.: It has not the accurate melting point. It began to sinter at 180–200°C and decomposed at 220–230°C.

Found: C, 30.74, 30.62; H, 2.87, 2.70; N, 25.61, 25.62, 25.65.

Calc. for $C_{14}H_{14}N_{10}O_{14}$: C, 30.77, H, 2.56, N, 25.64%.

It was also observed that the dipicrate was easily hydrolysed to give guanidine picrate,

1) K. Sugino, *J. Chem. Soc. Japan*, **60**, 111, (1939); *C.A.*, **34**, 2795 (1940).
2) Bamberger, *Ber.*, **26**, 1584, 1585 (1893).
3) Bell, *Sci. Proc. Roy. Dublin Soc.*, **18**, 207~10 (1926); *C.A.*, **21**, 2444 (1927).

TABLE I

Catholyte			Electrode		Cathodic current density	Time	Temp.	Quantity of electricity consumed*	pH of catholyte after electrolysis	Reaction Product			
Dicyandiamide	H_2O	Conc. of H_2SO_4	Cathode	Anode						(1) Picrate of intermediate product weighed	(2)** Guanidine picrate obtained by the hydrolysis of catholyte	(3)** Picrate of intermediate product calculated from (2)	Yield of intermediate product (Aminomethylene guanidine)
(g.)	(cc.)	(%)			(A/dm²)	(hr.)	(°C)	(Ahr.)		(g.)	(g.)	(g.)	(%)
1.00	100	1	Hg	Pt	0.8–1.0	2.3	20–24	1.103	acidic	1.91	—	—	—
1.00	100	1	Hg	Pt	1.0	2.0	26	1.031	acidic	1.72	1.01	1.91	29
1.00	100	1	Pb	Pb	1.0	2.5	23	1.010	acidic	2.80	1.61	3.05	47
1.00	100	1	Pb	Pb	1.0	2.5	23	0.982	acidic	2.77	1.62	3.07	47

* Theoretical value for intermediate product. 1.243.
** (2), (3): Quantitative determination of the new compound. It was carried out as follows:
This compound was converted to guanidine by the hydrolysis according to the reaction (2) in the catholyte and resulting guanidine was weighed as picrate, by which the amount of picrate of original intermediate compound was calculated.

TABLE II

Catholyte			Electrode		Cathodic current density	Time	Temp.	Quantity of electricity consumed	pH of catholyte after electrolysis	Reaction Product			
Dicyandiamide	H_2O	Concentration of H_2SO_4	Cathode	Anode						Guanidine picrate*		Amine-HCl** (mainly ammonium chloride)	
(g.)	(cc.)	(%)			(A/dm²)	(hr.)	(°C)	(Ahr.)		(g.)	(g.)	(g.)	(%)
1.01	100	1	Hg	Pt	1.0–0.46	—	20–23	2.66	alkali	1.56	46	Undetermined	—
1.00	100	1	Hg	Pt	1.0	7.6	20–23	3.76	alkali	1.31	38	0.40	62
1.01	100	1	Pb	Pb	1.0	6.3	20–23	2.96	alkali	0.89	26	0.88	138

* m.p. 320°C.
Found: N, 29.28.
Calc. for $C_7H_8N_6O_7$: N, 29.16%.
** m.p. above 250°C.
The existence of methylamine was verified by its characteristic odour and also the positive result for chloranil test.

ammonium picrate and formaldehyde almost quantitatively when its aqueous solution was boiled or made alkaline at room temperature.

Guanidine picrate: Yield: 94–120% of the theoretical value* m.p.: 320°C Found: C, 29.50; H, 2.77; N, 29.37 Calc. for $C_7H_8N_6O_7$: C, 29.17; H, 2.80; N, 29.16%.

Ammonium picrate: Long needle, m.p. 280°C (decomp.), Ammonia was evolved quantitatively by heating its aqueous solution with caustic alkali.

Formaldehyde: Yield, 93% of the theoretical value* (determined by the iodometric titration)

The compound itself, in the catholyte, was also found to be hydrolysed to give the same products when the catholyte was treated in the same manner as described above. From these observations, it was concluded that this compound has the constitution of amino-methylene guanidine.

$$NH_2\cdot C(NH)\cdot NH\cdot CH_2\cdot NH_2$$

The hydrolysis of the compound (and its dipicrate) may be represented by the following reaction.

$$NH_2\cdot C(NH)\cdot NH\cdot CH_2\cdot NH_2+H_2O=NH_2\cdot C(NH)\cdot NH_2+NH_3+CH_2O \quad \cdots\cdots(2)$$

$$C_2H_8N_4\cdot 2C_6H_2(NO_2)_3OH+H_2O=CH_5N_3\cdot C_6H_2(NO_2)_3OH+NH_3\cdot C_6H_2(NO_2)_3OH+CH_2O \quad \cdots\cdots(2')$$

II. The case in which the electrolysis was continued till the catholyte became alkaline.

When the electrolysis was continued till the catholyte became alkaline, reaction (2) occurred spontaneously and guanidine, ammonia and formaldehyde were obtained as the final products. But a small part of $C_2H_8N_4$ was reduced to guanidine and methylamine.

$$C_2H_8N_4+2H=NH_2\cdot C(NH)\cdot NH_2+CH_3\cdot NH_2 \quad \cdots\cdots(3)$$

An example of the results is shown in Table II.

In the high acid concentration of the catholyte, dicyandiamide was first hydrated to guanylurea, which was hardly further reduced in the acidic medium.

From the results of the author, he is induced to think that Bell's conclusion is erroneous and he agrees with Bamberger's one that dicyandiamide is directly reduced. But the author's final reduction products were entirely different from Bamberger's one. And the author's results showed that dicyandiamide should have both guanidine group and N-CN linkage, the latter of which behaves somewhat differently from usual nitrile. By referring the result of Hughe's X-ray analysis later published[4] (1940), the structure of dicyandiamide may be represented as guanylcyanamide rather than cyanoguanidine.

Laboratory of Organic Electrochemistry, Department of Chemical Engineering, Tokyo Institute of Technology

* Refer to the reaction (2).

4) Hughes, *J. Am. Chem. Soc.*, **62**, 1258 (1940).

Investigation on the Molecular Structure of Monochloroacetamide by Gas Electron Diffraction and Dipole Moment

By Masao KIMURA, Michiro AOKI, and Yukio KURITA

(Received May 6, 1954)

In the previous investigation, the molecular structures of acetamide and N-methylacetamide were determined by electron diffraction[1]. It was pointed out that the bond length of the peptide bond in gaseous acetamide is longer than that in the crystalline proteins determined by Corey et al.[2] and that the difference is due mainly to the hydrogen bond present in a crystal.

The present investigation deals with the structure of monochloroacetamide. Since the molecule has a carbon-carbon bond as a rotational axis, it is of interest to determine the rotational structure and the bond length of a peptide bond.

Experimental Method and Results

[I] Electron Diffraction.—Since monochloroacetamide is in the crystalline state at room temperature, it was vaporized through a high temperature nozzle[1]. The feature, and the positions of the maxima and the minima were estimated by a visual method and are shown in Fig. 2V and in Table I respectively. Here $q=10s/\pi$ and $s=4\pi\sin(\theta/2)/\lambda$. Since the observed q values

1) M. Kimura and M. Aoki, This Bulletin, **26**, 429 (1953).
2) R. B. Corey and J. Donohue, *J. Am. Chem. Soc.*, **72**, 2899 (1950).

TABLE I

OBSERVED q VALUES FOR MONOCHLOROACETAMIDE

Max.	Min.	q	Max.	Min.	q
1		10.6	7		42.7
	2	13.7		8	44.7
2		16.6	8		46.6
	3	19.3		9	49.7
3		21.5	9		52.6
	4	24.4	10		58.5
4		27.3	11		63.2
	5	30.0	12		68.2
5		32.5	13		73.8
	6	34.1	14		79.3
6		37.0	15		83.1
	7	39.7	(16)		91.4
			(17)		96.8

were inaccurate for the minima beyond $q=50$, they were omitted from Table I and were not used for the quantitative comparison with the theoretical values. In Fig. 2V, the features of the 16th and 17th maxima are drawn by a dotted line since they are not very accurate and the first maximum was estimated by use of the theoretical intensity curves to be mentioned later.

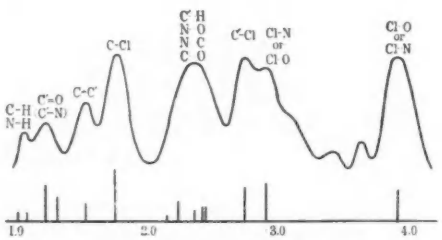

Fig. 1. The radial distribution curve for monochloroacetamide. The vertical bars under the curve show the interatomic distances r_{ij} and $z_i z_j / r_{ij}$ for the structure determined by the present investigation.

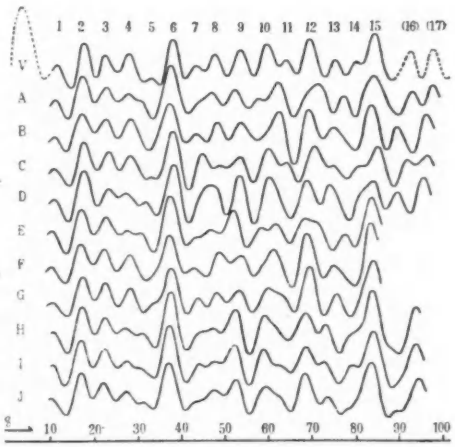

Fig. 2. The visual and theoretical curves for monochloroacetamide.

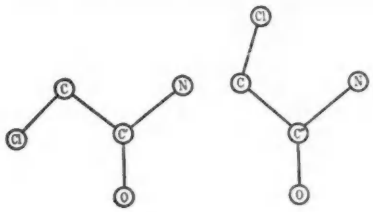

trans cis

Fig. 3. Monochloroacetamide.

The radial distribution curve,

$$rD(r)=\sum_{q=1}^{q_7} I(q)\exp(-aq^2)\sin(\pi qr/10),$$

calculated by use of the visual curve (Fig. 2V) is shown in Fig. 1, where a was chosen as $\exp(-aq^2_{\max})=0.1$. The pair of atoms corresponding to each peak is also indicated in Fig. 1. The peak corresponding to C-Cl bond is very sharp and its bond length was determined to be 1.75 Å. C-C′ and C′-Cl interatomic distances could also be determined to be 1.53 Å (the same value as those determined for C-C bond in acetamide, N-methylacetamide[1], glycyl-glycine, etc.[2]) and 2.73 Å respectively, although less accurate than that of a C-Cl bond. The other interatomic distances could not be determined owing to overlapping with the contributions from various interatomic distances (cf. Fig. 3). From the values obtained above, ∠C′CCl can be obtained to be about 113°. The peaks at 2.89 Å and 3.89 Å correspond to Cl···N and Cl···O interatomic distances. From these results alone, we cannot determine the form of the molecule. However, since two peaks are very distinct and are separated from each other by about 1 Å, it is reasonable to consider that the molecule is in the trans or cis configuration, at least approximately.

The theoretical intensity curves were calcutated with the simplified equation,

$$I(q)=\sum_{i\neq j}\sum z_i z_j \exp(-b_{ij}q^2)\sin(\pi r_{ij}q/10)/r_{ij}.$$

Here z_i and z_j are atomic numbers for the ith and jth atoms respectively, and r_{ij} is the interatomic distance between the ith and jth atoms. A factor $\exp(-b_{ij}q^2)$ is related to intramolecular vibrations. The intramolecular vibrations did not affect the features of the theoretical intensity curves, except the rotational vibration about a C-C′ bond. Therefore the theoretical curves were mostly calculated for fixed models. When the rotational vibration was taken into account, b_{ij} was taken as 0.0004 for both Cl-O and Cl-N. Some of the intensity curves are reproduced in Fig. 2.

Since there are many parameters involved, we had to be satisfied with an analysis with some assumptions. We used C-Cl=1.75 Å and ∠C′CCl

=113°, which were determined from the radial distribution curve, and also assumed the structure of gaseous acetamide determined by electron diffraction[1] (A form) or the structure of crystalline acetamide suggested by Corey et al. from a probable dimension of polypeptid chain (B form). These assumptions do not contradict with the result obtained from the radial distribution curve and appear to be reasonable since the molecule may be considered to take the structure nearly equal to that of acetamide in the gaseous as well as in the crystalline state (cf. Table II). These assumptions seem to be sufficient at least to estimate the position of C—Cl bond and a probable structure of monochloroacetamide. Thus the only parameter to be adjusted is the rotational angle about a C′—C bond.

TABLE II
THE STRUCTURE OF ACETAMIDE

	A form	B form
Authors	Kimura and Aoki	Corey and Donohue
C=O	1.21	1.23
C−N	1.36	1.32
C−C′	1.53	1.53
State	gas	crystal
method	electron diffraction	X-ray diffraction

In the case of A form, the theoretical intensity curves are shown in Fig. 2 for the models having 180° (the trans configuration, Fig. 2 A), 150° (Fig. 2 B), 30° (Fig. 2 C) and 0° (the cis configuration, Fig. 2D) as rotational angles (cf. Fig. 3). When rotational angles were given values ranging from 60° to 120° the theoretical intensity curves did not agree with the visual one, as expected from the radial distribution curve, and hence are not reproduced in Fig. 2. Curves E, F, G and H are the theoretical curves for the model with B form and the same rotational angle as in curves A, B, C and D respectively. These curves are in agreement to some extent with the visual curve for the maxima in the region $q<37$. But in both A and B form, the theoretical curves (A, B, E and F) for the models having the trans configuration exactly or approximately are not in agreement with the visual one, especially in regard to the 10th and 11th maxima. Moreover in the case of A form the theoretical curve for model C is in fair agreement with the visual one. But the calculated values for the maxima beyond $q=58$ shifted to q values larger than the observed values and the features of the 7th, 8th and 9th maxima were not in agreement with the visual curue. These curves were not in agreement with the visual one, even if we took into account the rotational vibration. In the case of B form, the curves G and H did not agree with the visual one in regard to the 13th and 14th maxima. For the model with the rotational angle of 15° (curve I), however, the theoretical curve was obtained in good agreement with the visual one. When we took into account the rotational vibration for this model, we obtained curve J. In this curve, the features of the 5th maximum, the 7th, 8th and 9th maxima and minima were improved, while the features of the 10th, 11th, 14th and 15th maxima became worse. These results are due entirely to the rather large value of b_{ij}, 0.0004, which was used in the case of taking into account the rotational vibration in N-methylacetamide. Thus the theoretical curve was obtained in good agreement with the visual one by taking into account the rotational vibration with an amplitude smaller than that in N-methylacetamide. The curve is not reproduced in Fig. 2.

Thus the structure of monochloroacetamide was determined as follows: C−Cl=1.75Å, ∠C′CCl =113°, N···Cl=2.89 Å and the twisted angle from the *cis* configuration is about 15°. For the structure of the part corresponding to acetamide the following structure was assumed. : C=O=1.23Å, C−C=1.53Å, C−N=1.32Å, C−H=1.09Å, N−H= 1.02Å, ∠C′CH=109°28′, ∠CC′O=121°, ∠OC′N= 122°, ∠CC′N=117°, ∠C′NH=107°. The interatomic distances r_{ij} and z_{iz_j}/r_{ij} for the structure obtained above are shown in Fig. 1 by means of vertical bars.

[II] Dipole Moment.—The measurement was made in benzene solution at 30°C. The apparatus and the method of measurements have already been reported[3]. The results are shown in Table III.

TABLE III
DIELECTRIC CONSTANT AND DENSITY INCREMENTS OF BENZENE SOLUTIONS AT 30°C
$\epsilon_B=2.2625$, $d_B=0.86629$

$w\times10^5$	$\Delta\epsilon\times10^4$	$\Delta d\times10^5$
30.3	25	—
64.6	60	31
85.5	58	30
88.1	72	—
130.1	76	39

The measurements of dielectric constants of monochloroacetamide could not be made on solutions of concentrations exceeding 0.1 weight percent, because the solubility in benzene is rather small*. Therefore it was difficult to determine the dipole moment of monochloroacetamide very accurately. From the results shown in Table III, the dipole moment of monochloroacetamide can be estimated to be 2.2D∼2.8D. The value thus obtained may be considered to be that in an unassociated state since it was obtained from the measurement on very dilute solutions, although it is known that the molecules of acetamide and its derivatives associate in benzene solutions[4].

The moment of monochloroacetamide was calculated by the use of the valence angles determined by electron diffraction and by assuming the three valence bonds of nitrogen directed in a plane with three valence angles equal to 120°. The bond moments used are:

3) Y. Kurita, T. Nozoe and M. Kubo, This Bulletin, **24**, 10 (1951).

4) W. W. Bates and M. E. Hobbs, *J. Am. Chem. Soc.*, **73**, 2151 (1952); M. E. Hobbs and W. W. Bates, *J. Am. Chem. Soc.*, **74**, 746 (1952).

* The solubility in carbon tetrachloride is smaller than that in benzene.

C—Cl=1.5 D, C—N=0.45 D, C—H=0.4 D, C=O =2.5 D and N—H=1.3 D. The results are 1.4 D, 1.7 D, 2.6 D, 3.5 D and 4.7 D for the configuration with the rotational angles of 0° (the *cis* configuration), 30°, 60°, 90° and 180° respectively. The calculated moment of acetamide is 3.2 D with the assumptions similar to those used for monochloroacetamide. The observed value is 3.44 D[4] in benzene solution. The difference between the calculated and the observed values of acetamide will be due to the values of bond moments used, resonance effect, induction effect and solvent effect. Since monochloroacetamide may be considered to have the same degree of these effects as in acetamide, the calculated value of monochloroacetamide to be compared with the observed one is about 0.2 D larger than those mentioned above. Therefore the configuration of monochloroacetamide may be concluded to take the rotational angle of 60~30° from a comparison of the calculated values with the observed one. Even if the crudeness of the observed and the calculated values is taken into account, the configuration of monochloroacetamide is definitely far from the *trans* configuration*. The discussion on this point will be given later in some detail.

Discussion

According to the results obtained by electron diffraction, C—Cl bond takes the *cis* position to C—N bond. This is due to an electrostatic interaction between C—Cl bond and C=O bond and to a hydrogen bond across Cl···N.

The part corresponding to acetamide does not take the structure of a gaseous acetamide molecule already determined[1], but that similar to a crystalline acetamide with intermolecular hydrogen bonds. This is likely to show a larger contribution of a polar resonance form to the structure of monochloroacetamide than to gaseous acetamide. The effects of an intermolecular hydrogen bond on bond lengths were already pointed out by us in the case of acetamide[1] and hydroquinone[5] by comparing the structure in the crystalline state with that in the gaseous state and by Vaughan and Donohue in carboxylic acids, a peptide and its related compounds from the change of bond lengths owing to the change of the number and the state of hydrogen bonds in crystal[6]. The present investigation shows that an intramolecular hydrogen bond also affects the bond lengths in the molecule.

The result obtained from the measurement of dipole moment is in fairly good agreement with the result obtained by electron diffraction regarding the position of C—Cl bond. As pointed out by Kumler[7], one must take into consideration the state, in which measurements are made, in comparing observed values with calculated ones. So far the effect of a hydrogen bond has not been taken into account by us. But according to the result by electron diffraction, an intramolecular hydrogen bond is present in a gaseous monochloroacetamide molecule. The displacement of charges due to such a hydrogen bond causes mainly the increase of polarity of C=O bond and the shift of a lone pair of an oxygen atom to a hydrogen atom*. As a result, the total moment of monochloroacetamide will increase. Therefore the theoretical moment of monochloroacetamide will possibly be greater than that calculated above. If such is the case, the twisted angle of C—Cl bond from the *cis* configuration becomes smaller and agrees with the result obtained by electron diffraction better than the result mentioned in the experimental part.

Vaughan and Donohue[6] estimated the double bond characters of C=O and C—N bonds to be 70 and 30% respectively in crystalline acetamide, yielding the bond lengths of C=O and C—N equal to 1.23 Å and 1.35 Å respectively**. These values are nearly equal to those obtained in monochloroacetamide. Therefore it is highly probable that an acetamide molecule in crystal has such a structure. Moreover, the contribution of a polar resonance form will probably be smaller in gaseous acetamide than that estimated by Vaughan and Donohue in crystalline acetamide, since the bond lengths are 1.21 Å for C=O and 1.36 Å for C—N in gaseous acetamide.

Summary

1) The structure of monochloroacetamide was determined by gas electron diffraction as follows: C—Cl=1.75 Å, ∠C'CCl=113°, N···Cl=2.89Å, and the twisted angle from the *cis* configuration is about 15°. The structure of the part corresponding to acetamide is nearly equal to that of acetamide with an intermolecular hydrogen bond. This suggests that a monochlorocetamide molecule has an intra molecular hydrogen bond.

* This conclusion is not altered even in the case of the three valence bonds of nitrogen taking a pyramidal form.

5) M. Kimura and S. Shibata, presented at the 4th annual meeting of the Chem. Soc. Japan held on April 7, 1951.

6) P. Vaughan and J. D. Donohue, *Acta Cryst.*, **5**, 530 (1952).

7) W. D. Kumler, *J. Am. Chem. Soc.*, **74**, 261 (1952).

* That the dipole moment of acetamide is 3.90 D in dioxane solution, may be considered to be due to an intermolecular hydrogen bond.

** This values are definitely different from the values obtained by F. Senti and D. Harker. *J. Am. Chem. Soc.*, **62**, 2008 (1940).

2) The dipole moment of monochloroacetamide was estimated to be 2.2 D~2.8 D from the measurement in benzene solution. The observed value was compared with the calculated one. The result agrees with that obtained by electron diffraction in regard to the position of C—Cl bond. The agreement becomes better if the effect of an intramolecular hydrogen bond is taken into account.

We wish to express our thanks to Professors S. Mizushima and Y. Morino of Tokyo University who supplied us with the sample of monochloroacetamide used in this experiment. We wish also to thank Professor M. Kubo of Nagoya University for his helpful advice.

Department of Chemistry, Faculty of Science, Nagoya University, Nagoya

*The Dipole Moments and Molecular Structures of Some Substituted Tropones**

By Yukio KURITA and Masaji KUBO

(Received May 12, 1954)

In our previous paper,[1] we have reported the results of measurements of the dipole moments of tropone and some of its derivatives. The high moment of tropone revealed the importance of contribution to the normal state by the electronic structures of dipolar character and the explanation was made in terms of resonance involving cycloheptatrienium oxide structure.[2] This feature was found to be common to all tropone derivatives including tropolone as well as substituted tropolones, giving rise to the quasi-aromatic properties and other characteristic behaviors of these compounds. The purpose of the present investigation is the elucidation of the effect of various substituents on the electronic state of the tropone ring. We have measured the dipole moments of five tropone derivatives having various substituents at a carbon atom or atoms adjacent to the carbon atom of carbonyl group. All of these substituents are π-electron donors. Some of the substituent groups have an axis of free rotation capable of affecting the value of the resultant moment. The present writers have undertaken to determine the geometrical arrangements of these substituents relative to the tropone ring by means of dipole moment measurements.

Experimental Method and Results

All the measurements were made in benzene solution at room temperature. The dielectric constants were measured with the apparatus described in one[3] of our previous reports. The materials used were synthesized and purified by Nozoe and his collaborators in the laboratory of organic chemistry, Tohoku University. The modified Hedestrand's method[4] was employed throughout. The results are shown in Tables I and II, where the same notations are used as those in the previous reports.

Discussion of Results

The dipole moments of 2-bromotropone, 2,7-dibromotropone and other 2-monosubstituted tropones are summarized in Table III, in which the observed moments are compared with calculated ones. These theoretical moments have been calculated with the following assumptions. (1) The cycloheptatrienone ring has a plane regular heptagon form composed of carbon atoms. Hence the angle between C=O direction and the carbon-substituent bond is equal to 51°26′. (2) The interactions between the tropone ring and the substituent groups have been neglected. In other words, the moment of a substituted tropone has tentatively been assumed to be equal to the vector sum of the moment of tropone, 4.17 D,[1] and the bond moment of the substituent. (3) The bond moments of the substituents in cycloheptatriene are equal to the moments of corresponding substituted benzenes. This assumption may be justifiable since the treatment by molecular orbital

* Read before a symposium on tropolone chemistry held by the Chemical Society of Japan on February 6, 1954.

1) Y. Kurita, S. Seto, T. Nozoe and M. Kubo, This Bulletin, **26**, 272 (1953).

2) W. von E. Doering and F. L. Detert, *J. Am. Chem. Soc.*, **73**, 876 (1951).

3) Y. Kurita, T. Nozoe and M. Kubo, This Bulletin, **24**, 10 (1951).

4) Y. Kurita, T. Nozoe and M. Kubo, This Bulletin, **26**, 242 (1953).

TABLE I

DIELECTRIC CONSTANT AND DENSITY INCREMENTS OF BENZENE SOLUTIONS AT 25°C

	Compounds	m. p.	$w\times10^5$	$\Delta\varepsilon\times10^4$	$\Delta d\times10^5$
I	2-Bromotropone	62°[a]	223	339	98
	at 30°C		483	693	—
			665	946	—
			1341	1919	588
II	2,7-Dibromo-	170[a]—171°	341	422	143
	tropone		558	667	264
			1116	1314	571
			1357	1622	697
III	2-Mercapto-	55°[b]	142	235	49
	tropone		436	675	129
			742	1133	210
			1231	1886	355
IV	2-Aminotropone	104[c]—105.5°	148	194	—
			161	209	57
			185	255	62
			285	366	88
			358	473	107
V	2-Methylmer-	43—44°[b]	221	387	57
	captotropone		536	903	145
			707	1150	199
			714	1160	199

(a) T. Nozoe, S. Seto and S. Matsumura, *Proc. Japan Acad.*, **28,** No. 9, 483 (1952).
(b) T. Nozoe, M. Sato and K. Matsui, *Science Repts. Tohoku Univ.*, I, **37,** 211 (1953).
(c) T. Nozoe, S. Seto, H. Takeda, S. Morosawa and K. Matsumoto, ibid., **36,** 126 (1952).

TABLE II

MOLECULAR POLARIZATIONS AND DIPOLE MOMENTS

	t(°C)	ε_1	d_1(g/cc)	α	β(g/cc)	$P_{2\infty}$(cc)	R_D(cc)	μ(D)
I	30	2.2638	0.86670	14.17	0.438	530.5±3.1	38.7	4.91±0.02
II	25	2.2740	0.87102	11.72	0.546	616.8±5.5	46.5	5.27±0.03
III	25	2.2741	0.87093	15.16	0.280	427.0±0.8	38.7	4.36±0.01
IV	25	2.2729	0.87101	13.00	0.256	326.4±7.3	34.4	3.78±0.05
V	25	2.2772	0.87104	15.66	0.290	483.7±4.1	43.4	4.64±0.02

method,[5,6] the results of ultraviolet absorption spectra,[7] and the studies in organic chemistry[8] have revealed that tropone bears resemblance to benzene in regard to the introduction of substituents in their rings and that the conjugation of the ring with Br, OH, SH, NH_2, etc. in substituted tropones is significant as in the case of substituted benzenes.

In the case of substituents other than bromine, one must take into account free rotation about a single bond between the carbon atom of the ring and oxygen, sulfur or nitrogen atom. In the case of oxygen- or sulfur-containing substituent groups, moments have been calculated for three conceivable configurations, viz., *cis*, *trans* and perpendicular forms. We mean by the *cis* form the configuration in which the hydrogen atom or the methyl carbon atom attached to oxygen or sulfur atom is in the plane of the ring and is near the carbonyl oxygen. The configuration in which the hydrogen atom or the methyl carbon atom is at the greatest distance from the carbonyl oxygen is called the *trans* form. The intermediate position resulting from the rotation of freely rotating atoms or groups about the respective axes of rotation through 90° from either *cis* or *trans* form is termed the perpendicular form. In the case of aminotropone, the configuration in which the two hydrogen atoms in question are equally distant from the carbonyl oxygen and are located at the side of the carbonyl group is designated as the *cis*

5) Y. Kurita and M. Kubo, This Bulletin, **24,** 13 (1951).
6) R. D. Brown, *J. Chem. Soc.*, **1951,** 2670.
7) M. Tsuboi, This Bulletin, **25,** 366 (1952).
8) See papers by T. Nozoe and his collaborators published for the most part in the *Proc. Japan Acad. and Science Repts. Tohoku Univ.* Series I since 1950.

form. The rotation of the hydrogen atoms through 180° and 90° gives *trans* and perpendicular forms respectively in the same manner as before.

For the *cis* and *trans* forms of tropolone, mercaptotropone and their derivatives as well as for the perpendicular form of aminotropone, the lone pair orbitals belonging to the substituent groups overlap with the π-orbital of the ring to the highest extent, favoring the conjugation between the ring and the substituents. On the other hand, the perpendicular forms of tropolone and its analogues as well as the *cis* or *trans* form of aminotropone decrease the conjugation between the ring and the substituent groups. Therefore the moments of the substituents will better be approximated byth ose of alkyl derivatives rather than by those of substituted benzenes. The calculated moments using the former data are given in parentheses in Table III.

TABLE III
DIPOLE MOMENTS OF SUBSTITUTED TROPONES

Substituents	μ_{obs}(D)	μ_{calc}(C)			
Br	4.94	5.3			
Br_2	5.27	6.1			
		cis	Perpendicular	*trans*	
OH	3.53[1]	3.1	4.5	5.5	
SH	4.36	4.2	4.8	5.4	
NH_2	3.78	2.7	3.8	4.7	
OCH_3	4.72[1]	3.0	4.1 (4.7)	5.0	
SCH_3	4.64	3.6	4.6 (5.0)	5.5	
$N(CH_3)_2$	—	2.7 (3.8)	3.6	4.2 (5.0)	

In the evaluation of the calculated moments given in Table III, it has been necessary to know the components of the moments of substituents along the direction parallel to the bond between the ring carbon and oxygen, sulfur or nitrogen atom, $\mu_{\parallel}$, and those perpendicular to this direction, $\mu_{\perp}$. These components have been calculated by means of a method similar to that used by Everard and Sutton.[9] These data are given in Table IV. The calculated moments in parentheses in Table III have been obtained using the data given in Table V.

TABLE IV
DIPOLE MOMENTS OF SUBSTITUTED BENZENES

Substituents	μ(D)	$\mu_{\parallel}$(D)	$\mu_{\perp}$(D)
Br	1.57[a]	1.57	0
OH	1.56[a]	0	—1.56
SH	1.19[b]	0.85	—0.83
NH_2	1.52[a]	—1.02	—1.13
OCH_3	1.28[a]	—0.39	—1.22
SCH_3	1.38[b]	0.40	—1.32
$N(CH_3)_2$	1.61[a]	—1.40	—0.79

(a) K. B. Everard, L. Kumar and L. E. Sutton, *J. Chem., Soc.*, **1951**, 2807.
(b) H. Lumbroso and C. Marschalk, *J. chim. phys.*, **49**, 385 (1952).

TABLE V
DIPOLE MOMENTS OF ALKYL DERIVATIVES

Substituents	μ(D)	$\mu_{\parallel}$(D)	$\mu_{\perp}$(D)
OCH_3	1.21	0.62	—1.07
SCH_3	1.57	1.01	—1.20
$N(CH_3)_2$	0.86	0.29	—0.81

9) K. B. Everard and L. E. Sutton, *J. Chem. Soc.* **1951**, 2818.

The moments calculated for 2-bromotropone and 2,7-dibromotropone are greater than the observed values. Presumably this is due to ortho effect, i. e., to the mutual electrostatic induction of bond moments and to the bond deflection caused by steric repulsion of bulky atoms in ortho position, both decreasing the resultant moments. If the correction is made for the effect of electrostatic induction in the same way as Sutton and his coworkers[10] have done, the moments of these two bromoderivatives are calculated as 5.1 D and 5.6 D respectively in fair agreement with the observed values. Mention should be made here that a similar behavior due to ortho effect has also been recognized in many of the brominated tropolones, phenyltropones and alkyltropolones having a bromine atom or atoms at ortho position to carbonyl carbon.[1,3,4,11]

The observed moments of tropolone and mercaptotropone are nearly equal to the values calculated for the *cis* form, while the moment of aminotropone is close to that of the perpendicular form. In these geometrical configurations, the conjugation between the ring and the substituent groups can attain its maximum possible extent. Moreover a hydrogen bond can be formed between the carbonyl oxygen and the substituent. The hydrogen bond formation will increase the

10) J. B. Bentley, K. B. Everard, R. J. B. Marsden and L. E. Sutton, *J. Chem. Soc.*, **1949**, 2957.
11) Y. Kurita, T. Mizuno, T. Mukai and M. Kubo, This Bulletin, **26**, 192 (1953).

trend of electron attraction of carbonyl oxygen, giving rise to the increase of the contribution of cycloheptatrienium oxide structure. This is in conformity with the fact that the observed moment of tropolone is slightly higher than the calculated moment in contradistinction to the case of bromo-derivatives. The magnetic susceptibility measurements by Maruha and Hazato[12] have also indicated that the contribution of the cycloheptatrienium oxide structure is greater in tropolone than in tropone.

The moments of methoxytropone and methylmercaptotropone can adequately be explained either by the perpendicular form or by the mixture of *cis* and *trans* forms. Although the dipole moment data are incapable of settling the problem of the alternative, we think the former viewpoint is nearer the truth on the basis of the following considerations. (1) The fact that the absorption spectra[7] of methoxytropone bear some resemblance to the spectra of tropone rather than to those of tropolone indicates that conjugation taking place between the tropone ring and the methoxy group is weak. (2) The plane configurations are unlikely in view of the steric hindrance acting between the methyl group and carbonyl oxygen or between the methyl group and the hydrogen atom at the position 3 of the tropone ring.

12) J. Maruha and G. Hazato, reported at the annual meeting of the Chemical Society of Japan on April 3, 1953.

Summary

The dipole moments of *ortho*-substituted tropones were measured in benzene solution at room temperature. The values obtained are as follows: 2-bromotropone, 4.94 D; 2,7-dibromotropone, 5.27 D; 2-mercaptotropone, 4.36 D; 2-aminotropone, 3.78 D; 2-methylmercaptotropone, 4.64 D. These values together with those of tropolone and methoxytropone were compared with the calculated moments and the following conclusions were derived. The moments of the bromotropones are lower than those calculated by simple vector addition owing to ortho effect. In tropolone, mercaptotropone and aminotropone, the substituent groups take such configurations that these groups are conjugated with the cycloheptatriene ring in the highest degree and that an intramolecular hydrogen bond is formed between the carbonyl oxygen and the hydrogen atom of each of the substituent groups. In methoxytropone and methyl mercaptotropone, on the other hand, the conjugation is weak and each of the substituent groups lies in a plane nearly perpendicular to the ring.

We wish to express our thanks to Prof. Nozoe and his collaborators in Tohoku University, who kindly provided us with samples used in this experiment. Our thanks are also due to the Ministry of Education in aid of this research.

Chemical Department, Faculty of Science, Nagoya University, Nagoya

Studies on Foams. VIII Effects of Alcohols on the Foaminess of Soap Solutions

By Masayuki NAKAGAKI and Kōzō SHINODA

(Received May 17, 1954)

In the previous papers in this series[1], the foaminess of aqueous solution has been explained, considering the work required to remove a unit area of adsorption layer. In the present report, this idea is extended qualitatively to three component systems, to elucidate the defoaming and foam-promoting action of alcohols on soap solutions.

As for the foaminess of ternary mixtures, systematic studies have not yet been made, except some solution containing electrolyte, or chemically complex substances, e.g. tannine, saponine, and proteins. Foaminess of aqueous solutions of two simple organic substances was studied by O. Bartsch[2] on nonanoic acid —ethyl alcohol—water, isoamyl alcohol—ethyl alcohol—water, isoamyl alcohol—benzyl alcohol—water, and *m*-cresol—benzyl alcohol—water, and studied by M. Nakagaki[3] on

1) M. Nakagaki, This Bulletin, **23**, 127 (1950); **24**, 269 (1951).

2) O. Bartsch, *Kolloid-Beih.*, **20**, 1 (1924).

3) M. Nakagaki, This Bulletin, **21**, 30 (1948); **22**, 21 (1949).

methyl alcohol—ethyl alcohol—water, and ethyl alcohol—grycerol—water. Few studies, however, on the effects of homologous series of alcohols to soap solution have been reported.

Experimental

Alcohols used were purified by fractional distillation using a glass packed column. A column of 2-ft in height was used for propyl-(b.p. 97.5°C.), and butyl-(b.p. 117°C.) alcohol, 3-ft column for isoamyl-(b.p. 131°C.), hexyl-(b.p. 156°C.), octyl-(b.p. 96°C./16 mmHg.), and decyl-(b.p. 101°C./5mmHg.) alcohol, and 1-ft column for nonyl-(b.p. 96~96.5°C./8 mmHg.), and undecyl-(b.p. 120.5°C./8 mmHg.) alcohol. Heptyl alcohol was Kahlbaum's pure grade material. All these showed definite boiling points.

In fatty acids, caproic-(b.p. 109.5°C./20 mmHg.) and caprylic-(b.p. 120.5°C./9 mmHg.) acids were purified by fractional distillation through a 3-ft column. Capric-(m.p. 31.5°C.), lauric-(m.p. 44.5°C.), and myristic-(m.p. 54.1°C.) acids were Nihon Yushi's purest grade materials. All these showed definite melting points the same as or somewhat higher than those cited in the literature.

Soap solutions were prepared by the neutralization of above acids with carbonate free potassium hydroxide. Stock solution was about four times as concentrated as the critical micelle concentration (C.M.C.), and 2% excess (to soap) of potassium hydroxide was added to supress hydrolysis of soap.

Foaminess was measured by shaking test in a test tube of 30 cc. in capacity, 15 cm. in height, using 5 cc. of solution. The test tube was immersed in thermostat water. After the temperature became constant, it was taken out and shaken 20 times in 10 sec. Foam height was read after 5 sec (or 30 sec for stable foams) and foam stability was measured as the time required for the foam height to become a half of its original height.

Foaminess of soap solution and alcohol solution

Foaminess of some soap solutions are shown in Figs. 1~3. Fig. 1 shows A_{30}-log C_s relations at 15°C., where A_{30} is the foam height after 30 sec. and C_s is the concentration of soap in mol./l. Fig. 2 shows $t_{1/2}$-log C_s curves at 15°C., where $t_{1/2}$ is the foam stability. Fig. 3 is A_{30}-log C_s relation at 35°C. The foaminess increases with the increase of concentration near to C.M.C. (shown in figures as vertical lines) and then becomes nearly constant or somewhat decreases. At

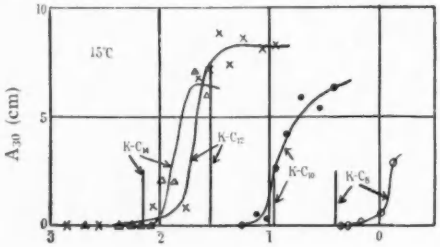

Fig. 1. Foam height of soap solutions at 15°C.

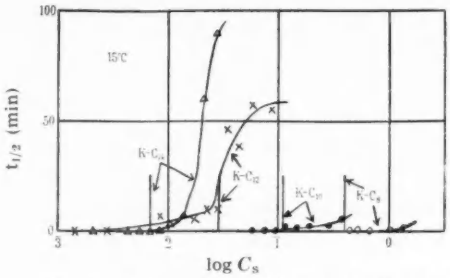

Fig. 2. Foam stability of soap solutions at 15°C.

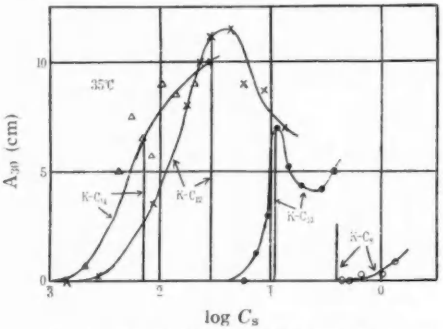

Fig. 3. Foam height of soap solutions at 35°C.

least in dilute solutions near C.M.C., the foam formation of soap solution may be ruled not by micelles but by single ions, since the single ion concentration increases up to C.M.C., and then remains nearly constant. This conclusion coincides with that previously obtained by the studies on the foaminess of dye solutions[4]. Comparing homologous series of soaps, foam height becomes maxi-

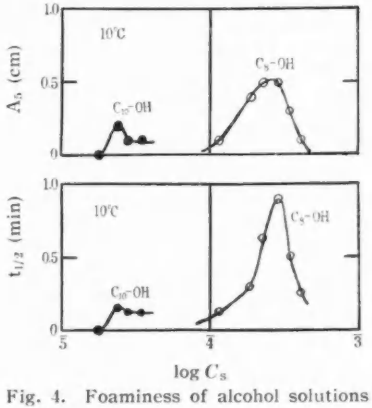

Fig. 4. Foaminess of alcohol solutions at 10°C.

4) M. Nakagaki, This Bulletin, **22**, 200 (1949); **23**, 47, 102 (1950).

mum at about K—C_{12}~K—C_{13} at ordinary temperature.

Foaminess of aqueous solutions of *n*-octyl- and *n*-decyl alcohol are shown in Fig. 4. It is ascertained that the foaminess of alcohol solution is far poorer than that of soap solution. Foam height measured after 5 sec. is smaller than 0.5 cm. for alcohol solutions, while, for soap solutions, it is several cm. even after 30 sec. Foam duration is smaller than 1 min. for alcohols and far more unstable than soap solutions. O. Bartsch[5] reported that the foam formation of homologous series of alcohols showed a maximum at about C_5-OH, and then decreased as alcohols were higher. The results shown here are coincident with Bartsch's, since the higher C_{10}-OH shows smaller foaminess than the lower C_8-OH.

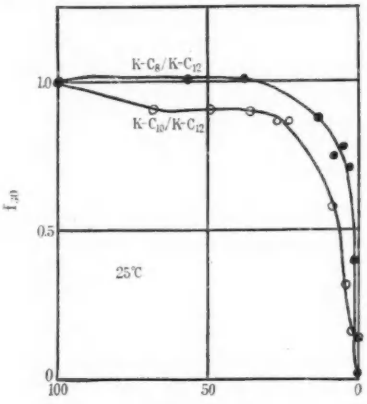

Fig. 5. Foam height of mixed soap solutions at C.M.C. (25°C.).

Foam height of mixed soap solution is measured at C.M.C., since the C.M.C. is considered as a corresponding state of soap solution. As in pure soap solution, C.M.C. can be determined also in mixed soap solution by the change in color of pinacyanol chloride[6]. Fig. 5 shows the relation between f_{30} and the mol. percents of K-C_{12} in two soaps, where f_{30} is defined as the ratio:

$$f_{30} = A_{30}/A^0_{30} \qquad \cdots\cdots(1)$$

A_{30} and A^0_{30} are foam height after 30 sec. for mixed solution and pure K-C_{12} solution at C.M.C., respectively. Foaminess decreases with the increase of the added amount of K-C_{10} or K-C_8. This coincides with the fact that the foaminess of pure soap solution at C.M.C. decreases, as shown in Fig. 1~3, in the sequence of K-C_{12}>K-C_{10}>K-C_8. Higher K-C_{12}, however, dominates the foaminess more influentially than lower K-C_{10} or K-C_8. This is explained by the theory that the nature of foam is dominated by molecules adsorbed at the surface, and the higher soap is adsorbed more strongly than the lower. This also explains the fact that higher K-C_{10} shows its effect at smaller addition than lower K-C_8.

Effects of Alcohols on Soap Solution

Effects of the homologous series of alcohols on the foam height of K-C_{10} and K-C_8 are measured, and f_{30} for K-C_{10} or f_5 (f-values after 5 sec.) for K-C_8 are shown in Fig. 6 as a function of $\log(C_{OH}/C_S)$. C.M.C. of mixed solution[7] is adopted as the concentration to be tested, since the C.M.C. is considered to be a corresponding state for mixed solution of soap and alcohol. C_{OH} and C_S are the concentrations of alcohol and soap in mol./l,

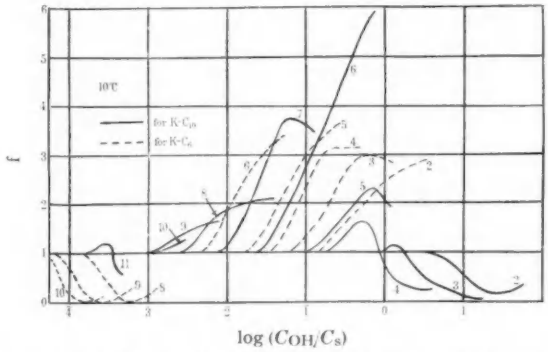

Fig. 6. Foam height ratio of soap-alcohol mixed solution at C.M.C. (10°C.). Numerals show numbers of carbon atoms of alcohol.

5) O. Bartsch, *Kolloid-Z.*, **38**, 177 (1926).
6) K. Shinoda, *J. Phys. Chem.*, **58**, No. 7, (1954).
7) K. Shinoda, *J. Phys. Chem.*, In Press.

respectively. Added amounts of alcohols were smaller than the solubilities of each kind of alcohol in distilled water[8]. In soap solutions, the solubilities of alcohols increase by solubilization, so that the deposition of alcohol drops on the surface cannot be expected.

The effects of alcohols on K-C_{10} are, first, discussed. As for C_2-and C_3-OH, little effects is observed in small addition, but foam height decreases distinctly when the amount of alcohol is increased to $1\sim10^2$ times that of soap. Also for C_4-OH, foam height decreases when the mol. ratio is greater than 1:1, though, at a smaller amount of alcohol, foaminess somewhat increases. The decreases of foaminess of the solution by large addition of lower alcohol (but within the limit of their solubilities) is explained as follows. As stated before[1], the foaminess of a solution is large when the work required to remove a unit area of adsorption layer is large. As the large amount of alcohol is added, the hydrocarbon chain of soap molecule is dissolved easily in bulk solution owing to the oil-dissolving ability of alcohol. The work then, to pull the soap molecule into the solution becomes small, to decrease the foaminess. This effect may be, therefore, named as the defoaming by solvent effect.

For higher alcohols, C_5-$\sim C_{10}$-OH, foam height becomes large with the addition of alcohol, at the ratio of $10^{-3}\sim1$ alcohol to soap. This is compared with the antifoaming action shown as these alcohols are sprinkled upon froth. Such an antifoaming action is explained by S. Ross[9] with a mechanism that a portion of foam membrane is substituted by an oil drop, and this portion becomes thinner to break the foam by the spreading of oil on the surface. In this case, it is necessary for alcohol to exist as an oil drop. When the oil dissolves homogeneously into the bulk after the long lapse of time, the solution becomes again foamable. As shown in Fig. 6, homogeneous dissolution of these alcohols increase foam height. As the number of carbon atoms of these alcohols is somewhat smaller than that of soap, the surface activities of alcohol and soap are about equal, since the hydrophilic property of -OH is weaker than $-COO^-$. Then, a simultaneous adsorption takes place and mixed monolayer is formed, and the surface viscosity may become large, as Matalon and Shulman[10] have shown on the penetration of Na-cetyl sulfate to cetyl alcohol monolayer. The foam promoting action may be attributed to the increase of surface viscosity.

The foam promoting action becomes maximum, as shown in Fig. 6, at C_5-OH and then decreases for higher alcohols. Higher alcohols, C_8-$\sim C_{10}$-OH, having greater surface activity than soap, may expel some of the soap molecules from the surface to decrease the foam height. At last, C_{11}-OH shows a defoaming action in extremely small addition. This alcohol is thought to be much higher in its surface activity than soap, to be adsorbed preferentially to the surface. Then, the greater part of the adsorption layer may be occupied by alcohol molecules, at the addition of $10^{-1}\sim10^{-3}$ to soap. Since the foam height of alcohol is much smaller than soap, the foam height of the mixed solution becomes very small. This effect may be named as defoaming by preferential adsorption.

The defoaming or foam promoting action of alcohol to soap solution is determined by the balance of surface activities between alcohol and soap. The same effects as shown by higher alcohol to higher soap will be shown by lower alcohol to lower soap. Taking the difference of the number of carbon atoms in alcohol and soap as a measure of relative surface activity, alcohols, having 8~6 carbon atoms less than soap, showed defoaming by solvent effect to K-C_{10}, 5~0 less showed foam promoting action, and 1 or more larger showed defoaming by preferential adsorption. Then, as for K-C_6 soap, C_2-$\sim$ C_5-OH should show foam promoting action, and alcohols higher than C_7-OH should show defoaming by preferential adsorption. Fig. 6 shows that this estimation is in good agreement with the experiments. C_2-OH and C_3-OH which always showed defoaming effect to K-C_{10} now show foam promoting action to K-C_6, and C_8-, C_9- and C_{10}-OH which always showed foam promoting action now show defoaming action. These three kinds of effects, defoaming by solvent effect, foam promoting action, and defoaming by preferential adsorptions, are entirely different in their phenomenological features, but are closely related in their essential nature.

The defoaming action by preferential adsorption at extremely small addition seems important in its application. The mechanism of defoaming by higher esters, amines, amides, ethers and so on, may be explained by it.

8) K. Kinoshita and K. Shinoda, presented before the 7th Annual Meeting of the Chemical Society of Japan (1954) at Tokyo.

9) S. Ross, *Rensselaer Polytech. Inst. Bull., Eng. Sci. Ser.*, No. 63 (1950).

10) R. Matalon and J. H. Shulman, *Trans. Faraday Soc.*, **43**, 479 (1947).

Summary

Foaminess of soap solution increases with the increasing concentration up to the C.M.C., and then becomes nearly constant. In homologous series, K-C_{12} or K-C_{13} show the greatest foaminess at ordinary temperature. Foaminess of alcohol solution is much smaller than the soap solution. In homologous series of alcohols higher than C_5-OH, the higher foams poorer. For the mixed solution of two soaps, the foaminess becomes smaller when the ratio of lower soap is larger.

The effects of homologous series of alcohols on soap solution are measured and three types are observed: defoaming by solvent effect (by C_2-$\sim C_4$-OH for K-C_{10}) is observed at $\log C_{OH}/C_S = 0 \sim 2$; foam promoting action (C_5-$\sim C_{10}$-OH for K-C_{10} and C_2-$\sim C_5$-OH for K-C_8) at $\log C_{OH}/C_S = 3 \sim 0$: and defoaming by preferential adsorption (C_{11}-OH for K-C_{10} and C_8-$\sim C_{10}$-OH for K-C_8) at $\log C_{OH}/C_S = \bar{5} \sim \bar{3}$. These three effects are correlated with each other.

Department of Chemistry, Faculty of Science, Tokyo University, and Department of Physical Chemistry, Faculty of Engineering, Yokohama National University Minamiku, Yokohama

---

The Catalytic Action of Organic Peroxides on the Polymerization of Ethenoid Compounds. III. The Effects of α-and β-Naphthoyl Peroxide on the Polymerization of Styrene

By Matsuji TAKEBAYASHI, Tadao SHINGAKI and Hisashi MATSUI

(Received May 25, 1954)

The reaction of free radicals in polymerization systems has been widely studied in particular as to the ability of a free radical to initiate and terminate reaction chains.[1] In the previous paper of this series,[2] the authors, studying the polymerization of styrene and of vinyl acetate in the presence of substituted benzoyl peroxides, observed that the activity of a radical derived from a peroxide was related to the distribution of electron density: thus electron repelling substituents increased the activity of a radical, and electron attracting substituents lowered the reactivity, and that the rate of polymerization was in a parallel relation with the rate of decomposition of peroxides, which generated active free radicals.

Recently, it has been found that some amines promote the decomposition of peroxides,[3] and that the peroxide-catalyzed polymerization of styrene is accelerated by adding tertiary amines[4] or polyamines.[5]

The experiments recorded in this paper have been carried out to investigate the effects of α-and β-naphthoyl peroxide on the polymerization of styrene and the influences of some tertiary amines on the effects of naphthoyl peroxides.

First of all, the rate of decomposition of the peroxide (1/6000 mol.) in styrene (1/30 mol.) was measured at 35°C. and 60°C. by the iodometric method. The results obtained are shown in Fig. 1. The date, given in Fig. 1, indicate that α-naphthoyl peroxide decomposes more rapidly than β-peroxide, accompanied by some extent of induced decomposition. Particularly at 60°C., α-peroxide

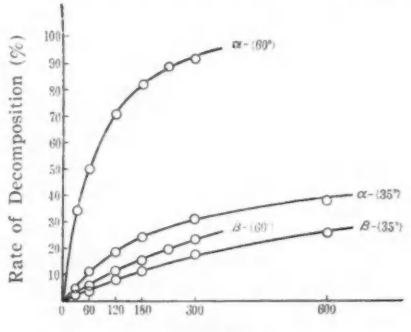

Fig. 1.

1) C. C. Price, "Mechanism of reactions of carbon-carbon double bonds", 70 (1946); W. Cooper, *Nature*, **162**, 897, 927 (1948).

2) M. Takebayashi and T. Shingaki, This Bulletin, **26**, 137 (1953); M. Takebayashi, T. Shingaki and Y. Ito, ibid., **26**, 475 (1953).

3) P. D. Bartlett and K. Nozaki, *J. Am. Chem. Soc.*, **69**, 2299 (1947).

4) L. Horner, *Angew. Chem.*, **61**, 311 (1949); M. Imoto and S. Sai Unpublished; J. Elly, R. N. Haward and W. Simpson, *J. Appl. Chem.*, **1**, 347 (1951).

5) R. Spolsky et al., *Ind. Eng. Chem.*, **42**, 1847 (1950).

decomposed to the extent of 92 per cent, while β-peroxide to that of only 22 per cent during five hours. The decomposition of β-peroxide was observed to be of nearly first order, and the rate was almost equal to that of benzoyl peroxide at 60°C.

In another experiment, the decomposition products of the peroxides in styrene were examined. It was recongnized that the peroxide decomposed to produce mainly naphthoate radical and naphthyl radical, generating carbon dioxide, and that α-naphthoate radical and β-radical did not isomerize each other during the reaction.[6]

If the radicals produced from the peroxides are active ones, the rate of polymerization of styrene will be in a parallel relation with that of decomposition of the peroxides. The above expectation was satisfied in the case of the experiments with 1/30 mol. of styrene and 1/6000~1/3000 mol. of the peroxide at 35°C. and 60°C. in the absence of air. The results are summarized in Table I, and a result obtained for benzoyl peroxide is added to it for the sake of comparison.

TABLE I

Peroxide	Temp. (°C.)	React. time (hr.)	Rate of Polymerization (%)
α-Naphthoyl (1/6000 mol.)	35	10	22
β-Naphthoyl (1/6000 mol.)	35	10	4
α-Naphthoyl (1/6000 mol.)	35	26	34
β-Naphthoyl (1/6000 mol.)	35	26	10
α-Naphthoyl (1/6000 mol.)	60	5	22
β-Naphthoyl (1/6000 mol.)	60	5	16
α-Naphthoyl (1/3000 mol.)	60	5	28
β-Naphthoyl (1/3000 mol.)	60	5	20
β-Naphthoyl (1/3000 mol.)	60	18	89
Benzoyl (1/3000 mol.)	60	18	82
None	60	18	1

In the next place, the influence of tertiary amines (1/6000~1/30000 mol.) on the rate of decomposition of the peroxides (1/6000 mol.) in styrene (1/30 mol.) was examined at 35°C. The data obtained are given in Fig. 2 and 3.

Aromatic amines such as dimethyl aniline and ethyl-benzyl aniline, and urotropine accelerate the decomposition of the peroxides remarkably, while heterocyclic amines such as pyridine and quinoline show practically no influence on the rate of the decomposition in the experimental conditions.

Then the polymerization of styrene with the peroxides and tertiary amines was carried out at 35°C. in the absence of air. The rate of the polymerization and the degree of it (P) are listed in Table II.

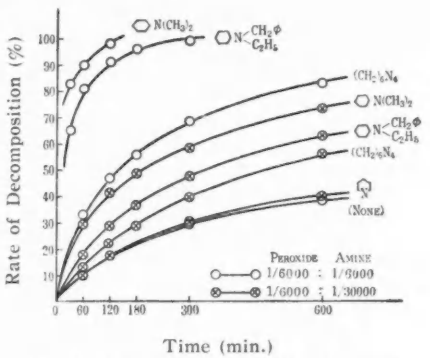

Fig. 2. Rate of decomposition of α-naphthoyl peroxide in the presence of tertiary amines at 35°C.

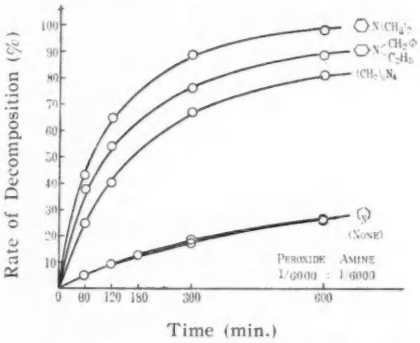

Fig. 3. Rate of decomposition of β-naphthoyl peroxide in the presence of tertiary amines at 35°C.

In the experiments using α-peroxide, the presence of aromatic amines such as dimethyl aniline and ethyl-benzyl aniline, and urotropine show a retarding influence on the rate of polymerization. It has been known that the presence of a little amount of amine accelarates the peroxide-catalyzed polymerization, while a larger amount of amine rather retards.[7] In an experiment, the polymerization was carried out adding a less amount of amines, but a similar result was obtained. It seems that the amines accelarate the decomposition of peroxide so rapidly that the radicals, produced from the peroxide, react to some extent upon each other or combine with other radicals besides reacting as the initiator of reaction chains.

In the experiments using β-peroxide, on

6) Kharasch also has observed this fact in carbon tetrachioride. M. S. Kharash and R. L. Dannley, *J. Org. Chem.*, **10**, 406 (1945).

7) M. Imoto and S. Sai, Unpublished.

TABLE II

In the presence of	React. time (hr.)	Rate of polymerization (%)	$v_t \times 10^9$ mol./l., min.	$\bar{P}$
α-Peroxide (1/6000 mol.) Dimethyl aniline (1/30000 mol.)	10	14.3	18	430
α-Peroxide (1/6000 mol.) Ethyl-benzyl aniline (1/30000 mol.)	10	17.1	24	400
α-Peroxide (1/6000 mol.) Urotropine (1/30000 mol.)	10	17·7	26	380
α-Peroxide (1/6000 mol.)	10	20.3	30	370
α-Peroxide (1/6000 mol.) Pyridine (1/6000 mol.)	26	40.9	20	400
α-Peroxide (1/6000 mol.) Quinoline (1/6000 mol.)	26	40.5	20	400
α-Peroxide (1/6000 mol.)	26	38	19	410
β-Peroxide (1/6000 mol.) Dimethyl aniline (1/6000 mol.)	5	28.9 (60°C.)		
β-Peroxide (1/6000 mol.) Ethyl-benzyl aniline (1/6000 mol.)	5	24.9 (60°C.)		
β-Peroxide (1/6000 mol.) Dimethyl aniline (1/6000 mol.)	10	16.0	17	520
β-Peroxide (1/6000 mol.) Ethyl-benzyl aniline (1/6000 mol.)	10	14.3	14	560
β-Peroxide (1/6000 mol.) Urotropine (1/6000 mol.)	10	3.4	1.3	1400
β-Peroxide (1/6000 mol.)	10	4.0	2.0	1100
β-Peroxide (1/6000 mol.) Pyridine (1/6000 mol.)	26	10.5	2.2	970
β-Peroxide (1/6000 mol.) Quinoline (1/6000 mol.)	26	10.3	2.2	970
β-Peroxide (1/6000 mol.)	26	10.0	2.1	1000

the contrary, dimethyl aniline and ethyl-benzyl aniline influence the peroxide, causing it to accelerate the polymerization. The results indicate that the increase of the rate of polymerization is affected not only by the increase of the amount of active radicals, but also by the activity of β-peroxide-radicals on the initiation of the reaction.

Heterocyclic amines such as pyridine and quinoline manifest practically no influence either on the rate of decomposition of peroxides or on that of the peroxide-catalyzed polymerization of styrene.

The accelerating action of aromatic amines on the decomposition of naphthoyl peroxides seems to be elucidated as follows for the case of dimethyl aniline. The decomposition may be initiated by the addition of dimethyl aniline with its lone-pair of electrons on nitrogen atom to the positively polarized part of the peroxide, giving rise to the formation of an iminium salt.[8] The salt may decompose to produce radicals: RCOO· and R· (R indicates naphthyl radical), ions: $RCOO^+$ and $RCOO^-$, and a radical-cation of dimethyl aniline. Here the radicals, RCOO· and R·, initiate the polymerization, and sometimes react on the peroxide, amine or other radicals. The anion $RCOO^-$ probably forms RCOOH with H^+, and the radical-cation dimerizes giving out H^+, or comes into play for the polymerization.[9]

Heterocyclic amines showed practically no influence on the decomposition of the peroxides in the experimental conditions. However, it has been reported that the decomposition of benzoyl peroxide is accelerated in pyridine.[10] Therefore, the concentration of amine in reaction systems might come in question,

Pyridine, contrary to dimethyl aniline, can hardly be added with its nitrogen atom to naphthoyl peroxide owing to the steric

8) L. Horner and K. Scherf, *Ann.*, **573**, 35 (1951).

9) L. Horner and E. Schwenk, *Ann.*, **566**, 69 (1950).

10) K. Nozaki and P. D. Bartlett, *J. Am. Chem. Soc.*, **78**, 1686 (1946).

strain[11] between them. If the decomposition should be accelerated by pyridine the reaction might be induced by the mutual interaction between pyridine and peroxide radicals.

Experimental

Materials—For the preparation of α-naphthoyl peroxide a modification of the method used by Kharasch and Dannley[6] was found to be useful. α-Naphthoyl chloride was dissolved in 40 cc. of anhydrous toluene; the solution was then added slowly to a vigorously stirred solution of 5 g. of sodium peroxide in 50 cc. of cold water. The temperature was not allowed to rise above 0°C. The stirring at 0° C. was continued for about three hours. Then the α-naphthoyl peroxide separated out as a pale precipitate. The precipitate was collected on a filter, washed with water, and dried. It was then dissolved in chloroform and fractionally precipitated by pouring the solution into methanol on stirring. The procedure was repeated several times. Yield: 55 %. The purity was found to be of 90 per cent by titration. A pure sample decomposed sharply at 98°C. The preparation of β-peroxide was similar to that of α-peroxide, the temperature of the reaction being held at 5~7° C. Yield: 76 %. A sample, the peroxide content of which was 95 %, decomposed sharply at 138° C..

The styrene employed was distilled with steam, dried over a small amount of calcium chloride, and was distilled under reduced pressure just before use. B.p. 63°C./55 mm. The absence of peroxides was ascertained by the test with ferrous ammonium sulfate and ammonium thiocyanate. The aromatic and heterocyclic amines employed were distilled under reduced pressure just before use.

Decomposition of Peroxides—The decomposition of peroxide was carried out in sealed reaction tubes. The tubes were treated with warmed cleaning solution for several hours, left standing in a dilute solution of sodium bisulfate for a short time, then rinsed with distilled water, and dried. The definite amount of the peroxide and amine were mixed with 1/30 mol. of styrene in the reaction tube, the tube was cooled in an ice-salt-bath, then was evacuated and sealed off. The sealed tube was immersed in a thermostat. After the required time the tube was cooled again, and opened. The content of the tube was mixed with 40 cc. of purified acetone in a glass-stoppered flask, and then titrated by the standard solution (1/10N) of sodium thiosulfate according to the direction of Blomquist and Buselli.[12] It was ascertained that no reaction took place between iodine and amine during the titration.

Polymerization of Styrene—The definite amount of the peroxide and amine were mixed with 1/30 mol. of styrene in a reaction tube, evacuated as described above, and then immersed in a thermostat for the reaction time. When the reaction time was over, the tube was cooled in an ice-salt-bath. The reaction products were dissolved in benzene, the polymer produced was precipitated by adding methanol to the solution, and the weight of polystyrene was measured. The molecular weight of the polymer was determined by the viscosity method.

Summary

(1) The rates of polymerization of styrene with α-and β-naphthoyl peroxide have been found to be in a parallel relation with the rates of decomposition of the peroxides at 35° and 60°C.

(2) Aromatic amines such as dimethyl aniline and ethyl-benzyl aniline, and urotropine accelerate the decomposition of the peroxides.

(3) In the experiments using α-peroxide, the presence of the aromatic amines and urotropine show a retarding influence on the rate of the polymerization. In the experiments using β-peroxide, on the contrary, dimethyl aniline and ethyl-benzyl aniline influence the peroxide to accelerate the polymerization.

(4) Heterocyclic amines such as pyridine and quinoline manifest practically no influence either on the rate of decomposition of the peroxides or on that of the peroxide-catalyzed polymerization of styrene.

(5) In respect to the action of amines, a tentative theory has been made.

The authors express their hearty thanks to the Ministry of Education for a Grant in Aid for Scientific Research.

Chemical Laboratory, South College, Osaka University, Osaka

11) H. C. Brown et al., *J. Am. Chem. Soc.*, **64**, 374, 378, 1452 (1945), ibid., **64**. 325 (1942), ibid., **70**, 2878 (1948), ibid., **71**, 445 (1949).

12) A. T. Blomquist and A. J. Buselli, *J. Am. Chem. Soc.*, **73**, 3883 (1951).

Manufacture of Levulose from Jerusalem Artichoke

By Junzo YAMAZAKI

(Received May 25, 1954)

In eight years since 1941, the Japan Levulose Company manufactured 127 tons of pure crystalline levulose (D-fructose) from 6000 tons of tuber of Jerusalem artichoke.

Here will be shown, together with a diagram, the details of the operation performed in 1948, the year of complete mastery of the manufacturing technique.

Fig. 1. Cultivation of Jerusalem artichoke in the end of June at Eniwa, Hokkaido.

Cultivation and Drying of Artichoke Tuber

The artichoke used as the raw material for the manufacture of levulose was cultivated mainly in a field (400 acres) of Eniwa, near Sapporo in Hokkaido, using animal power for cultivation and harvesting, as shown in Fig. 1 (photograph). The variety of Jerusalem artichoke used was of a family of white cortex, and the crop was 9 tons per acre. The fresh tuber was washed with water, sliced into cossette, and dried to a water content of 15 percent by the use of a rotary drier. Thus one ton of dried material was obtained from 5 tons of fresh tuber. To this end 800 kg. of coal was required.

TABLE I

ANALYSIS OF JERURALEM ARTICHOKE

(Cultivated in 1947 at Eniwa, Hokkaido)

	Moisture (%)	Solid matter (%)	After hydrolysis: Total reducing sugar(%)	After hydrolysis: Levulose (%)
Fresh tuber*	80.00	20.00	14.80	11.56
Dried tuber**	15.11	84.89	53.35	40.17

* Mean of the analytical values of 11 samples, converted to the basis of moisture content of 80 percent.

** Mean values of 123 tons of the dried cossette.

The dried cossette can well be preserved, is very little damaged by insects, and is suitable for levulose manufacture throughout the year.

The results of analysis of the tubers, both fresh and dried, are shown in Table I.

Manufacture of Levulose

The dried artichoke used for levulose manufacture from 1941 to 1948 amounted to 1142 tons, corresponding to 6000 tons of cultivated fresh artichoke. The average content of levulose in the dried artichoke was 41.3 percent, the maximum content of year average being 44.0, the minimum 38.0 percent. The crystalline levulose manufactured from these material was 127.4 tons in quantity, the average yield being 11.2 percent of the dried artichoke, corresponding to 27.0 percent of the levulose contained in the raw materials.

In order to explain the details of the levulose production we will illustrate the data obtained in 1948. By this year we mastered the technique of manufacture, producing 16.7 tons of crystalline levulose from 123 tons of dried artichoke during the period from January to July.

In Fig. 2 is illustrated each process of manufacture as well as its material balance in the form of a diagram, where the description of water content and thermal data are eliminated. The width of the figure represents the ratio of solid matter, while the content of levulose is shown numerically. All the numerals in Fig. 2 represent those values recalculated from the data totally obtained during this period, so as to correspond to one ton of the material for manufacture.

Diffusion of Dried Cossette

We have used a diffusion apparatus of a type of semi-counter-current diffusion battery which is usually employed for the extraction of beet sugar. This consists of twelve cells, each of 320 l. in capacity, connected with each other in the form of a circle. Each cell is charged with 63 kg. of the material, and hot water is circulated through the cells, so as to extract the contained fructan. Extraction is in general completed when the liquid

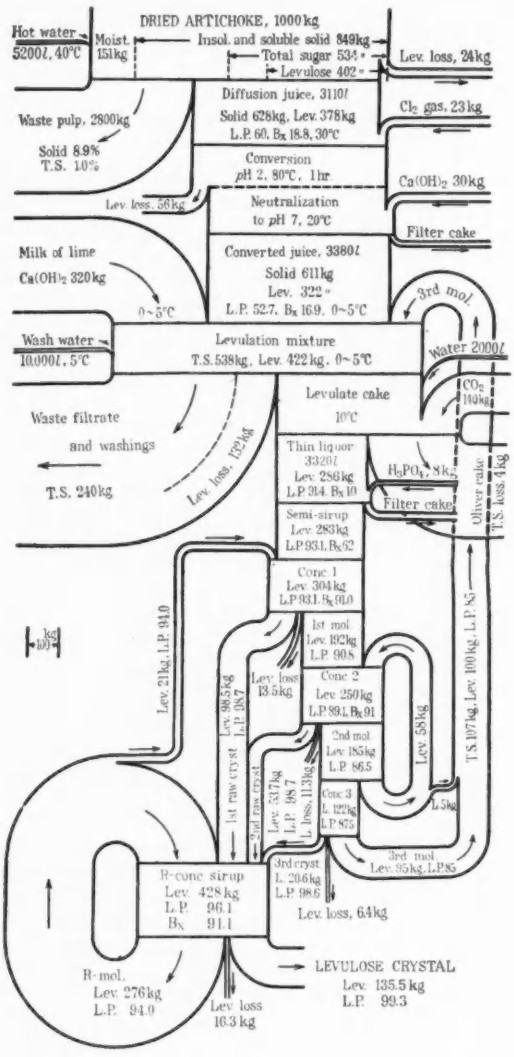

Fig. 2—A process flow diagram of levulose manufacture.

Abbreviations:

T.S.:	Total sugar
L.P.:	Levulose purity
Conc.:	Concentrated sirup
Bx:	Refractometric Brix (% solid)
R:	Refined
Mol.:	Molasses
Lev., L.:	Levulose

passes through ten of the cells, the refractometric solid in the liquid amounting to 18–19 percent. This "diffusion juice" is obtained in a quantity of 200 l. per one charge, is brown in appearance, the total sugar purity (T. S. × 100/solid) being 81, and the levulose purity (Levulose ×100/solid) 60. The yield of levulose of this procedure is 94 percent.

Conversion and Neutralization

A wood tank, 2 m. in height, is filled with this diffusion juice, and chlorine is blown into it at a temperature of 30°C. This is a patented process[1], the characteristic of which is that chlorine destroys any coloring matter, coagulates a part of the impurities, and the hydrochloric acid thereby formed promotes the hydrolysis of polyfructosans. It was once reported[2] that in the oxidation of invert sugar by chlorine, levulose is oxidized at 15°C. to a range of 10 percent, while glucose is destructed by it to the large extent of 80 percent. It is, however, experienced that during the seven months' period the

1) *Japanese Pat.*, 92201 (1931).
2) S. Ochi and M. Nakamura, *Repts. Tokyo Imp. Ind. Res. Inst. Lab.*, **24**, No. 5, 46 (1929) (in Japanese).

extent of decomposition or loss in this procedure amount to 14.8 percent for levulose, and to 16.8 percent for other reducing sugars.

It is no doubt possible to prevent the destruction of levulose to a far lesser degree, if hydrochloric acid is used for conversion in place of chlorine, but in this case the filtration of the treated liquor becomes difficult, and, moreover, decolorization as well as clarification can not be carried out with satisfaction. It should be mentioned further that treatment with chlorine has another advantage; this is that in the sugar liquor the growth of moulds is prevented, and thus subsequent operation can easily be performed. The introduction of chlorine is continued until the liquor shows a *p*H between 1.8 and 2.0, and conversion is completed by keeping the liquor at 80°C. for one hour. The liquor is then cooled down to 20°C., and some milk of lime is added to a *p*H 7, when proteinous matters, pectins, etc. are coagulated. On filtering these precipitates a "converted juice" is obtained. The yield of levulose in this process is 85.2 percent.

Precipitation of Levulose ("Levulation Process")

The converted juice is cooled down to 0°–5°C., and milk of lime of the same temperature is added. The necessary quantity of the lime is 1.45 times the quantity equivalent to the total sugar in the hydrolyzate. It is desirable to employ lime of good quality containing more than 67 percent of available CaO, and especially consisting of fine powder. The quality and the quantity of lime has a remarkable effect on the yield of levulose as well as on the amount of carbon dioxide necessary for neutralization. The most important point of this procedure lies in obtaining a compound between levulose and lime ($C_6H_{12}O_6 \cdot CaO \cdot XH_2O$, "lime levulate") in the form of granular precipitate filtrable as easily as possible. Either when the juice is too thick, or when the mixing of the liquors is too rapid, undesirable blocks or fine precipitates are readily formed. To prevent this it is necessary to mix the juice with milk of lime gradually and alternately, and to keep the mixture constantly in a medium of a little excess of lime by stirring well at the temperature between 0° and 5°C. It is, however, unnecessary to add crystal seeds of lime levulate, as already pointed out by Jackson[3]. After thorough mixing for some time, the precipitate is filtered through a filter press, and washed with cold water of 5°C. Washing is continued till the filtrate becomes colorless. The filter cake ("levulate cake") is mixed with cold water, transferred to a carbonator as a thick suspension, and carbon dioxide is introduced until the liquor shows a *p*H 8, keeping the temperature below 10°C. Here levulose is liberated, and by filtering the precipitate of $CaCO_3$ on an Oliver filter, a "thin liquor" of light yellow coloration is obtained. This liquor has a concentration of 10 percent, and a levulose purity (L.P.) 90 to 99 (av. 91.4). In later operations the final (third) molasses, which is removed from raw crystal, is diluted and subjected to levulation process for recovery of levulose, either solely or in admixture with the converted juice.

The process of levulation must be carefully performed, since the loss of levulose in this process is the greatest in the whole procedure, often becoming equal, in quantity, to the final product. The yield of levulose is 65 percent with respect to the artichoke juice, and 80 percent to the molasses. In this illustration the two are mixed and treated, so the yield becomes 68.7 percent on the average.

Evaporation to "Semi-Sirup"

The thin liquor is, while still cold, neutralized with phosphoric or oxalic acid to a *p*H 5.8. After filtration the liquor is concentrated to 62 percent in a vacuum evaporator, and preserved in a tank. The calcium salt in the solution separates out gradually, and finally the value of L.P. increases to 93 on the average.

Crystallization of Raw Crystals

The sirup which has been blended from a few lots of semi-sirups, so as to make the L.P. value to 94, is again thickened by heating in a vacuum evaporator to a "concentrated sirup" having a concentration of 91 percent as regards to solid. This thick sirup is then introduced into a crystallizer, seeded at 52°C. with a fine powder of crystalline levulose, gradually cooled down with constant gentle stirring, so that the seed can grow up sufficiently. Thus the content will be in the state of massecuite, when the temperature is lowered to 30°C. within 24 hours. Then the molasses is removed by means of a centrifuge, where the first raw crystal is obtained. The former (the first molasses), on concentrating, is subjected to repeated (twice) crystallization. In a similar manner the second and the third crop of levulose crystal is obtained, thereby the value of

3) R. F. Jackson, C. G. Silsbee, and M. J. Proffitt, *Sci. Papers Bur. Standards*, No. 519, **20**, 609 (1926).

L.P. is hardly lowered as to the crystal, but is depressed to 85 with the molasses. This molasses with a low L.P., being unfavorable for crystallization, is returned for recovery of levulose to the above mentioned process of levulation.

In practice, the second molasses is concentrated to obtain a third crop of crystal, in so far as the L.P. value is above 87.5. If below, the molasses is blended to a sirup of L.P. 89 by adding the first molasses, and made to yield the second crystal. With the depression of L.P. value the yield of levulose crystal suddenly falls with respect to massecuite, and also the crystallization process becomes tedious, as shown in Table II.

TABLE II
CRYSTALLIZATION OF LEVULOSE

Crystal	No. of Crystallization	Crystals obtained (kg.)	Crystals per one Cryst'n (kg.)	Av. Purity of "Conc."	Yield of Cryst. as to Massecuite (Solid/solid)(%)	Time required for Cryst'n (day)
1st raw	42	12,290	292.6	93.1	29.6	1
2nd raw	35	6,706	191.6	89.1	19.4	2
3rd raw	17	2,574	151.4	87.5	15.1	6
Refined	57	16,810	294.9	96.1	30.7	0.8—1

Crystallization of Refined Crystal

The raw crystal and the sirup (R-mol. of Fig. 2), which is removed from the refined crystal, are made up to a L.P. of 96, decolorized with active carbon, and subjected to crystallization. The crystals, after centrifugation, are washed with a little distilled water, and dried in vacuum at 40°C.

The refined crystals thus obtained are colorless, tilted cubes of a relatively uniform size (from 0.5 to 1 mm.). The L.P. is 99.3 on an average, well in agreement with the Japanese Pharmacopoeia. By recrystallizing from dilute methanol or ethanol we are able to obtain easily a sample of highest purity[4].

In order to obtain further crystals from the mother sirup (L.P. 94) of the refined levulose, some raw crystal is dissolved into it, the excess sirup being returned to the stage of the first raw crystal. Such a somewhat complicated method of preparing refined crystal is, in reality, a most economical process, and favorable for keeping constant the quality of the product.

Steam, Electric Power and Labor

The manufacture of levulose consumed, per one ton of dried artichoke, 6 tons of steam, 1500 KWH of electric power, 345 man hours of labor (in the case of all-night operation) and the chemicals indicated in Fig. 2.

Analytical Procedure

It is of the utmost necessity, for chemical control, to carry out the exact analysis of levulose and the accurate determination of its purity. A number of various analyses were made for each lot of the raw material as well as its intermediates, and finally summed up. The value of refractometric solid was assumed directly as the value of solid in aqueous solutions. The total reducing sugar (T.R.S.) was measured by the titrimetric method of Lane and Eynon[5], after the test liquid was hydrolyzed by hydrochloric acid. The levulose ratio (L.R.) was obtained according to Jackson and Mathews[6] from the titre of T.R.S. and the saccharimetric polarization. It was very fortunate that both of these methods enabled us to perform rapid and accurate determinations. The levulose content (L.) is obtained by means of an equation: $L. = T.R.S. \times L.R.$, and likewise the levulose purity (L.P.) by a relation: $L.P. = L. \times 100/S.$ All the analytical procedures required considerable skill and precision; nevertheless, after some experiences, accurate and consistent values were constantly obtained. (Here allow us to mention that Messrs. M. Nakamura†, K. Nishiki, and S. Kidooka of this factory helped us to systematize these analytical methods and carry out practical determinations).

Utilization of Waste Liquor

It is possible to collect nearly 90 percent of the total waste sugar in a concentration of 5 percent from the waste filtrate of the levulate, when combined with the first portion of the filtrate obtained by washing.

This liquor, on neutralizing with carbon

4) Y. Tsuzuki, J. Yamazaki, and K. Kagami, *J. Amer. Chem. Soc.*, **72**, 1071 (1950).

5) J. H. Lane and L. Eynon, *J. Soc. Chem. Ind.*, **42**, 32T (1923), **44**, 150T (1925), A. O. A. C., 5th ed. pp. 498~9 (1940).

6) R. F. Jackson and J. A. Mathews, *Bur. Standards J. Res.*, **8**, 435 (1932).

dioxide or with sulfuric acid, proved to be an active culture media for yeasts.

Experiments culturing Fleischmann's yeast by the so-called "Zulaufsverfahren" with a concentrated liquor, to which was added some ammonium sulfate and phosphate showed that sugar consumption is 92.6 percent and the yield of dry yeast is 49.7 percent with respect to the sugar present in the liquor. The effect was even superior to a control experiment done with malt juice, where sugar consumption was 90.2 percent, yield 49.5 percent[7].

It is, therefore, possible to produce even 1200 lb of fresh yeast by utilizing the waste liquor produced from one ton of dried artichoke.

Cost and Mode of Manufacture

In Japan at present, the mill cost of levulose can not be lowered below $3 per kg., owing to the high price of Jerusalem artichoke. Consequently. raw sugar (sucrose) or beet molasses has been used as the raw materials for levulose manufacture since 1949. It is certain that Jerusalem artichoke has no advantage as raw material, unless the price of fresh artichoke is less than 1/20 of that of sucrose. However, if there is any possibility of utilizing fresh artichoke directly the cost will be equal to that of sucrose, even if the artichoke is, in price, as high as 1/7 of sucrose.

Since the price of this tuber is, in general, lower than this, the cost will be considerably decreased, if such a scheme of production is adopted. If it is possible to produce yeast at the same time, further decrease of the cost by 10 to 20 percent will be expected. One of the best schemes to realize this would be to cultivate Jerusalem artichoke in the vicinity of a beet sugar factory with an attached yeast manufacturing factory, to extract fresh artichoke tuber by using a large diffusion battery during the winter, to preserve the concentrated converted juice till the spring of the next year, and by utilizing the season of cessation of beet sugar production to carry on levulose manufacture. This appears to be a most economical form of levulose production, considering the circumstances that direct extraction of fresh artichoke is at some important points more profitable than the use of dried artichoke.

Japan Levulose Co.,
385 Ichinotsubo, Kawasaki

7) T. Asai, H. Arioka, C. Sakurai, and S. Takahashi, *J. Agr. Chem. Soc. Japan*, **22**, 136~9 (1949) (in Japanese).

Über die Wirkung von Alkynolen als Säurebeizinhibitor

Von Kazumi YAMAMOTO

(Eingegangen am 26. April, 1954)

Einleitung

Zur Entfernung des Rostes von Eisen oder Stahl durch Säurebeize werden verschiedene Substanzen als Beizinhibitor verwendet, die die Auflösung von Eisen oder Stahl an sich schützen. Als solche Substanzen sind Stärke, Mineralöl, organische Basen, Salze des Arsens oder Antimons, Jodide, Phosphate, Benzoate, organische Schwefelverbindungen usw. schon wohl bekannt.

Jüngst hat Reppe[1] in seinem Buche veröffentlicht, dass Propargylalkohol und Butin-2-diol-1.4, welche beide aus Acetylen und Formaldehyd unter erhöhtem Druck hergestellt werden können, vorzügliche Säurebeizinhibitor sind, jedoch eingehende Data sind noch unbekannt.

In vorliegender Abhandlung sollen die Wirkungen der Alkynole erörtert werden.

Arbeitungsmethode

Experiment wurde nach der Einweichungsmethode durchgeführt, unter Verwendung von Probestücken des wohl polierten schweissbaren Stahls in einer Form rechteckiger Platte.

Fünf bis sechs Probestücke wurden in der Inhibitor enthaltenden wässrigen Säurelösung unter Rührung bei einer konstanten Temperatur eingeweicht und einer nach dem andern mit der bestimmten Zeit aufgehoben und nach der Wäsche mit Wasser und Alkohol, in Exsikkator getrocknet und dann gewogen.

Die Ätzung wurde durch den Zerfressungsgrad, der nach folgender Gleichung defeniert wird, ausgedrückt.

1) W. Reppe, "Acetylene Chemistry," Charles A. Meyer Co., N. Y. (1949), S. 96.

$$Z = \frac{\text{Gewichtsverlust des Probestücks (g.)}}{\text{Spezifisches Gewicht Probestücks} \times \text{Oberfläche desselben (cm}^2\text{.)}}$$

Demnach soll der Zerfressungsgrad Z die Dimension von cm. haben und die Tiefe der Ätzung für je eine Einheitsoberfläche des Probestücks bedeuten.

Experiment wurde zuerst in bezug auf die Inhibitorwirkung des Propargylalkohols für Salzsäure bis ins einzelne ausgeführt und danach hinsichtlich der verschiedenen Abkömmlinge.

Experimentelle Resultate

A. Der Effekt der Menge des Propargylalkohols. — Bei der praktischen Rostentfernung wird 8 bis 10 %-ige Salzsäure verwendet. Ich habe jedoch ziemlich konzentrierte Salzsäure, d. h., 20 %-ige, zum Versuch angestellt, um die Wirkung von der Probe auszudehnen. Experimentelle Resultate, die bei 24°C. erhalten wurden, sind in Figur 1 (dicke Linie) und 2 dargestellt.

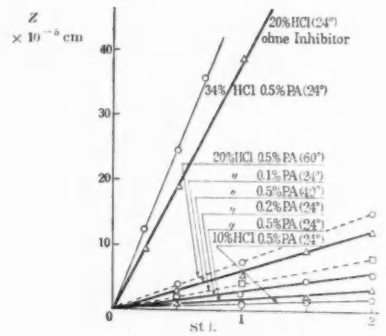

Fig. 1

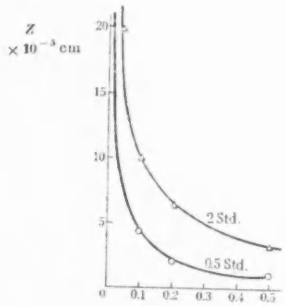

Fig. 2

Bei der Auflösung von Eisen durch Salzsäure ist es schon bekannt, dass sie gegen die Laufzeit in linearem Verhältnis steht. Das ist der Fall auch hier. Von obigen Figuren kann man verstehen, dass die Inhibitorwirkung des Propargylalkohols sehr bemerkenswert ists und eine wirksame Grenzkonzentration desselben (0.5%) vorhanden ist.

Auf solche Weise kann der Zerfressungsgrad im Falle der Anwesenheit von Propargylalkohol mit $Z = 1.75 \times 10^{-5}\, t$, wobei t die Laufzeit (Std.) bedeutet, ausgedrückt werden, dementgegen im Falle der Abwesenheit desselben mit $Z = 3.75 \times 10^{-4} t$ (Fig. 1).

B. Einfluss der Temperatur.—Unter der Verwendung von 20%iger Salzsäure, in der Propargylalkohol (0.5%) enthalten ist, wurde der Zerfressungsgrad bei 24°, 40° und 60°C. bestimmt. Die Resultate sind in Figur 1 (punktierte Linie) und 3 dargestellt, von welchen man verstehen kann, dass eine Steigerung der Temperatur die Inhibitorwirkung des Propargylalkohols vermindert.

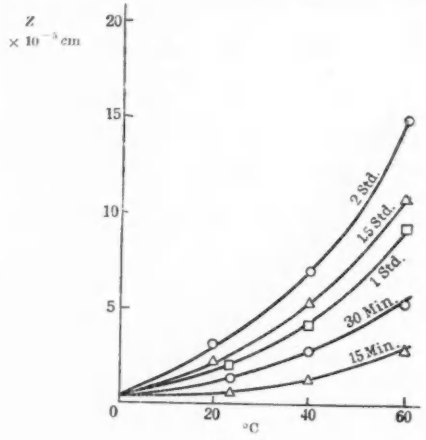

Fig. 3

C. Konzentration der Salzsäure.—Die Auflösung von den Probestücken durch Salzsäure verschiedener Konzentrationen, in der je 0.5 % Propargylalkohol enthalten ist, wurde bei 24° beobachtet.

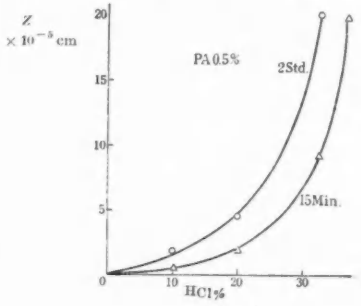

Fig. 4

Die Resultate sind in Figur 1 (dünne Linie) und 4 dargestellt.

Bei der Konzentration von Salzsäure über 25% ist die Inhibitorwirkung eindeutig dahingeschwunden. Es scheint mir, dass dies seinen Ursprung darin habe, dass des Propargylalkohols eigentümliche dreifache Bindung verloren geht, da es wohl bekannt ist, dass Propargylalkohol unter Bildung von Chlorallylalkohol leicht Chlorwasserstoff addiert.[2)]

D. Sparbeizwirkung von anderen Abkömmlingen.—Aus dem Gesagten wurde es klar dass Propargylalkohol bemerkenswerte Sparbeizwirkung hat. Demnach habe ich die Wirkung der unten zusammengefassten verschiedenen Abkömmlinge und der einigen olefinischen und gesättigten Alkohole untersucht, um den Mechanismus der Inhibitorwirkung derselben klar zu erkennen.

Verbindung	Formel	Abbreviation
Propargylalkohol	$HC{\equiv}C\text{-}CH_2OH$	PA
Butin-2-diol-1.4	$HOCH_2C{\equiv}C\text{-}CH_2OH$	BDO
3-Methylbutin-1-ol-3	$(CH_3)^2C(OH)\text{-}C{\equiv}CH$	MB
1,1,4,4-Tetramethylbutin-2-diol-1.4	$(CH_3)_2C(OH)C{\equiv}C\text{-}C(OH)(CH_3)_2$	TMBDO
Hexadiin-2.4-diol-1.6	$HOCH_2C{\equiv}C\text{-}C{\equiv}C\text{-}CH_2OH$	HDDO
Allylalkohol	$H_2C{=}CH\text{-}CH_2OH$	AA
n-Propylalkohol	$CH_3\text{-}CH_2\text{-}CH_2OH$	NPA

Experimente wurden in bezug auf 20%-ige Salzsäure, die je 0.5% von Inhibitor enthielt, bei 24° durchgeführt und deren Resultate sind in Figure 5 illustriert.

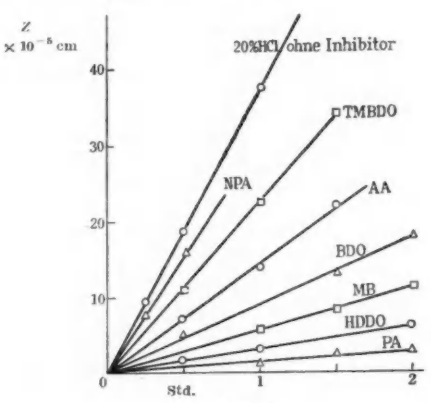

Fig. 5

Wie man von Figur 5 verstehen kann, werden die folgenden Schlüsse gezogen:

1. In bezug auf die gleiches Kohlenstoffatom besitzenden Alkohole nimmt deren Wirkung mit Zunahme von Unsättigungsgrad zu. (PA>AA>NPA)

2. Die Zunahme von Methylgruppe erniedrigt die Wirkung von Acetylenalkohol. Es scheint mir dies auf eine sterische Hinderung zurückzuführen. (PA>MB, BDO>TMBDO)

3. Hexadiindiol ist auch so wirksam wie Propargylalkohol.

E. Das Andere.—Die Sparbeizwirkung von Propargylalkohol für Schwefelsäure anstatt Salzsäure wurde ebenfalls probiert. Diese Resultate sind in Figur 6 gezeigt.

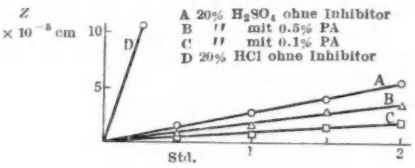

Fig. 6

Nicht nur die Probestücke von Eisen sondern auch die von Zink und Aluminium wurden unter Verwendung von 20%-iger Salzsäure, die 5% von Propargylalkohol enthält ausprobiert. Jedoch Propargylalkohol hat die Inhibitorwirkung für solche Metalle beinah nicht gezeigt.

Betrachtung der Resultate

Der Mechanismus der Sparbeizwirkung bisher bekannter Inhibitoren wird ungefähr in drei Klassen eingeteilt.

1) Inhibitor, der auf der Oberfläche des Eisens unlöslichen, dünnen Film bildet, wie Phosphate, Benzoate. 2) Inhibitor, der an sich positiv geladen ist und der auf der Grenzlinie des Kristalls von Metall, die die Anode der Lokalbatterie bildet, absorbiert wird, wie Stärke, organische Basen, Arsenverbindungen usw. 3) Inhibitor, der die Diffusionsgeschwindigkeit des Metallions auf dem Metall verspätet, wie Mineralöl usw.

Jedoch scheint es mir, dass die Wirkung der Alkynole keiner Gruppe angehört.

Jüngst hat Lüttringhaus[3)] die Sparbeizwirkung der Trithion und der Alkynole durch die chemisch-morphologische $\text{-}C{\equiv}C\text{-}CH_2OH$-Gruppen-Theorie erklärt.

Nur, mit diesem Experiment möchte ich nicht schliessen und stelle darüber eine Erläuterung auf.

In meiner Arbeit wurde gezeigt, dass auch Methylbutinol, die oben besagte $\text{-}C{\equiv}C\text{-}CH_2OH$ Gruppe nicht hat, die die Sparbeizwirkung bietet, und dass selbst Allylalkohol, wenn es

2) W. Reppe u. a., *DRP* 764595.

3) A. Luttringhaus, H. Goetze, *Angew. Chem.*, **64**, 66 (1952).

auch gering ist, die Wirkung hat. Aber die experimentellen Resultate hinsichtlich der Alkynolabkömmlinge stellen dar, dass die Existenz der Methingruppe (HC≡) nicht gerade bedeutsam ist.

Folglich scheint es mir, dass doppelte oder dreifache Bindung in Molekül auf die Wirkung wesentlich Beziehung habe. Das heisst, die Rolle von OH-Gruppe ist nichts anderes als der Beitrag zur Löslichkeit für wässrige Säurelösung.

Meiner Meinung nach würde π-Bindung ungesättigter Verbindungen auf dem ferromagnetischen Metall wie Eisen durch eine Art induzierter, magnetischer Polarisation aufgebrochen. Und dann würden diese Verbindungen an Oberfläche—Fe—Atome mit Koördinationsbindung unter Bildung von dem Schutzfilme verbunden.

Schlusswort

Gemäss der Suggestion von Reppe wurde Sparbeizwirkung von Propargylalkohol und dessen Abkömmlingen ausgeprobt.

Es wurde beobachtet, dass Acetylenalkohole und Glykole mehr oder wenig Sparbeizwirkung haben und deren Unterschied hauptsächlich auf den sterischen Faktor der Verbindungen zurückzuführen ist.

Diese Wirkung wäre auf Grund der Koördinationsbindung von ungesättigten Verbindungen mit Oberfläche—Fe—Atome zu erklären.

Den Herren Dr. K. Yoshikawa und K. Maki danke ich für ihre fördernde Unterstützung und stetige Leitung zu dieser Arbeit.

Diese Arbeit wurde am 21. Feb. 1953 im Rahmen der Versammlung der japanischen chemischen Gesellschaft-Kyushu-Zweigabteilung in Omuta mündlich veröffentlicht.

Mitsui Chemical Industry Co.
Miike Dyestuff and Chemical Works,
Omuta, Fukuoka

Über die Herstellung von Styrol und Benzol aus Acetylen

Von Kazumi YAMAMOTO und Mitsuo OKU

(Eingegangen am 26. April, 1954)

Einleitung

Reppe[1] hat über die cyclisierende Polymerisation von Acetylen veröffentlicht, die in zwei Gruppen eingeteilt wird, wie folgt:

1) Bildung von Cycloöktateraen unter Tetramerisation von Acetylen

2) Bildung von Benzol unter Trimerisation von Acetylen, und hat gezeigt, dass bei der zweiten Reaktion Styrol als Nebenprodukt erhalten wurde, d.h., 88% Benzol neben 12% Styrol, wovon etwa die Hälfte als polymeres Produkt anfällt.

Cycloöktatetraen, Kohlenwasserstoff von 8-Gliederring, entspricht dem Isomer von Styrol und die Isomerierungswärme zum Styrol ist endothermisch (-36.1 Kcal./Mol.)[2].

Solche leichte Bildung von Styrol oder Benzol zeigt so die Möglichkeit, dass Styrol aus Acetylen, die Reaktionsbedingung gut gewählt, unmittelbar erhalten werden kann. Unsere Arbeit wurde von diesem Standpunkt durchgeführt.

Herstellung von Katalysator

1) Herstellung von Triphenylphosphin: Triphenylphosphin, das der Ausgangsstoff für den Katalysator Bistriphenylphosphin-Nickeldicarbonyl ist, wurde nach Wurtz-Reaktion aus Monochlorbenzol, Phosphortrichlorid und metallischem Natrium hergestellt:

$$3C_6H_5Cl + PCl_3 + 6Na \longrightarrow (C_6H_5)_3P + 6NaCl$$

2) Herstellung von Bistriphenylphosphin-Nickeldicarbonyl: Rose[3] hat Bistriphenylphosphin-Nickeldicarbonyl $(Ph_3P)_2Ni(CO)_2$, wobei Ph den Phenylrest ausdrückt, dadurch hergestellt, ätherische Lösung von Triphenylphosphin bei deren Kochpunkt mit Nickelcarbonyl einwirken zu lassen.

$$2Ph_3P + Ni(CO)_4 \longrightarrow (Ph_3P)_2Ni(CO)_2 + 2CO$$

Smp. 209°

Die Resultate unserer Nachprobe sind in Tabelle I zusammengefasst.

TABELLE I

HERSTELLUNG VON $(Ph_3P)_2Ni(CO)_2$

Ph_3P (g.)	$Ni(CO)_4$ (cc.)	Lösgmittel (cc.)		Reakt.-temp. (°C.)	Ausbeute von Komplex (g.)	Ausbeute von Komplex (% d. Th.)
13.1	3.2	Äther	30	35	14.6	91.4
13.1	3.2	Benzol	30	55	12.3	77.0
10.0	2.5	Methanol	50	50	9.6	78.7
10.0	3.8	Butanol	50	50	9.5	77.7

4) W. Reppe u. a., *Ann.*, **560**, 104 (1948).
2) W. Johnson, *J. Am. Chem. Soc.*, **72**, 626 (1950).
3) J. D. Rose, *J. Chem. Soc.*, **1950**, 69.

Die Ausbeuten sind zwar ziemlich gut, aber dieses Verfahren an und für sich ist unangenehm, da man sehr giftiges Nickelcarbonyl behandeln muss.

Wir fassten ins Auge, dass Nickelcarbonyl sich leicht durch Einwirkung des unter Druck stehenden Kohlenoxyds auf reduziertes Nickel bildet.

Dann stellten wir auf die Probe, die Komplexverbindung durch Reaktion von Kohlenoxyd mit methanolischer Lösung von Triphenylphosphin, in welcher reduziertes Nickel suspendiert ist, unter erhöhtem Druck und bei erhöhter Temperatur herzustellen.

$$2Ph_3P + Ni + 2CO \longrightarrow (Ph_3P)_2Ni(CO)_2$$

Triphenylphosphin wurde so überschüssig verwendet, dass kein freies Nickelcarbonyl blieb. Das Experiment wurde gemäss 4×4-Latin Quadratverfahren in Bezug auf drei Faktoren, Anfangsdruck von Kohlenoxyd, Reaktionstemperatur und Laufzeit durchgeführt. Die Bedingungen waren wie folgt:

Anfangsdruck von CO	11	20	45	60	in at.
Temperatur	50	90	130	170	in °C.
Laufzeit	0:30	1:00	2:00	4:00	in Std.: Min

Andere konstante Bedingungen:

Autoklav	100 ccm. Inhalt
Triphenylphosphin	9 g., Methanol 50 ccm.
Reduziertes Nickel	3 g.

Verarbeitung von Reaktionsprodukt.—Nach Entfernung von nicht umgesetztem Triphenylphosphin mit heissem Methanol extrahiert man den Komplex, der in festem Zustand zurückgeblieben ist, mit Benzol. Der Komplex wird aus der Benzollösung als feiner, schöner Kristall erhalten. Die Resultate sind in Tabelle II zusammengefasst.

TABELLE II

UNMITTELBARE HERSTELLUNG VON KOMPLEX

CO-Atm.	Reaktemp. (°C.)	Laufzeit. (Std. Min.)	Komplex- (g.)	Zurückgewonn. Ph_3P (g.)	Komplex-Ausbeute (%)
11	130	2:00	2.6	5.2	56.1
60	170	0:30	9.2	1.7	100
11	90	4:00	1.0	8.1	91.1
60	130	1:00	8.4	1.0	93.0
11	170	1:00	4.2	4.3	73.2
45	90	1:00	2.6	5.9	69.8
20	90	0:30	1.1	7.5	60.1
60	90	2:00	3.2	5.4	74.2
45	50	2:00	3.4	3.7	52.6
45	170	4:00	11.3	0	100
45	130	0:30	4.2	4.1	70.3
20	130	4:00	4.7	3.9	72.6
11	50	0:30	0.5	7.8	35.6
60	50	4:00	5.5	3.9	88.3
20	50	1:00	0.9	8.1	81.9
20	170	2:00	9.3	0.6	91.2

Erläuterung von Resultaten

1) Betreffs der Ausbeuten wurde ein bedeutender Unterschied in Bezug auf drei Faktoren nicht erkannt. 2) Betreffs der Umsetzung kann man darauf schliessen, dass die Umsetzung des Triphenylphosphins von dem Druck des Kohlenoxyds ziemlich und von der Temperatur bedeutend abhängig ist.

Folglich wurden die besten Bedingungen (60 Atm. CO-Druck, 170°, 30 Min.) bestimmt, worunter der Komplex bei der Feststellungsprobe mit der Umsetzung von 88.5% und der Ausbeute von 100% festgesetzt wurde.

Vorläufige Betrachtung über die Bildung von Styrol

Wie oben gesagt, ist bekannt, dass man bei der cyclisierenden Polymerisation des Acetylens unter Verwendung von Bistriphenylphosphin-Nickeldicarbonyl und einem Lösungsmittel wie Benzol, 88% Benzol und 12% Styrol, wovon etwa die Hälfte als polymeres Produkt sich ausscheidet, erhalten kann.

(1) $3CH{\equiv}CH \rightarrow C_6H_6$

(2) $4CH{\equiv}CH \rightarrow C_6H_5CH{:}CH_2$

Am Anfange unserer Arbeit, die Ausbeute von Styrol zunehmen zu lassen, betrachteten wir zuerst danach, auf welchen Mechanismus die Reaktion (2) verläuft. So nahmen wir folgende vier Reaktionen an:

a) $C_6H_6 + C_2H_2 \longrightarrow C_6H_5{-}CH{:}CH_2$

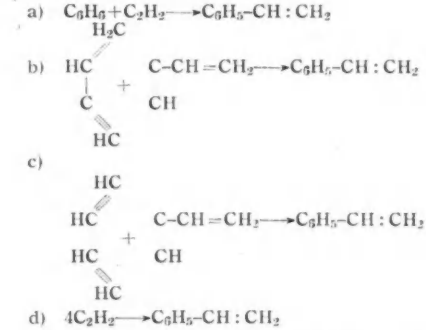

d) $4C_2H_2 \longrightarrow C_6H_5{-}CH{:}CH_2$

Reaktion a), die unter Vinylierung von Benzol verstanden werden kann, muss wahrscheinlich ausserordentlich schwer sein. Reaktion b), die Dimerisation von Monovinylacetylen umfasst, das sich durch Dimerisation von Acetylen bildet, wird aus der Untersuchung von Dykstra[4] vermutet, in der er Styrol aus Monovinylacetylen unter Anwendung von Säure bei 105° mit Ausbeute von 20 bis 50% erhielt. Wir liessen Monovinylacetylen unter Anwendung von besagtem Komplexkatalysator und von Benzol bei 80° während 5 Stunden polymerisieren, aber konnten kein Styrol erhalten, sondern nur gelatineartiges, unlösliches Polymerisat.

4) H. B. Dykstra, *J. Am. Chem. Soc.*, **56**, 1626 (1934).

Demnach berechneten wir die Möglichkeit von Reaktion (c) und (d) thermodynamisch. Wärmetönungen von beiden Reaktionen wurden wie folgt berechnet:

c) $2C_2H_2+C_4H_4 \rightarrow C_6H_5\text{-}CH:CH_2+138.4$ Kcal.

d) $4C_2H_2 \rightarrow C_6H_5\text{-}CH:CH_2+82.6$ Kcal.

Aus diesen Werten wurden Gleichgewichtskonstanten (log Kp) nach Annäherungsgleichung von Nernst ausgerechnet.

TABELLE IV

GLEICHGEWICHTSKONSTANTEN

Temp. °C.	70	80	90	100	110	120
Log Kp (c)	72.74	70.20	67.80	65.52	63.38	61.19
Log Kp (d)	44.90	43.40	41.97	40.61	39.33	38.00

Von diesen wurden Freienergie (konst. Vol.) berechnet.

TABELLE V

FREIEENERGIE

Temp. °C.	70	80	90	100	110	120
$-\Delta Y$ (c) Kcal./Mol.	113.4	111.9	111.1	110.3	109.5	108.2
$-\Delta Y$ (d) Kcal./Mol.	69.8	69.4	69.0	68.4	68.1	67.5

Die Vorzüglichkeit der Reaktion (c) zeigt sich von obigen Werten. Dann haben wir über Mischpolymerisation von Acetylen und Monovinylacetylen gearbeitet.*

Verfahren, worin Monovinylacetylen mit Lösungsmittel in Reaktionsgefäss eingesetzt ist.

Monovinylacetylen wurde unter Anwendung von Nieuwlands Katalysator nach Verfahren von Shimo[5] hergestellt. Die Entfernung von Acetaldehyd, das den Katalysator vergiftet, wurde vorsichtig durchgeführt.

Ein Gemisch von gereinigtem Benzol und Komplexkatalysator Bistriphenylphosphin-Nickeldicarbonyl und Monovinylacetylen wird in Druckgefäss von 300 cc. Inhalt eingesetzt. Man presst nun unter Erwärmen ein Gemisch von 1 Teil Stickstoff und 1 Teil Acetylen auf, bis der Druck 20 at. beträgt. Bei etwa 110° setzt die Reaktion ein. Durch Nachpressen von frischem Acetylen hält man den Druck (ca. 30 Atm.) konstant. Die Temperatur kann im Laufe der Umsetzung auf 60 bis 70° gesenkt werden. Wenn die Absorption von Acetylen langsam wird, so wird das Reaktionsgemisch aus dem Druckgefäss nach Abkühlung herausgenommen, gewogen und mit Wasserdampf abdestilliert. Styrolgehalt in der Oelschicht wird nach KBr-$KBrO_3$-Verfahren bestimmt. Die Ausbeute von Styrol und Benzol wird unter Abziehung der Mengen von Benzol, ausgerechnet, das als Lösungsmittel eingesetzt wurde. Wenn Polyolefin sich nebenbei bildet, soll diese analytische Methode dementsprechenden Fehler begleiten. Aber das Resultat des Feststellungsversuches von Dibromstyrol (Smp. 73°) zeigte, dass Olefin ausschliesslich des Styrols beinahe abwesend war. Das nicht umgesetzte Monovinylacetylen konnte nicht zurückgewonnen werden, da es sich mit dem Abgase bei der Entspannung des Restdrucks im Autoklav verliert.

Die experimentellen Resultate sind in Tabelle VI zusammengefasst.

TABELLE VI

HERSTELLUNG VON STYROL UND BENZOL

Nr.	Bzl. (g.)	Kat. (g.)	MVA (g.)	Temp. (°C.)	Laufzeit (Std.)	Inkremt. (g.)	Benzol (g.)	Benzol (%)	Styrol (g.)	Styrol (%)	S/B
S-1	50	3	5	70–127	15	44.5	19.7	44.2	9.35	21.0	0.48
4	40	3	10	80–110	23	65	35.8	55.0	15.23	23.4	0.43
5	40	3	10	70–110	20	62	34.5	55.7	15.6	25.2	0.45
6	60	3	10	70–100	9	74	25.4	34.3	12.65	17.1	0.5
9	60	3	15	80–120	nicht reagiert						
11	60	3	20	80–120	nicht reagiert						
B-10	50	3	0	70–80	10	100	80.0	80.0	8.0	8.0	0.1

Bemerkungen: S/B ist das Verhältnis der Ausbeuten von Benzol und Styrol. Inkrement bedeutet die Summe von eingesetztem Monovinylacetylen und polymerisiertem Acetylen. Die Ausbeute sowohl von Benzol als von Styrol ist in diesem Inkrement begründet.

1) Mit dem Reaktionsverlaufe (als aufgenommene Acetylenmenge 15 bis 20 l.) wird die Reaktionsgeschwindigkeit langsam. Folglich muss man die Reaktionstemperatur auf 90 bis 120° steigern. Diese Temperatur ist um 20 bis 30° höher als die in dem Falle, in welchem Monovinylacetylen nicht verwendet wird. Es scheint, dass dies seinen Ursprung von höherer Konzentration des Monovinylacetylens hat, die den Verlust von der Aktivität des Katalysators durch Bildung eines schädlichen Nebenproduktes bringt.

5) K. Shimo, Gosei Gomu, S. 168 (1940).

* K. Yamamoto und M. Oku, *J. P.* 198913.

2) Die Ausbeute von Styrol, worin polymeres Styrol nicht umfasst wird, nimmt eindeutig mit Vergleich von der Ausbeute von Nr. B-10 zu.

3) Aus obigen Resultaten wird geschlossen, dass die am Anfange eingesetzten Mengen von Monovinylacetylen ihre Grenzen (bis ca. 20% auf Basis von Benzol) haben und dass auch die Zunahme von der Ausbeute des Styrols also ihre Grenze haben muss.

Verfahren, worin Monovinylacetylen mit Acetylen in Reaktionsgefäss eingepresst wird

Um den oben erwähnten Nachteil zu beseitigen, nahmen wir ein anderes Verfahren auf, worin Monovinylacetylen mit Acetylen in das Reaktionsgefäss nachgepresst wird. Acetylen wird durch druckfesten Verdampfer, worin Monovinylacetylen eingesetzt ist, in

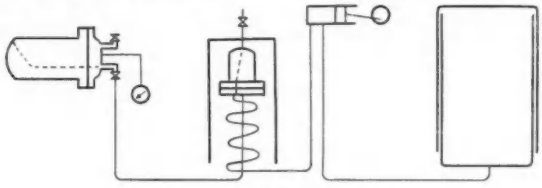

Fig. 1

das Reaktionsgefäss eingepresst. Das Molverhältnis von Acetylen zu damit begleitetem Monovinylacetylen wird durch Regelung der Temperatur von dem Verdampfer willkürlich bestimmt. Die Skizze von dem Reaktionsapparat ist in Figur 1 angegeben.

In Tabelle VII sind Sättigungsdruck von Monovinylacetylen bei verschiedener Temperatur, und in Tabelle VIII Molverhältnisse von dem unter 30 Atm. Druck stehenden, gesättigten Acetylen-Monovinylacetylen-Gasgemisch angegeben.

TABELLE VII

SÄTTIGUNGSDRUCK VON MVA

MVA-Dampfdruck in Atm.	1	1.82	3.16	5.4	16.98	29.9
Temp. °C.	5	22.4	40	50	110	120

TABELLE VIII

C_2H_2: MVA. BEI 30 ATM. IN MOL.

°C.	C_2H_2	MVA.
22	16	1
60	5	1
80	2	1

Wenn die Reaktion nach folgendem Schema dargestellt wird, so kann man verstehen, dass die Temperatur von dem Verdampfer bei etwa 80° gehalten werden muss.

$$2C_2H_2 + C_4H_4 \rightarrow C_6H_5\text{-}CH : CH_2$$

Geringe menge Pyrogallol setzten wir in den Verdampfer ein, um die Polymerisation von Monovinylacetylen darin zu hemmen. Experimentelle Resultate nach diesem Verfahren sind in Tabelle IX gegeben.

TABELLE IX

HERSTELLUNG VON STYROL UND BENZOL

Nr.	Bzl. (g.)	Kat. (g).	MVA. (g.)	Verdamp. temp. (°C.)	Reakt.-temp. (°C.)	Laufzeit (Std.)	Inkrement (g.)	Benzol (g.)	Benzol (%)	Styrol (g.)	Styrol (%)	S/B
S13	50	3	4	25	70–90	12	54	35.2	67.7	14.9	28.6	0.42
14	50	3	5	25	70–90	14	76	43.4	57.1	18.6	24.5	0.43
18	50	3	12	60	70–80	11	57.5	25.6	44.5	14.4	25.0	0.56
19	50	3	30	80	70–90	7	50	13.5	27.0	28.5	57.0	2.11

Wie erwartet, nahm die Ausbeute von Styrol desto mehr zu, je grösser Verhältniss MVA/C_2H_2 wird (d.h., je höher die Temperatur von dem Verdampfer wird). Es ist bemerkenswert, dass die Ausbeute von Styrol in Nr. S19 mehr als die von Benzol wurde.

Auf solche Weise haben wir Styrol mit Ausbeute von 57% auf Basis von dem Inkremente erhalten können, das die Summe von aufgenommenem Acetylen und verwendetem Monovinylacetylen bedeutet.

Schlusswort

Bei der cyclisierenden Polymerisation des Acetylens erfolgt die Verwendung von Bistriphenylphosphin - Nickeldicarbonyl - Katalysator die Bildung von Benzol und Styrol und die von Nickelcyanidkatalysator[6] dementgegen die Bildung von Cyclopolyolefin wie Cyclooktatetraen. Diese zwei Katalysatoren müssen in wohl verschiedenen Mechanismen

6) W. Reppe, *Ann.*, **560**, 1 (1948).

einwirken. Der extreme Beweis dafür ist deren Verhalten bei Mischpolymerisation von Acetylen und Monovinylacetylen. In unserem Experiment, in welchem der erstere verwendet wurde, nahm die Bildung von Styrol zu, aber in dem von Hagiwara[7], in welchem der letztere angewandt wurde, dementgegen die Bildung von Cyclopolyolefin hoher Glieder, wie $C_{10}H_{10}$, $C_{12}H_{12}$. Der Mechanismus der Bildung von Benzolring an Komplexkatalysator ist ein Gegenstand späterer Arbeit. Wir haben dargestellt, dass Styrol sich durch Mischpolymerisation von Acetylen und Monovinylacetylen bildet, das durch Dimerisation von Acetylen erhalten wird, d.h.,

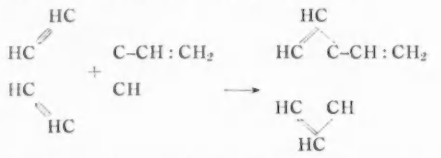

Darüber hinaus haben wir einen neuen Weg erschliessen können, bei welchem Styrol in unserem Lande aus leicht zugänglichem Rohstoff wirtschaftlich gut hergestellt werden kann.

7) N. Hagiwara, *J. Chem. Soc. Japan*, **73**, 323 (1952).

Diese Arbeit wird zusammengefasst, wie folgt:

1) Im Verfahren, worin Monovinylacetylen mit Lösungsmittel in dem Reaktionsgefäss eingesetzt ist, betrugen die Ausbeuten von Benzol und Styrol 50 bis 60% und 30 bis 20% beziehungsweise. Die Mengen von dem in Reaktionsgefäss eingesetzten Monovinylacetylen haben ihre Grenzen (bis ca. 20% auf Basis von einem Lösungsmittel).

2) Im Verfahren, worin Monovinylacetylen mit Acetylen in das Reaktionsgefäss eingepresst wird, betrugen die Ausbeuten von Benzol und Styrol 27% beziehungsweise und 57%.

Herr Dr. K. Yoshikawa hat uns immer bei unserer Arbeit geleitet und ermutigt. Ihm und der Mitsui Chemical Industry Co., die uns die Veröffentlichung unserer Arbeit erlaubte, sagen wir unseren herzlichen Dank.

Diese Arbeit wurde am 1. IV, 1954 im Rahmen der 7. Jahresversammlung der japanischen chemischen Gesellschaft in Tokyo mündlich veröffentlicht.

Mitsui Chemical Industry Co., Ltd. Miike Dyestuff and Chemical works, Omuta, Fukuoka

Kupferchromit als Katalysator bei der Propargylalkoholsynthese

Von Kazumi YAMAMOTO, Yōichi HIRUSAWA und Minoru YOSHIMURA

(Eingegangen am 26. April, 1954)

Einleitung

Es ist bekannt, dass Butindiol-1.4 und Propargylalkohol durch die von Reppe[1] gefundene Alkynolsynthese aus Acetylen und Formaldehyd in Anwesenheit von Kupferacetylid als Katalysator unter erhöhtem Druck erhalten werden.

Zur Gewinnung des Propargylalkohols, der wichtiger Ausgangsstoff für organische chemische Industrie ist, handelt es sich darum, auf welche Weise man die Bildung von Butindiol, das sich leichter als Propargylalkohol bildet, hemmen kann.

Murahashi[2] hat mit seinem Mitarbeiter hinsichtlich sowohl des Einflusses des Acetylendruckes als der Reaktionstemperatur und als der Wasserstoffionenkonzentration veröffentlicht. Yamamoto[3] von den Verfassern hat erfunden, dass das als Hydrierungskatalysator wirksame Kupferchromit von Adkins auch für Alkynolsynthese die spezifische Aktivität besitzt.

Wir haben also Reaktionsbedingung unter Anwendung von diesem Katalysator untersucht, Propargylalkohol vorzüglich zu gewinnen. Ferner haben wir die neue Erkenntnis über Selektivität des Chromitkatalysators für einseitige Umsetzung von Acetylen bei Äthinyrierung von Formaldehyd erhalten.

Arbeitungsmethode

Die verwendeten, verschiedenen Kupferchromite wurden gemäss Adkinsscher[4] Methode dargestellt. Das Experiment wurde im allgemeinen wie folgt durchgeführt:

In einem Autoklav von 600 cm^3. Inhalt, der

1) W. Reppe, "Acetylene Chemistry," Charles A. Meyer Co. N. Y. 1949, S. 84.

2) S. Murahashi, B. Ryutani, Mundliche Veröffentlichung bei der 3. Jahresversammlung der japanischen chemischen Gesellschaft, Osaka (1950).

3) K. Yamamoto und K. Sato, *J. P.* 187633.

mit Verdichter durch biegsames Kapillarrohr verbunden ist, erhitzt man Formalin-Kontakt Gemisch bei 120° unter Schüttelung und presst reines Acetylen auf 30 Atm. ein. Durch Nachpressen von Acetylen wird dieser Operationsdruck während des Reaktionsverlaufes, konstant gehalten. In manchen Fällen wurde ein Lösungsmittel wie Methanol oder Aceton verwendet.

Die nach der Filtration von Katalysator befreite Reaktionslösung lässt sich durch Widmersche Kolonne 2 m. lang fraktionieren. Dabei kann Propargylalkohol unter Bildung von Azeotrope mit 56%-igem Wassergehalt bei 97° erhalten werden. Von konzentrierter Mutterlauge wird Butindiol durch Destillation unter vermindertem Druck zurückgewonnen.

Die Ausbeute von Propargylalkohol wurde jodmetrisch bestimmt[5] und die von Butindiol wurde durch Destillation geschätzt.

Experimentelle Resultate und deren Betrachtungen

a) Einfluss der Konzentration von Formaldehydlösung.—Die Resultate der Experimente, in welchen 10 g. von 25 KAF.-Kupferchromit von Adkins als Vertreter, verwendet wurden, sind in Tabelle I zusammengefasst.

TABELLE I

EINFLUSS DER CH_2O-KONZENTRATION

Nr.	Konz. von CH_2O (%)	BDO-Ausbeute (g.)	BDO-Ausbeute (%)	PA-Ausbeute (g.)	PA-Ausbeute (%)	Umgesetzt.CH_2O (%)	PA/BDO in Gew.
708	36.9	22.5	57.0	13.5	26.2	38.2	0.61
710	,,	23.0	58.2	13.9	26.8	85.0	0.62
715	17.9	17.4	44.0	17.7	34.4	78.4	1.02
717	11.9	19.2	48.6	19.6	38.1	86.7	1.02
721	,,	19.0	48.2	19.2	37.3	85.5	1.01
723	9.0	15.3	38.7	19.4	37.7	76.3	1.27
727	,,	15.3	38.7	20.1	31.0	78.3	1.33
724	7.4	8.3	31.3	13.7	39.8	71.1	1.65
726	,,	8.5	32.0	13.0	37.9	69.9	1.53
728	6.2	6.5	24.6	14.2	41.3	65.9	2.18
730	,,	6.6	24.8	13.0	37.9	62.7	1.96

BDO = Butindiol-1.4 PA = Propargylalkohol

Auch bei dem Kupferchromit-Katalysator nimmt die Bildung des Propargylalkohols je nach der Verminderung der Konzentration von Formaldehyd zu.

b) Effekt des Lösungsmittels. — Von der unten gezeigten zwei Gleichungen soll vermutet werden, dass die Ausbeute von Propargylalkohol durch Verdünnung von Formaldehyd mit so geeignetem Lösungsmittel, wie das Acetylen gut löst, verbessert werden kann.

$$CH{\equiv}CH + HCHO \longrightarrow CH{\equiv}C{-}CH_2OH$$

$$CH{\equiv}CH + 2HCHO \longrightarrow HOCH_2{-}C{\equiv}C{-}CH_2OH$$

Reppe[1,6] hat Tetrahydrofuran als solches und Kupferacetylid als Katalysator verwendet und Propargylalkohol mit Ausbeute von 59% erhalten können. Wir haben den Einfluss von Methanol und Aceton, unter Anwendung von 10 g. 25-KAF-Chromit erforscht. Die Resultate sind in Tabelle II gezeigt.

TABELLE II

EFFEKT DES LÖSUNGSMITTELS

Nr.	Lösungsmittel (g.)	37%-CH_2O (g.)	BDO-Ausbeute (g.)	BDO-Ausbeute (%)	PA-Ausbeute (g.)	PA-Ausbeute (%)	Umgesez. CH_2O (%)	PA/BDO in Gew.
723	Wasser 225	75	15.3	38.7	19.4	37.7	76.3	1.27
727	Wasser 225	75	15.3	38.7	20.3	39.6	78.3	1.33
666	Aceton 225	75	12.4	31.3	25.0	48.5	79.8	2.02
667	Aceton 225	75	10.8	27.3	25.4	49.2	76.5	2.34
674	Methanol 225	75	3.7	9.4	11.3	21.8	31.2	3.06
675	Methanol 225	75	3.8	9.6	10.8	19.6	30.4	2.38

Wie Tabelle II zeigt, ist Aceton als Lösungsmittel besser denn Methanol. Jedoch eine Sache von grösster Besorgnis ist es, dass Aceton, das auch aktive Carbonyl-Gruppe besitzt, durch das unter Druck stehende Acetylen äthinyliert werden könnte.

4) H. Adkins, *J. Am. Chem. Soc.*, **53**, 1095 (1931); **54**, 1138 (1932).

5) K. Yamamoto, M. Yoshimura, und M. Tanaka, Dieses Bulletin, **24**, 151 (1951).

6) W. Reppe, *J. P.* 148,022.

Es war nicht der Fall. Wie das Fraktionierungsdiagramm (Fig. 1.) zeigt, konnte keine Bildung von Methylbutinol, das bei 82 bis 83° mit Wasser azeotropisch destilliert werden soll, beobachtet werden.

$$CH_3COCH_3+CH{\equiv}CH\longrightarrow (CH_3)_2C(OH)-C{\equiv}CH$$

c) Einfluss der Acetonmenge.—Unter Anwendung besagten Katalysators wurde der Einfluss der Acetonmenge untersucht. Die Resultate sind in Tabelle III gezeigt.

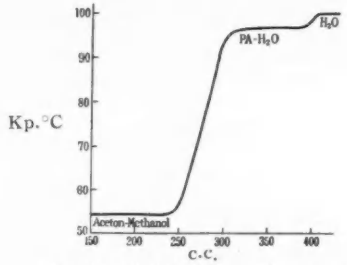

Fig. 1. Fraktionierungskurve von Reaktionsprodukt

TABELLE III

EINFLUSS DER ACETONMENGE

Nr.	36.9% HCHO (g.)	Aceton (g.)	BDO-Ausbeute (g.)	BDO-Ausbeute (%)	PA-Ausbeute (g.)	PA-Ausbeute (%)	Umgesetzt. CH_2O (%)	PA/BDO in Gew.
780	75	—	22.5	57.0	13.5	26.2	83.2	0.6
645	75	75	16.3	41.2	19.9	38.6	79.8	1.22
644	75	112.5	13.6	34.3	19.0	36.9	71.2	2.14
648	75	150	12.6	31.8	20.6	40.0	71.8	1.63
639	75	225	14.6	36.9	22.5	43.7	80.6	1.54
653	50	200	8.5	32.1	18.6	54.0	86.1	2.18
711	50	250	9.0	34.0	19.5	56.6	90.6	2.17

Wie vermutet wurde, ist sowohl die Umsetzung des Formaldehyds als auch die Ausbeute von Propargylalkohol desto höher, je mehr die Acetonmenge steigt. Auf solche Weise haben wir Propargylalkohol mit der Ausbeute von 55 % unter hoher Umsetzung erhalten können.

d) Vergleich der verschiedenen Kupferchromite.—Adkins[4] hat verschiedene Kupferchromite, die kleine Mengen Erdalkalimetall enthalten, entwickelt, wie 25-KAF (Ba), 30-RAC (Ba), 40-KAF (Sr), 39-KAF (Ca). Die zum Vergleich der Aktivität benützte Kontaktmenge war je 10 g.

Auf Tabelle IV ist eindeutig zu sehen dass von diesen Chromiten hinsichtlich der Umsetzung von Formaldehyd und der Ausbeute des Propargylalkohols 25-KAF am wirksamsten ist. Die verwendeten Mengen von 37%-igem Formaldehyd und Aceton waren beziehungsweise 75 g. und 225 g.

TABELLE IV

VERGLEICH DER VERSCHIEDENEN KUPFERCHROMITKATALYSATOREN

Katalysator	BDO-Ausbeute (g.)	BDO-Ausbeute (%)	PA-Ausbeute (g.)	PA-Ausbeute (%)	Umgesetzt CH_2O (%)	PA/BDO in Gew.
25-KAF Cu-Ba-CrO	9.8	24.7	24.1	46.3	71.0	2.46
,,	10.8	27.3	26.1	50.2	77.5	2.60
30-RAC Cu-Ba-CrO	13.3	33.0	24.0	46.1	79.1	1.80
,,	13.7	34.6	24.4	47.3	81.9	1.78
40-KAF Cu-Sr-CrO	14.5	36.7	20.5	39.8	76.5	1.41
,,	14.7	37.2	22.5	43.6	80.8	1.53
39-KAF Cu-Ca-CrO	6.8	17.2	16.7	32.3	49.5	2.45

e) Effekt der Essigsäurenwäsche von 25-KAF.—Im allgemeinen hat üblicher Kupferoxydkatalysator (wesentlich Kupferacetylid) die Neigung zur Butindiolbildung. Dementgegen ist gezeigt worden, dass Kupferchromitkatalysator spezifisches Verhalten bietet. Dies wird durch folgenden Vergleich des Effektes der Essigsäurenwäsche von 25-KAF-Chromit dargestellt. Geröstetes, rohes Chromit wurde in zwei Teile geteilt. Ein Hälfte wurde, so wie sie ist, verwendet, während die andere Hälfte nach der Wäsche mittels 50 %-iger Essigsäure bei 50° unter Rührung während einer Stunde von beigemengtem Kupferoxyd befreit wurde. Katalytische Wirkung dieser beiden Chromite wurde unter Verwendung 75 g. von 37%-igem Formaldehyd mit 225 g. Aceton verglichen (Tabelle V).

Tabelle V

Effekt der essigsäurenwäsche von 25-KAF

	BDO-Ausbeute (g.)	(%)	PA-Ausbeute (g.)	(%)	umgesetzt. CH_2O (%)	PA/BDO in Gew.
Rohes Chromit	14.3	36.2	21.4	41.6	77.8	1.50
,,	14.6	36.9	22.5	43.7	80.6	1.54
Gewasch. Chromit	9.8	24.7	24.7	46.3	71.0	2.46
,,	10.8	27.3	27.3	50.2	77.5	2.60

Die gefundenen, analytischen Zusammensetzungen beider Chromite zeigen, dass das Atomverhältnis Cu: Cr unter Berücksichtigung von dem mit Barium sich zu verbindenden Chromatom, nahe an dem Wert von Stroupe[7] 1 : 1 ist.

	Cu %	Ba %	Cr %	Cu:Ba:Cr
Rohes Chromit	31.98	7.71	29.09	10:2.8:10.7
Gewasch. Chromit	22.29	10.06	30.62	10:5.4:16.9

f) Selektvität des Chromitkatalysators.— Die Bildung von Butindiol aus Acetylen und Formaldehyd ist so zu erklären, dass sich zuerst Propargylalkohol aus Acetylen und einem Molekül Formaldehyd auf Katalysator bildet und dann ferner mit einem Molekül Formaldehyd Butindiol ergibt. So soll vermutet werden, dass Chromitkatalysator gegen sekundäre Reaktion, Butindiol aus Propargylalkohol und Formaldehyd, inaktiver als Kupferoxyd (wesentlich Kupferacetylid) sei.

Das experimentelle Resultat, das unter folgenden Bedingungen erhalten wird, ist in Tabelle VI dargestellt.

Ausgangsstoffe; 37% Formaldehyd 30g. (HCHO 11.10 g), Propargylalkohol 9.225g, Katalysator 5 g.

Experiment wurde in Abwesenheit von Luft bei 120° während einer Stund durchgeführt.

Diese Resultate erweisen die Selektivivität des Chromitkatalysators, die auch durch den Effekt der Essigsäurenwäsche von Kupferchromit dargestellt wurde.

7) T. D. Stroupe, *J. Am. Chem. Soc.*, **71**, 569 (1949).

Tabelle VI

Butindiol aus propargylalkohol

Katalysator	Reaktionsgemisch HCHO (g.)	PA (g.)	BDO (g.)	BDO-Ausbeute. % d. Th. an PA
25-KAF	10.38	8.88	0.34	2.40
CuO	9.58	6.89	2.82	19.9
,,	9.45	5.55	3.21	22.7

Schlusswort

Wir haben über die Synthese von Propargylalkohol unter Anwendung von Kupferchromit, das von Adkins als Hydrierungskatalysator entwickelt worden ist, gearbeitet. Und wir haben nicht nur die optimalen Bedingungen darüber finden können, sondern auch die Erkenntnis erhalten, dass die katalytische Wirkung von Kupferchromit von der des Kupferoxyds ziemlich verschieden ist.

Es sei uns gestattet, dem Herrn Dr. K. Yoshikawa, auf dessen Anregung vorliegende Arbeit entstanden ist, an dieser Stelle unseren ergebensten und herzlichsten Dank auszusprechen für die warme und fördernde Leitung an unserer Arbeit.

Diese Arbeit wurde am 20. I, 1951 im Rahmen der japanischen chemischen Gesellschaft Kyushu-Zweigabteilung in Fukuoka mündlich veröffentlicht.

Mitsui Chemical and Industry Co., Miike Dyestuff and Chemical Works, Omuta, Fukuoka

Über die neue synthetische Methode von Carbonäsuren durch Carbonylierung von aromatischen, halogenierten Kohlenwasserstoffen

Von Kazumi Yamamoto und Kazutoshi Sato

(Eingegangen am 26. April, 1954)

Einleitung

In der Arbeit über die Herstellung von Adipinsäure durch Carbonylierung von Butandiol-1.4 haben wir die Tatsache gefunden, dass Benzoesäure sich durch Einwirkung von Kohlenoxyd auf Monochlorbenzol bildet, welches als Lösungsmittel verwendet wurde.

Auf Grund dieser Erfindung der neuen Reaktion haben wir Carbonylierung von verschiedenen halogenierten, aromatischen

Kohlenwasserstoffen durchgeführt und entsprechende aromatische Carbonsäure erhalten können.

Diese neue Reaktion verläuft wie allgemeine Carbonylierung von Alkohol[1] in Anwesenheit von Wasser und unter Anwendung von carbonylbildungsfähigem Metall oder dessen Halogenid als Katalysator bereits bei 250 bis 300° und 200 bis 300 Atm.

z. B. 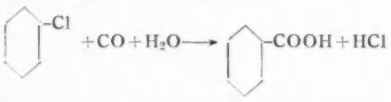

Diese neue Reaktion wird folglich die Verwendbarkeit von aromatischen halogenierten Kohlenwasserstoffen in der organischen synthetischen Chemie vergrössern, d. h., die Herstellung der Benzoesäure aus Chlorbenzol, die der Terephthalsäure aus *p*-Dichlorbenzol, welche als Rohmaterial der synthetischen Faser insbesondere wichtig ist.

Wir wollen etwas über die bisher veröffentlichten, analogen Reaktionen sprechen, bevor wir unsere Arbeit beschreiben.

Hopf[2] hat Essigsäure aus Chlormethan und Kohlenoxyd unter erhöhter Temperatur in Anwesenheit von Aluminiumchlorid erhalten. Frank[3] und Theobold[4] haben auch Essigsäurechlorid oder dessen chloriertes Derivat aus mono- oder polychloriertem Methan unter ähnlichen Bedingungen hergestellt.

$$CCl_4 + CO \rightarrow CCl_3COCl$$
$$HCCl_3 + CO \rightarrow HCCl_2COCl$$
$$H_3CCl + CO \rightarrow H_3CCOCl$$

Groombridge[5] hat auch gefunden, dass oben beschriebene Reaktionen unter katalytischer Einwirkung von Nickel oder dessen Salze glatt verlaufen.

Wir haben am Anfange dieser Arbeit keine Beschreibung über die Reaktion von aromatischem, halogeniertem Kohlenwasserstoff und Kohlenoxyd in einer Literatur finden können.

Unsere Arbeit, wobei ein Autoklav von 18:8 Stahl verwendet wurde, war nicht gerade vollständig, da fortlaufender Versuch wegen der Ätzung der Gefässwand, die auf Einwirkungen von gebildeten Säuren zurück zuführen ist, abgebrochen werden musste.

Beschreibung der Versuche

1. Arbeitungsmethode. Im Autoklav (18:8 Stahl) von 100 cc. Inhalt wird das Gemisch von aromatischem, halogeniertem Kohlenwasserstoff, Wasser und Katalysator eingeschaltet und Kohlenoxyd von 150 bis 200 Atm. nach Verdrängung von Luft eingepresst. Wird das Reaktionsgemisch auf 250 bis 300° gehitzt, so beobachtet man das Auftreten der Umsetzung durch plötzlichen Druckabfall. Die Umsetzung verläuft im allgemeinen in weniger als 30 Minuten.

Als Katalysator gilt in erster Linie Nickel oder dessen Halogenide, insbesondere Nickeljodid. Die Umsetzung verläuft ohne Zugabe von einem Medium, aber im allgemeinen ist die Zugabe von geeignetem Lösungsmittel, wie Glykol, Ester, Benzol usw. erwünscht.

Das Reaktionsgemisch lässt sich aus dem Autoklav herausnehmen und mit Natronlauge behandeln und filtrieren. Gebildete Carbonsäure wird von der auf solche Weise erhaltenen Lösung des Natriumsalzes mit Schwefelsäure niedergeschlagen und umkristallisiert.

2. Experimentelle Resultate. Unsere typenhaften, experimentellen Resultate sind in folgenden Tabellen zusammengefasst.

a) REAKTIONSBEDINGUNGEN

Nr.	Ronstoff (g.)		H_2O (g.)	Katalysator (g.)		Medium (g.)		Reakt.temp. (°C.)	Max. Druck (Atm.)
1	Chlorbenzol	10	10	$NiJ_2$6 Ni	1	Butandiol	15	300	280
2	〃	10	10	$NiJ_2$3 Ni	1	Butylacetat	10	290	261
3	Jodbenzol	10	10	$NiJ_2$3 Ni	1	〃	10	250	250
4	〃	10	10	Ni 3		—	—	300	260
5	*p*-Dichlorbenzol	10	10	$NiJ_2$3 Ni	1	Butylacetat	10	300	240
6	*o*-Chlortoluol	10	10	$NiJ_2$2 Ni	1	〃	10	300	320
7	*β*-Chlornaphthalin	10	10	$NiJ_2$3 Ni	1	〃	10	280	235
8	*p*-Chlorphenol	10	10	$NiJ_2$3 Ni	1	〃	10	280	240
9	Jodbenzol	10	10	Ni 3		Methanol	10	300	310

b) RESULTATE

Nr.	Druckabfall (Atm.)	Carbonsäureausbeute (g.)		(%)	Nebenprodukt
1	80	Benzoesäure	7.1	65.3	Adipinsäure, Valeriansäure
2	31	〃	10.3	95	Essigsäure, 〃

1) W. Reppe, "Neue Entwicklungen auf dem Gebiet der Chemie des Acetylens und Kohlenoxyds", Springer Verlag (1949) S. 110.
2) H. Hoff, *Ber.*, **64**, 2739 (1931).
3) C. Frank u. a., *Ind. Eng. Chem.*, **41**, 2061 (1949).
4) C. Theobold, *A. P.* 2378048; *C. A.*, **39**, 4084 (1945).
5) W. Groombridge, *E. P.* 621520; *C. A.*, **43**, 6650 (1949).

3	21	〃	6.3	100	〃 〃
4	18	〃	5.5	92	Diphenyl*
5	30	Terephthalsäure	3.5	31	Benzoesäure 4.9 g.*
6	15	*o*-Toulylsäure	6.5	60.5	Essigsäure, Valeriansäure
7	15	*β*-Naphthoesäure	5.5	52.4	Naphthalin 1 g.*
8	Keine Umsetzung				
9	10	Benzoesäuremethyl	1	—	Essigsäure, Methylacetat

* Daneben wurden Essig- und Valeriansäure isoliert.

Betrachtung der Resultate

Die Reaktion verlief langsam ohne Zusatz von Reaktionsmedium. Butylacetat liess die Umsetzung als solches glatt verlaufen, wenn gleich es an sich zum Teil durch den Angriff von Kohlenoxyd gemäss der folgenden Gleichung Essig- und Valeriansäure lieferte:

$$CH_3COO\text{-}C_4H_9 + CO + H_2O \rightarrow CH_3COOH + CH_3CH_2CH_2CH_2COOH$$

Der Verlust von Kohlenoxyd betrug im allgemeinen 200 bis 300% an theoretischer Menge, die zur Bildung aromatischer Carbonsäure erforderlich ist. Auch oben erwähnte Nebenreaktion ist natürlich eine der Ursachen, aber eine hauptsächliche Ursache ist die Wassergasreaktion, die durch das Sein von Wasserstoff und Kohlensäure im Abgase bewiesen werden kann.

$$H_2O + CO \rightarrow H_2 + CO_2$$

Wie es in Nr. 5 erkannt wird, bildet sich Benzoesäure, deren Bildung auf die Kohlensäureabspaltung von zuerst gebildeter Terephthalsäure gegründet werden muss.

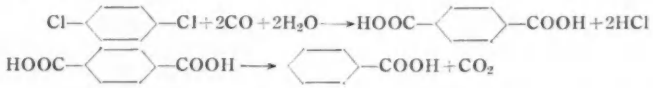

Man kann Terephthalsäure durch einen anderen, zweckmässigeren Weg herstellen, d. h., durch Oxydation von leicht umkristallisierbarer *p*-Toluylsäure, die nach der neuen Reaktion von *p*-halogeniertem Toluol mit Kohlenoxyd in guter Ausbeute erhalten werden muss. Die Umsetzung von Chlorbenzol verlief bei 290° bis 300°, aber die von Jodabkömmling trat bei 250° unter Anwendung von Nickeljodidkatalysator zusammen mit Nickelpulver als Hilfskatalysator ein. Wenn Alkohol wie Methanol im Reaktionssystem vorhanden ist, so könnte man die Bildung von aromatischem Carbonsäureester vermuten. Unter solcher Annahme wurde das Experiment Nr. 9 durchgeführt. Jedoch Methylbenzoat bildete sich nur in geringem Umfang. Dies soll zeigen, dass die Carbonylierung aromatischen Halogenkohlenwasserstoffes im Vergleich mit der des Methanols bei weitem schwieriger ist. In solchem Falle wurde also die Bildung von Essigsäure und deren Methylester stets beobachtet.

$$CH_3OH + CO \rightarrow CH_3\text{—}COOH \quad \text{und}$$
$$2CH_3OH + CO \rightarrow CH_3COOCH_3 + H_2O.$$

Der Mechanisumus der neuen Carbonylierung des aromatischen, halogenierten Kohlenwasserstoffes ist noch nicht aufgeklärt, aber es scheint uns, dass der Abbruch der Bindung zwischen dem Halogen- und Kohlenstoffatom die wichtigste Stufe dieser Umsetzung, von den experimentellen Tatsachen aus gesehen, z. B. die leichtere Umsetzbarkeit von Jodbenzol mit Vergleich von Chlorbenzol oder die beobachtete Bildung von Diphenyl (vgl. Nr. 4), ist.

Die zweite Stufe ist wahrscheinlich die Bildung von Säurechlorid, das sodann durch Verseifung mit Wasser die entsprechende Carbonsäure liefert. Das zur Entwicklung der neuen Reaktion schwierigste Problem ist die Ätzung von Reaktionsgefäss, die ihren Ursprung in erzeugter Salzsäure und Carbonsäure hat und die so heftig war, als dass wir diese Arbeit hätten fortsetzen können.

Wir möchten hier hinzufügen, dass unsere Arbeit unter neuer Gegenmassnahme fortgesetzt wird.

Schlusswort

Wir haben die neue Reaktion zur Synthese von Carbonsäuren aus aromatischen halogenierten Kohlenwasserstoffen in Anwesenheit von Wasser bei erhöhter Temperatur unter erhöhtem Druck von Kohlenoxyd unter Anwendung von Nickelverbindung als Katalysator gefunden.

Diese neue Reaktion gibt die Möglichkeit, dass wichtige Zwischenprodukte für organische chemische Industrie, wie Benzoesäure, Phthalsäure, Terephthalsäure usw., von billigen, leicht zugänglichen Rohstoffen aus mit guter Ausbeute hergestellt werden können.

Für dieses Verfahren zur Herstellung von aromatischen Carbonsäuren haben wir japanisches Patent am 13. Juni 1951 angemeldet.[6]

Zum Schluss sprechen wir dem Herrn Dr.

6) K. Yamamoto und K. Sato, *J. P.* 196859.

K. Yoshikawa für seine Anregung und stetige Leitung zu dieser Arbeit unseren besten Dank aus.

Darüber hinaus zum Teil von Forschungskosten für diese Arbeit wurde die Unterstützung für wissenschaftliche Forschung des Jahrganges 1952 von dem Unterrichtsministrium verwendet. Wir sagen unseren verbindlichsten Dank dafür.

Diese Arbeit wurde am 2. IV. 1953 in der 6. Jahresversammlung der japanischen chemischen Gesellschaft in Kyoto mündlich veröffentlicht.

Mitsui Chemical and Industry Co. Ltd.
Miike Dyestuff and Chemical Works
Omuta, Fukuoka

LETTER

On the Heterogeneity of Calf Thymus Histone

By Nobuo Ui

(Received May 24, 1954)

Since the studies of Kossel and Lilienfeld[1], histones have been a well-known class of proteins, but their chemical and physicochemical properties are not yet clearly understood. Recent workers[2] have discovered a heterogeneity of calf thymus histone, but because of the preparation methods employed in these investigations it is possible that some changes in the protein had been produced during the purification processes.

In the present investigation histone was prepared carefully from acid extracts of calf thymus gland, and examined for its heterogeneity. An attempt was also made to fractionate the preparations.

Method 1. Fresh calf thymus glands were frozen, minced, homogenized in 0.05 M sodium citrate at *p*H 7.0 (or in dilute citric acid) and centrifuged. The sediment was washed with the solvent several times to remove cytoplasmic contaminants and then the histone was extracted from the sediment with 0.1 or 0.2 N sulfuric acid (Extract A). After clarifying "Extract A", the histone was precipitated by addition of two volumes of ethanol at low temperature (sometimes below 0°C.) and reprecipitated several times.

The preparation obtained was free from deoxypentose nucleic acid and its nitrogen content was 18.2%. Tryptophane content was estimated to be less than 0.2%. This preparation was found to be inhomogeneous both in electrophoresis and ultracentrifuge.

Fractional precipitation of the purified histone preparation by ethanol yielded mainly two fractions. Fraction I, precipitated at lower ethanol concentrations, revealed two components in the ultracentrifuge, the sedimentation constants ($s_{20,w}$) of which were 1.9 S and about 7 S respectively in an acetate buffer of *p*H 5.0 and ionic strength 0.2. The heavier component amounted to about one-third of fraction I and its sedimentation constant varied with different preparations. Fraction II, precipitated at higher ethanol concentrations, was ultracentrifugally almost homogeneous ($s_{20,w}$=1.0 S), but electrophoretically not homogeneous.

Fraction II differed from fraction I in the fact that it could not be precipitated by addition of ammonia to its solution, but like fraction I was soluble in H_2SO_4-$HgSO_4$ reagent[3].

Method 2. From the above-mentioned "Extract A" histone could also be salted out by addition of ammonium sulfate. The fraction, which was obtained at 80% saturation of ammonium sulfate, contained two components ($s_{20,w}$=2.1 and 12 S). A second fraction, which precipitated between 80% and 100% saturation of ammonium sulfate, was also inhomogeneous ($s_{20,w}$=0.8, 1.9 and 15 S).

Method 3. According to the method of Mirsky and others[3,4] histone was extracted from thymus nuclei with 0.2 N hydrochloric acid and precipitated by bringing the dialyzd extract to a *p*H value of about 10 by sodium hydroxide. Fractional precipitation, by in-

1) A. Kossel, "The Protamines and Histones," London and New York (1928).

2) L. Ahlström, *Arkiv. Kemi. Mineral. Geol.*, **24**A, No. 31 (1947); E. Stedman and E. Stedman, *Phil. Trans. Roy. Soc. London*, Ser. B. **235**, 565 (1951); J. Grégoire, J. Grégoire, and J. Reynand, *Compt. rend.*, **236**, 1922 (1953).

3) A. E. Mirsky and A. W. Pollister, *J. Gen. Physiol.*, **30**, 117 (1946).

4) M. M. Daly, A. E. Mirsky and H. Ris, *J. Gen. Physiol.*, **34**, 439 (1951).

creasing the *p*H of the solution, yielded at least three different fractions, and a final fraction soluble in alkaline solution was precipitated by adding ethanol at *p*H 10.9. None of these fractions were homogeneous in the ultracentrifuge.

From the above observations it was concluded that calf thymus histone is not a homogeneous protein, but consists of many fractions having different molecular weights and charges.

Studies on the homogeneity of the histone sample which was prepared without using acid are now in progress and will be published soon with the details of the present investigations.

The author wishes to express his sincere thanks to Assistant Professor I. Watanabe for his kind advices and encouragement.

Institute of Science and Technology,
Tokyo University, Komaba-machi
Meguro-ku, Tokyo

Paper Fraction Analyzer

By Nobuo TAMIYA, Yukichi YOSHINO and Tokuro SODA

(Received March 6, 1954)

Since its invention, the fraction collector proved to be widely applicable in various fields of chemistry. The authors tried to construct a very simple apparatus (see Fig. 1) capable of collecting fractions drop by drop on a long moving strip of filter paper[1], and obtained satisfactory results. The drops of the liquid collected on the filter paper were treated by suitable techniques such as are used in paper chromatography.

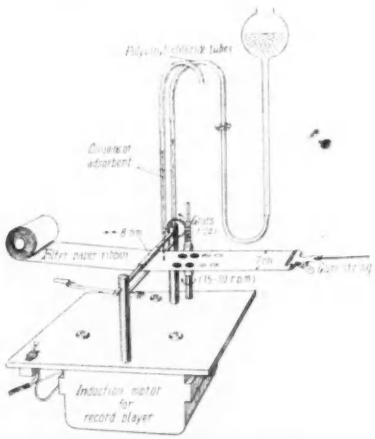

Fig. 1 "Paper fraction collector"

Using a small amount of ion-exchange resin as adsorbent, different metallic ions[2] were collected separately on different parts of the moving paper, as may be seen in Fig. 2. After spraying them with ammonium sulfide solution, the strips of the filter paper were dipped in melted paraffin in order to make the filter paper transparent and in order to stabilize the colors, and the metallic sulfides on the paper were estimated colorimetrically. The coloration is proportional to the concentration of dropped solution, provided that it is not less than 0.030 M/l.

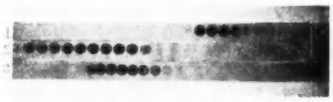

Fig. 2 Strips of filter paper, the colorimetric data of which are shown in Fig. 3. (photographed under ultraviolet light) 1—HgS, 2—CdS, 3—CuS.

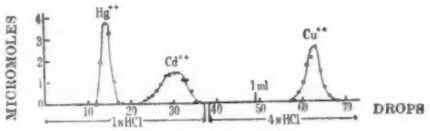

Fig. 3 Separation of Hg^{++}, Cd^{++} and Cu^{++} ions by the paper fraction analyzer. 10 micromoles each of mercuric, cadmium and cupric ions were adsorbed on a column of 0.45 ml. (5.1 cm. in height) of Amberlite IR 120 (180–250 mesh) from sulfates solution (0.033 M/l respectively) in 0.31 N nitric acid. After washing with distilled water, the cations were eluted by hydrochloric acid (1 N and 4 N) at a velocity of 1 drop per minute.

Fig. 4 shows the result of an experiment

1) B. Drake, *Nature*, **160**, 602 (1947).
2) R. Wickbold, *Zeit. anal. Chem.*, **132**, 26 (1951).

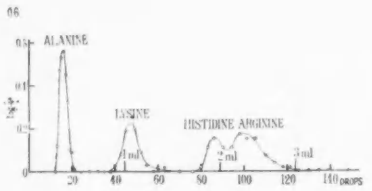

Fig. 4 Separation of amino acids by the paper fraction collector. 1 Micromole each of alanine, lysine, histidine and arginine were chromatographed by a column of Amberlite XE 64 (0.24 ml., 5.0 cm. in height) with a buffer of *p*H 5.95 (mixture of 0.2 M sodium citrate buffer and 0.2 M sodium phosphate buffer at the ratio of 2:1 in volume[4]) at the same rate as in the above experiment.

by this "paper fraction analyzer" in which basic amino acids and alanine were separated by Amberlite XE 64[3,4]. The amino acids on the filter paper were colorimetrically determined after treatment with ninhydrin solution[5] and melted paraffin. Amino acid-ninhydrin coloration thus treated did not change for several months.

The Chemical Institute, Faculty of Science, Tokyo University

3) C.H.W. Hirs, S. Moore, and W.H. Stein, *J. Biol. Chem.*, **200**, 493, (1953).
4) S. Ishii, and T. Ando, "Symposium on Biological Chemistry", October, 1953 (Tokyo).
5) R.R. Redfield, and E.S.G. Barron, *Arch. Biochem. and Biophys.*, **35**, 443 (1952).